Data-driven MRI modelling for the characterization, staging, and subtyping of frontotemporal dementia

Jillian McCarthy

Integrated Program in Neuroscience

McGill University, Montreal

December 2021

A thesis submitted to McGill University in partial fulfillment of the requirements of the degree of Doctor of Philosophy.

Abstract

Frontotemporal dementia (FTD) is a heterogenous neurodegenerative disease characterized by impairments in behaviour, language, and/or cognition. FTD has a significant genetic component; up to a third of cases are caused by an autosomal-dominant genetic mutation. It is crucial to accurately identify FTD before extensive neuronal damage has occurred, when treatment interventions will likely have the greatest effect. As such, there is a critical need for early diagnostic and prognostic biomarkers. Improving MRI-based biomarkers is ideal, given that MRI is already part of standard clinical practice. However, development is limited by a lack of knowledge of the progression of brain changes that begins several years before symptoms occur. This thesis uses advancements in computational modelling, including machine learning and multivariate statistical modelling, to study MRI-based biomarker progression throughout the early stages of FTD. Chapter 1 provides a brief overview of the problem and sets out the objectives of the thesis. Chapter 2 provides a review of the literature on biomarker development in FTD, with a focus on MRI measures and disease progression modelling. Chapter 3 describes a systematic review of the current state of the literature using morphometric MRI and machine learning to aide in FTD diagnosis. We found that morphometric MRI shows potential as an early diagnostic biomarker of FTD, however studies which use rigorous methodology and validate findings in an independent real-life cohort are necessary before recommendation for clinical use. Chapter 4 describes the methodology used to study the presymptomatic phase of FTD, using genetically at-risk individuals, who will eventually develop FTD symptoms. In chapter 5, we show that an unsupervised machine learning algorithm can identify data-driven disease stages in a heterogeneous sample combining different mutations and disease stages of genetic FTD using only MRI metrics. In chapter 6, we show that MRI metrics are insufficient to recover genetic subtypes

in the same sample, likely due to the high number of early presymptomatic individuals included. Chapter 7 attempts to untangle the underlying mechanisms of disease progression in genetic FTD using a multifactorial mechanistic model and suggests that this challenging task may require more complete data from individuals across the full disease course as well as a wider variety of potential biomarkers in combination. Finally, chapter 8 discusses the contributions, limitations, and future directions of these studies. Taken together, this thesis provides novel insights into the value of data-driven methods of biomarker development in genetic FTD, as well as some of the challenges of applying these methods to complex neurodegenerative diseases.

Résumé

La démence frontotemporale (DFT) est une maladie neurodégénérative hétérogène caractérisée par des troubles du comportement, du langage et/ou de la cognition. La DFT a une composante génétique importante; jusqu'à un tiers des cas sont causés par une mutation génétique autosomale dominante. Il est essentiel d'identifier avec précision la DFT avant que des dommages neuronaux importants ne se soient produits: c'est-à-dire la période de la maladie où les interventions thérapeutiques auront probablement le plus grand effet. Dans ce contexte, il existe un besoin critique pour des biomarqueurs diagnostiques et pronostiques précoces. L'amélioration des biomarqueurs basés sur l'IRM est idéale, étant donné que l'IRM fait déjà partie de la pratique clinique habituelle. Cependant, le développement des biomarqueurs est limité par le manque de connaissances sur la progression des changements cérébraux qui commencent plusieurs années avant l'apparition des symptômes. Cette thèse utilise les avancements de la modélisation informatique, y compris l'apprentissage machine et la modélisation statistique multivariée pour étudier la progression des biomarqueurs basés sur l'IRM tout au long des premiers stades de la DFT. Le chapitre 1 donne un bref aperçu du problème et expose les objectifs de la thèse. Le chapitre 2 présente une revue de la littérature sur le développement de biomarqueurs dans la DFT, en mettant l'accent sur les mesures IRM et la modélisation de la progression de la maladie. Le chapitre 3 décrit une revue systématique de l'état actuel de la littérature utilisant l'IRM morphométrique et l'apprentissage machine pour faciliter le diagnostic de la DFT. Nous avons constaté que l'IRM morphométrique présente un potentiel en tant que biomarqueur de diagnostic précoce de la DFT, mais des études utilisant une méthodologie rigoureuse et validant les résultats dans une cohorte indépendante dans la vie réelle sont nécessaires avant de recommander une utilisation clinique. Le chapitre 4 décrit la méthodologie utilisée pour étudier la phase

présymptomatique de la DFT, en utilisant des individus génétiquement à risque, qui finiront par développer des symptômes de la DFT. Dans le chapitre 5, nous montrons qu'un algorithme d'apprentissage machine non supervisé peut identifier les stades de la maladie basés sur les données dans un échantillon hétérogène combinant différentes mutations et différents stades de la maladie de la DFT génétique en utilisant uniquement des mesures de l'IRM. Dans le chapitre 6, nous montrons que les mesures IRM sont insuffisantes pour retrouver les sous-types génétiques dans le même échantillon, probablement à cause du nombre élevé d'individus présymptomatiques précoces inclus. Le chapitre 7 tente de comprendre les mécanismes sous-jacents de la progression de la maladie dans la DFT génétique à l'aide d'un modèle mécaniste multifactoriel et suggère que cette tâche difficile peut nécessiter des données plus complètes des individus tout au long de l'évolution de la maladie, ainsi qu'une combinaison d'une plus grande variété de biomarqueurs potentiels. Enfin, le chapitre 8 aborde les apports, les limites et les orientations futures de ces études. Dans son ensemble, cette thèse fournit de nouvelles informations sur la valeur des méthodes de développement de biomarqueurs basées sur les données dans la DFT génétique, ainsi que sur certains des défis liés à l'application de ces méthodes aux maladies neurodégénératives complexes.

Table of Contents

Acknowledgements

Throughout these past six years, many people advised me and provided invaluable assistance with my doctoral research. First and foremost, I would like to thank my supervisor Simon Ducharme and my co-supervisor Yasser Iturria-Medina for their guidance. Second, to my committee members, Sylvia Villeneuve and Boris Bernhardt for their advice and suggestions. Thanks to Ed Ruthazor for stepping in when necessary and providing valuable mentorship.

Thanks to all my fellow lab members in the Ducharme and Iturria-Medina labs for all their support, especially Teodora Yaneva and Jake Levy (I had fun sharing a workspace with you while it lasted). Special thanks to Teo for translating my abstract into French. Thanks to Robert Baumeister for helping me out with methodology and coding questions.

I would like to thank Natasha Rajah and Sylvia Villeneuve for taking me on as rotation student. Thanks as well to each of their lab members for their helpful advice and support. Special thanks to Stamatoula Pasvanis for teaching me all about fMRI processing and analysis. Thanks to Melissa Savard for her assistance with the diffusion weighted image processing used in this thesis. Thanks also for teaching me about fMRI processing and coding when I was a rotation student.

I would also like to acknowledge GENFI for providing the data used in this research; special thanks to each of the GENFI members who provided valuable feedback on my manuscript. Thanks also to Dr. Louis Collins for his valuable comments and advice on my first paper. I would also like to thank FRQS for funding my research.

Finally, I would like to thank my parents, Alison, and Toby for their constant support, advice, encouragement, and many visits and much needed distractions. You're the best!

Contributions of Authors

Chapter 3 (including all tables and figures), section 8.3.1 and parts of sections 8.4.3 and 8.5 of Chapter 8 are modified with permission from the published paper,

McCarthy, J., Collins, D. L., & Ducharme, S. (2018). Morphometric MRI as a diagnostic biomarker of frontotemporal dementia: A systematic review to determine clinical applicability. *NeuroImage: Clinical*, *20*, 685–696. https://doi.org/10.1016/J.NICL.2018.08.028

on which I am the first author. I conducted the literature review, reviewed all papers, interpreted the results, and wrote the manuscript including all tables and figures.

Co-author contributions:

Louis Collins: reviewing the manuscript

Simon Ducharme: Study design, reviewing the manuscript

All data used in the analyses presented in Chapters 4-7 were obtained from the Genetic Frontotemporal Dementia Initiative (GENFI). The models implemented in Chapters 5-7 (the contrastive trajectory inference (cTI) and the multifactorial causal model (MCM)) were developed by Yasser Itturia-Medina. I conducted all image processing and quality assessment, conducted the statistical analyses, visualized and interpreted the results, and wrote the chapters including all tables and figures.

Chapters 4 and 5 and parts of sections 8.2, 8.4.1, and 8.5 of Chapter 8 are modified with permission from a manuscript which has been accepted for publication in *Human Brain Mapping*, on which I am the first author.

Co-author contributions:

Simon Ducharme: Data collection (GENFI), study supervision, review and editing of the manuscripts.

Yasser Iturria-Medina: Assistance with image processing, statistical analyses, review of the manuscripts.

GENFI Principle Investigators*: GENFI study design and data collection, review of the manuscript.

*Barbara Borroni, Raquel Sanchez-Valle, Fermin Moreno, Robert Laforce Jr, Caroline Graff, Matthis Synofzik, Daniela Galimberti, James B Rowe, Mario Masellis, Maria Carmela Tartaglia, Elizabeth Finger, Rik Vandenberghe, Alexandre de Mendonça, Fabrizio Tagliavini, Isabel Santana, Chris Butler, Alex Gerhard, Adrian Danek, Johannes Levin, Markus Otto, Giovanni Frisoni, Roberta Ghidoni, Sandro Sorbi, Lize C. Jiskoot, Harro Seelaar, John C. van Swieten, Jonathan D Rohrer.

Additional Contributions:

Melissa Savard: Assistance with processing of diffusion weighted imaging tractography used in Chapter 7.

Robert Baumeister: Assistance with and review of the methodology in Chapter 7.

Chapter 1

Introduction

1.1 Overview of the problem – general context

Dementia is a major global health challenge, with more than 40 million people currently living with dementia worldwide, a number that is expected to grow dramatically as the population continues to age (Nichols et al., 2019; Prince et al., 2013). While much attention has focused on Alzheimer's disease (AD), other less common causes of dementia remain poorly understood. Frontotemporal dementia (FTD) is relatively rare in the overall population, but is one of the most common forms of early-onset dementia, occurring with similar frequency to AD in people under the age of 65 (Onyike & Diehl-Schmid, 2013). The majority of cases occur between the ages of 40-70, although up to 25% of cases occur in those over 65 (Onyike & Diehl-Schmid, 2013). FTD presents with unique challenges because of its young age of onset, as affected individuals are often still working and caring for children, and results in a substantial economic burden (Galvin et al., 2017).

FTD is currently difficult to diagnose, as validated diagnostic methods are inadequate, particularly in the early stages. The overlap between symptoms of FTD and other better known conditions (most significantly, behavioural changes seen in FTD and those seen in primary psychiatric disorders) often results in erroneous diagnosis and prolonged periods of uncertainty for patients and their families, which can last more than three years (Woolley et al., 2011). While there are several promising candidates in development (Tsai & Boxer, 2016), there are currently no disease-modifying treatments for FTD. The ability to enroll very early stage FTD patients and

accurately monitor and predict disease progression in these individuals is extremely important for the success of any clinical trial of a potential disease-modifying treatment.

There is therefore a critical need for improved methods of diagnosis and disease monitoring in FTD, but advancements have been limited. One likely reason is disease heterogeneity; FTD is best described as a group of related disorders, which encompass multiple clinical, genetic, and pathological variations, complicating diagnosis and making it difficult to accurately identify those individuals with similar disease progression, who may benefit from the same treatment. Furthermore, neurodegenerative disorders such as FTD progress for years, potentially decades, prior to the emergence of clinical symptoms. Individuals therefore need to be identified and targeted for disease-modifying treatments while still in this presymptomatic phase when irreversible neuronal damage is minimal and further progression can be prevented.

For these reasons, the development of improved biomarkers (indicators of specific changes that characterize the disease in question) is highly relevant to aide in early diagnosis and treatment. The lack of validated biomarkers for FTD means a difficulty in diagnosing and monitoring early-stage disease, both clinically and in future clinical trials of disease-modifying treatments. Sensitive biomarkers which characterize the full spectrum of FTD across the disease course, from presymptomatic stages to clinical FTD, are therefore essential.

1.2 Objectives

A promising tool which is already routinely used in clinical practice to aid in FTD diagnosis is magnetic resonance imaging (MRI). With advancements in image processing techniques, MRI-based measures of structural and functional brain changes have been investigated extensively in recent years as potential biomarkers. Furthermore, computational models including discriminative

machine learning methods and disease progression modelling are emerging technologies for aiding in the diagnosis and monitoring of neurodegenerative diseases. These methods mean the ability to detect data-driven biological patterns in FTD, across multiple potential biomarkers in combination. The overall objective of this thesis is therefore to explore the use of computational methods in the application of MRI techniques as early-stage biomarkers in FTD. Specific objectives from each chapter that constitute original research are described below.

Chapter 3 describes a systematic review of the literature on the use of morphometric MRI techniques on an individual level in the diagnosis of FTD. Morphometric MRI has found distinct patterns of atrophy in FTD; applying techniques to discriminate between subjects on an individual level could provide necessary assistance to clinicians in the differential diagnosis of FTD, particularly in the early disease stages. These methods have been widely studied, typically using discriminative machine learning methods, yet have not made it into clinical practice. A systematic review of these studies was conducted to evaluate the current state of this research and determine if the methods have clinical utility.

Chapters 5, 6, and 7 present two different models of multifactorial biomarker progression throughout presymptomatic and symptomatic FTD using genetically at-risk individuals, while Chapter 4 describes the participants and image processing methods used in these analyses. Asymptomatic individuals who carry FTD-causing genetic mutations will eventually develop the clinical disease. Genetic FTD therefore provides a unique opportunity to study the presymptomatic disease stage. Existing research focuses on single MRI measures; there is a lack of models incorporating multiple measures in an integrative framework, an important step to develop data-driven biomarkers of early stage FTD.

Chapter 5 describes the application of a data-driven unsupervised machine learning model

for staging disease to presymptomatic and symptomatic individuals with genetic FTD. High variance in structural and functional MRI metrics across clinical and genetic FTD variants, both symptomatically and in presymptomatic gene carriers, makes these single measures less effective to stage the disease in individuals. Unifying biomarkers which can accurately stage FTD cases across the full disease course, despite heterogeneity, are therefore needed.

Chapter 6 describes an extension of the unsupervised machine learning model from Chapter 5 to data-driven subtyping of genetic FTD. The ability to predict subsets of individuals with similar disease progression patterns would open the possibility of improving future clinical trials by selectively enrolling a more homogeneous group of participants who may benefit from the same treatment.

Chapter 7 describes the application of a multifactorial causal model to genetic FTD, to identify in a data-driven way the earliest changes in MRI-based biomarkers in preclinical and early clinical stages. Studies of MRI-based biomarkers in presymptomatic genetic FTD suggest a possible pattern of brain changes prior to symptom onset, however research typically assumes biomarker independence. No studies to date have attempted to characterize the interactive spreading of multiple factors throughout the brain during disease progression. The model used in this analysis allows the data-driven exploration of multiple interacting biological factors. Knowledge gained from these types of models can aid the development of sensitive biomarkers.

Chapter 2

Review of the literature

2.1 Overview of FTD

Frontotemporal dementia (FTD) is a neurodegenerative disease presenting most commonly with changes in behaviour, language and/or cognition. FTD has a relatively fast rate of decline, but progression varies widely across individuals (Garcin et al., 2009; Onyike & Diehl-Schmid, 2013). FTD is an umbrella term describing a heterogeneous group of diseases that are associated with degeneration of the frontal and/or temporal lobes, referred to as frontotemporal lobar degeneration (FTLD). It encompasses a variety of clinical, pathological, and genetic variants.

There are two main clinical syndromes: behavioural variant FTD (bvFTD) and primary progressive aphasia (PPA). bvFTD is the most common syndrome and presents with personality changes such as apathy, loss of empathy, and disinhibition (Rascovsky et al., 2011). Primary progressive aphasias (PPA) are associated with language deficits. PPA is further divided into three variants - semantic (svPPA), nonfluent (nfvPPA), and logopenic (lvPPA) (Gorno-Tempini et al., 2011). Patients can also develop concomitant parkinsonism or motor neuron disease (MND), so that the clinical spectrum of FTLD includes amyotrophic lateral sclerosis (ALS), progressive supranuclear palsy (PSP), and corticobasal syndrome (CBS). FTD is associated with abnormal accumulation of one of several misfolded proteins; the most common being microtubule-associated protein tau and transactive response DNA-binding protein with molecular weight 43 kDa (TDP-43), and, less commonly, fused in sarcoma (FUS) protein (Rademakers et al., 2012). FTD also has a significant genetic component. Up to one third of cases are caused by an autosomal-dominant genetic mutation, with the majority being caused by mutations in progranulin *(GRN)*,

microtubule-associated protein tau *(MAPT)* and expansions of chromosome 9 open reading frame 72 *(C9orf72)* (Rademakers et al., 2012).

The complexity of FTD is exacerbated by the lack of clear correspondence between clinical, pathological, and genetic variations (Figure 2.1). Clinical presentation reflects regional patterns of neurodegeneration; the underlying pathology cannot be accurately predicted by clinical syndrome. Some clinical syndromes are more commonly associated with a specific underlying pathology, such as svPPA and FTD with MND (called FTD-MND or FTD-ALS) with TDP-43 (Josephs et al., 2011). lvPPA, while frequently classified under the umbrella of FTD clinical syndromes, is most commonly an atypical form of Alzheimer's disease (AD) in terms of pathology (Gorno-Tempini et al., 2011). bvFTD, however, does not have a strong association with a single pathology. Unlike sporadic cases, FTD caused by genetic mutations have predictable underlying pathology; GRN mutations and C9orf72 expansions have TDP-43 pathology while MAPT mutations are associated with tau pathology. While some clinical presentations are associated with specific genotypes, such as ALS with C9orf72 expansion, correlations between genotype and phenotype are generally poor (Lashley et al., 2015). The most common clinical presentation in all genetic forms is bvFTD, but all phenotypes can occur (Lashley et al., 2015).

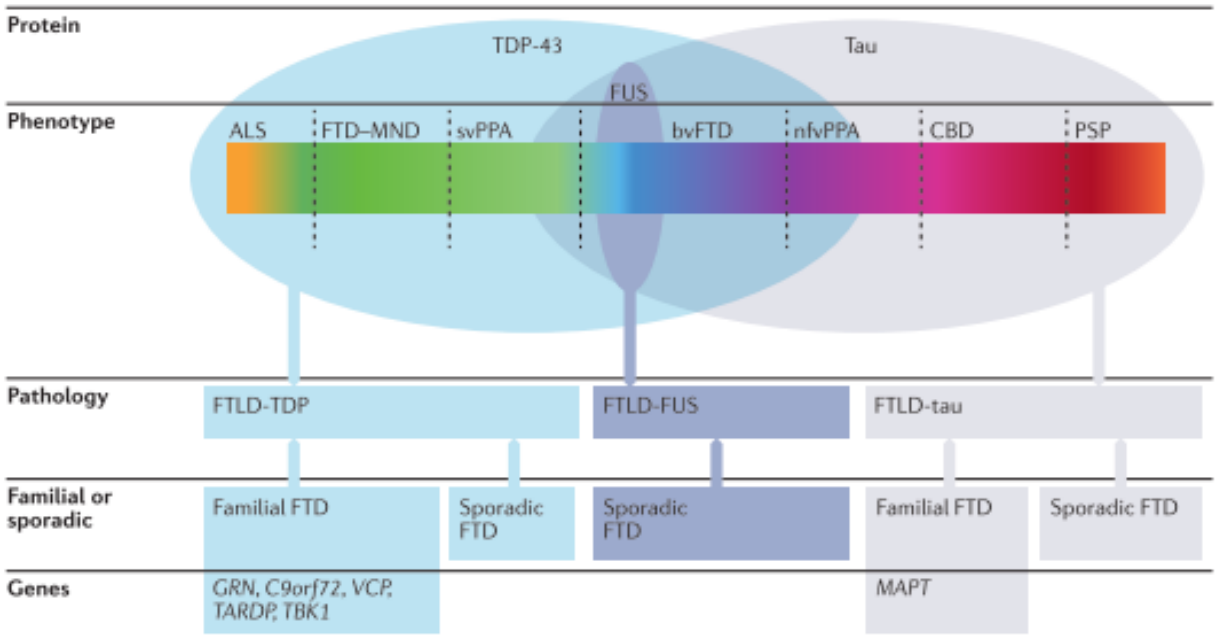

Figure 2.1: Relationship between clinical, genetic, and pathological FTD variants. Genetic forms of FTD have predictable pathology: GRN mutations and C9orf72 repeat expansions result in TDP-43 pathology, whereas MAPT mutations result in tau pathology. By contrast, variable underlying pathologies and genetic forms are found across the clinical spectrum of FTD. VCP, TARDP and TBK1 are rare FTD-causing genes. bvFTD = behavioural variant FTD; CBD = corticobasal degeneration; FUS = RNA-binding protein FUS; nfvPPA = nonfluent variant primary progressive aphasia; PSP = progressive supranuclear palsy; svPPA = semantic variant primary progressive aphasia; TDP-43 = transactive response DNA-binding protein 43. Figure and caption adapted with permission from (Meeter et al., 2017).

2.2 Clinical diagnosis

FTD is currently a major challenge to diagnose. FTD symptoms overlap considerably with primary psychiatric disorders and other dementias (Ducharme et al., 2015). The diagnosis of bvFTD is especially difficult in the real-life context of patients presenting with adult-onset (i.e., more than 40 years old) behavioral changes. Evidence suggests as many as 50% of people with bvFTD are initially diagnosed with a primary psychiatric disorder (Woolley et al., 2011). Standard neuropsychological test batteries of cognitive performance are unreliable to distinguish between

the two groups (Vijverberg et al., 2017). Furthermore, significant memory impairment can exist in bvFTD, comparable to that seen in AD, particularly in individuals with an older age of onset (Bertoux et al., 2014; Mansoor et al., 2015).

Current diagnostic guidelines include the use of structural MRI for visualization of atrophy in frontal and temporal brain regions and PET using a 18 F-fluorodeoxyglucose tracer (FDG-PET) for visualization of abnormalities in metabolism (Gorno-Tempini et al., 2011; Rascovsky et al., 2011). However, these methods are insufficient in the early stages; in a mixed neuropsychiatric population that is representative of clinical practice, a standard MRI with visual review had insufficient sensitivity (70%) to identify cases of bvFTD at baseline, while specificity of FDG-PET was poor (68%) (Vijverberg et al., 2016). There is no FTD equivalent to the concept of mild cognitive impairment, a clinical syndrome which often represents an early phase of AD, and helped transform diagnosis and treatment in that disease (Rosen et al., 2020). Although attempts have been made to define an MCI-like stage in FTD (Ismail et al., 2017; Jiskoot et al., 2019), these definitions do not capture the full range of clinical symptoms, including early stage PPA, and the prognostic value of this concept has not been established (Rosen et al., 2020).

2.3 FTD biomarkers

Over the past two decades, considerable efforts have been made to develop sensitive biological markers of FTD. Ideally, biomarkers should precisely and reliably detect a fundamental feature of the disease using a procedure that is inexpensive, noninvasive, and easy to perform (Meeter et al., 2017). Diagnostic biomarkers need to distinguish between FTD subtypes and non-FTD disorders, as well as between clinical, genetic, or pathological subtypes, while staging biomarkers need to monitor disease progression across the full disease course, and encompass the

substantial heterogeneity in FTD (Meeter et al., 2017). To date, validated biomarkers for diagnosis and disease monitoring remain limited (Meeter et al., 2017).

Potential biomarkers in neurodegenerative diseases include those derived from imaging (typically MRI and PET) and fluid-based methods (cerebrospinal fluid (CSF) and blood derived biomarkers). Validated diagnostic biomarkers in AD (including CSF and PET amyloid tracers) can be used in the differential diagnosis of FTD from AD, as FTD will likely be negative for these (Meeter et al., 2017), however FTD-specific CSF biomarkers or tau tracers are not currently available. Much research has focused on MRI-based biomarkers; MRI is non-invasive, is less costly than alternatives such as PET, and is already used regularly in clinical practice. MRI studies in FTD have focused on measures of grey matter atrophy, diffusion tensor imaging, and resting-state fMRI.

2.4 MRI changes in clinical FTD syndromes

2.4.1 Grey matter atrophy

Grey matter structural changes have been most frequently studied as potential FTD biomarkers using T1-weighted MRI. Quantitative morphometric MRI techniques, most commonly grey matter volume and cortical thickness, have demonstrated specific patterns of frontal and temporal grey matter atrophy on a group level in FTD clinical syndromes (Meeter et al., 2017) (Figure 2.3). This is distinct from psychiatric disorders such as depression and anxiety disorders, in which no clinically significant cortical atrophy is expected. These patterns also differ from those seen in other dementias (such as hippocampal atrophy found in AD). BvFTD is associated with atrophy primarily in the frontal lobe, insula, anterior cinguate cortex and basal ganglia (Meeter et al., 2017; Pan et al., 2012; Schroeter et al., 2014). PPA is primarily associated with left-sided

atrophy (the language dominant hemisphere) in the initial disease stages; nfvPPA with inferior frontal and insular atrophy, svPPA with anterior temporal atrophy, and lvPPA with posterior temporal and parietal atrophy (Bisenius et al., 2016; Meeter et al., 2017; Mesulam et al., 2009; Rogalski et al., 2014).

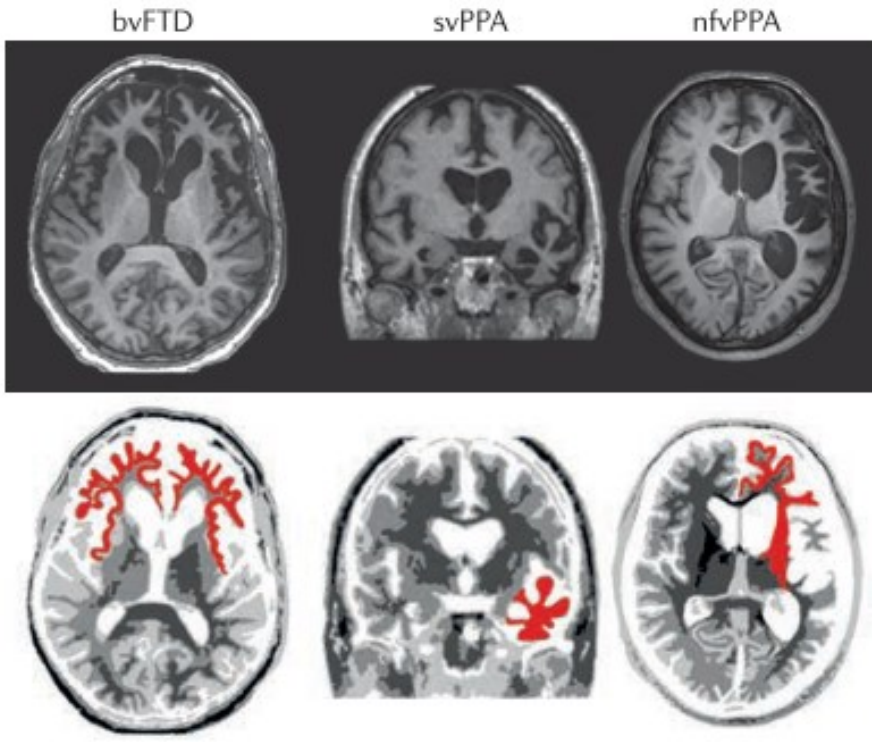

Figure 2.2: Grey matter atrophy in clinical syndromes of FTD. Characteristic group-level patterns of grey matter atrophy (highlighted in red) in different clinical subtypes of FTD. Atrophy is typically found in frontal, insular and anterior cingulate regions in bvFTD, left-sided temporal atrophy is typically seen in svPPA, and left frontal and insular atrophy is typically found in nfvPPA. Figure and caption adapted with permission from (Meeter et al., 2017).

2.4.2 Diffusion tensor imaging

Diffusion tensor imaging (DTI) has typically been used to measure white matter changes. DTI uses the directional diffusion of water to obtain metrics of microstructural integrity, most commonly fractional ansiotrophy (FA) and mean diffusivity (MD), based on the idea that water

diffuses differently depending on tissue type, integrity, and the presence of barriers (Soares et al., 2013). In white matter water tends to diffuse directionally along the axon (anisotropic). In grey matter diffusion is less anisotropic and in CSF is unrestricted in all directions (isotropic) (Soares et al., 2013). A decrease in FA and increase in MD is expected with neurodegeneration. White matter changes mirror grey matter atrophy patterns in FTD but extend beyond these regions, with overlapping patterns found in each clinical syndrome, most consistently identifying tracts in the frontal and temporal regions including the uncinate fasciculus, cingulum bundle, corpus callosum and superior and inferior longitudinal fasciculi (Agosta et al., 2012, 2015; Lam et al., 2014; Mahoney et al., 2013, 2014, 2015; Schwindt et al., 2013; Tu et al., 2015; Whitwell et al., 2010; Zhang et al., 2013). The more widespread changes in white matter indicate that white matter changes could precede grey matter atrophy or that white matter DTI measures may simply be a more sensitive biomarker. DTI has been infrequently studied in grey matter, but one study found patterns of grey matter microstructure alterations (seen via increases in MD) mirrored volumetric grey matter atrophy in the clinical syndromes (Whitwell et al., 2010).

2.4.3 Resting-state fMRI

Changes in spontaneous neural activity have frequently been measured using resting-state functional MRI (fMRI). fMRI uses blood oxygen level–dependent (BOLD) contrast imaging to measure localized increases in oxygenated blood flow, which are coupled with increased neural activation (Lv et al., 2018). Most research focuses on changes in functional connectivity, which measures the correlation of spontaneous fluctuation in the BOLD signal between different brain regions. This method has identified several brain networks, formed from regions which are said to be functionally connected when they exhibit correlated fluctuations (Lv et al., 2018). Changes have been detected in the salience network in bvFTD and semantic variant PPA, a brain network

involved in emotional processing, which includes the insula and the anterior cingulate cortex. While several studies report decreased connectivity in this network (Barbara Borroni et al., 2012; Farb et al., 2013; Filippi et al., 2013; Whitwell, Josephs, et al., 2011; Zhou et al., 2010), some studies have found no change or increased connectivity (Hafkemeijer et al., 2015; Rytty et al., 2013). Changes in measures of regional functional activity have also been identified, including in fALFF (fractional amplitude of low frequency fluctuations), which measures signal strength within brain regions (Zou et al., 2008). Alterations in fALFF have been detected in the insula of individuals with bvFTD and svPPA (Day et al., 2013; Farb et al., 2013).

2.5 The presymptomatic phase

It is now understood that the neurodegenerative disease process begins many years before symptom onset, with the symptomatic period representing the later stages of the disease. For instance, brain atrophy and changes in amyloid and tau were detected in familial AD up to 25 years before expected symptom onset (Bateman et al., 2012). This presymptomatic phase is widely considered to be the ideal time for intervention, when irreversible neuronal loss is minimal and clinical function is still preserved (Rohrer et al., 2015). The failure of several clinical trials in mild to moderate stage AD (Salloway et al., 2014) further indicates the importance of targeting the presymptomatic and early symptomatic phases for disease prevention. The development of CSF and PET amyloid tracers has proven massive for AD diagnosis and treatment (Cohen et al., 2019) and allows for the targeting of asymptomatic individuals at high risk of developing clinical AD.

Research into these preclinical biomarkers has led to the development of neurodegenerative disease progression models which suggest low rates of change in biomarkers in the presymptomatic phase which accelerate near the start of the symptomatic phase (Rosen et al., 2020), including the highly cited observational model of AD progression (Jack et al., 2013), which

hypothesized the trajectories of the most commonly researched biomarkers over the disease course. This type of biomarker progression model has been applied to other neurodegenerative disorders, including FTD (Figure 2.2). However, while knowledge of this presymptomatic stage has become more frequently studied in recent years (reviewed in the next sections), no presymptomatic biomarkers of FTD are currently available.

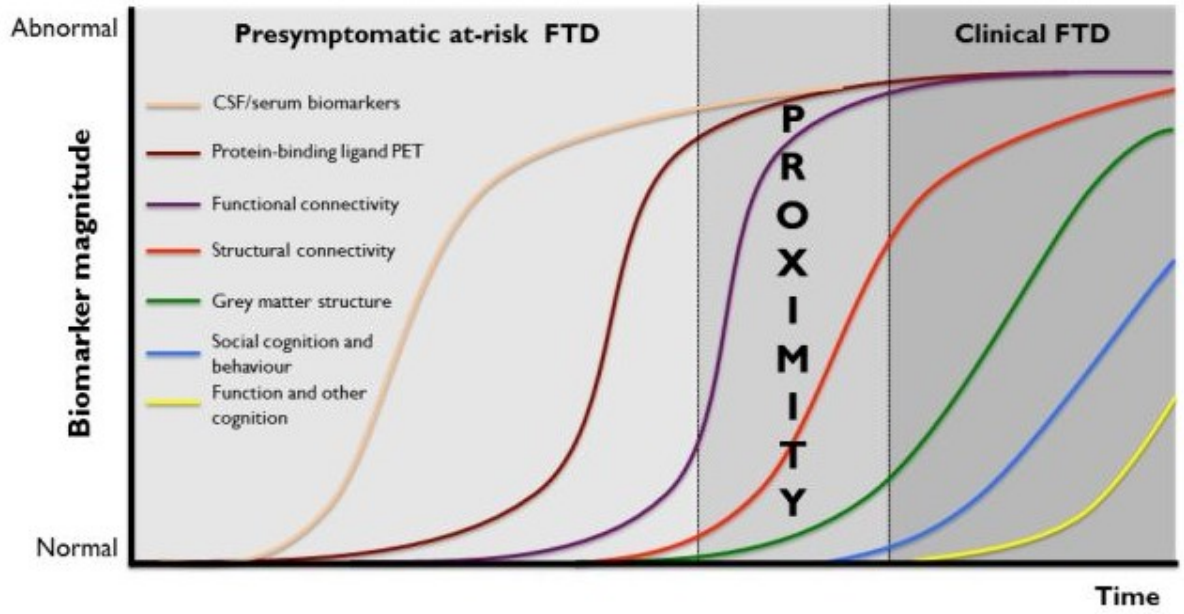

Figure 2.3: Hypothetical model of biomarker progression in FTD. CSF and PET based biomarkers are hypothesized to become altered first, followed by MRI changes, with functional changes preceding structural changes (structural connectivity is referring to white matter microstructural changes). Finally, behavioural/cognitive impairment begins to immerge. Figure adapted with permission from (Gordon et al., 2016).

2.6 Genetic FTD

Knowledge of the brain changes occurring in the earliest disease stages is an important step in the development of early-stage biomarkers, but knowledge of the presymptomatic and early symptomatic stages remains limited in FTD. Genetic FTD provides an opportunity to study the presymptomatic stage which is not available in sporadic FTD; the most common FTD-causing

genetic mutations (*C9orf72, GRN or MAPT*) have near to full penetrance (Rademakers et al., 2012), meaning asymptomatic individuals who carry the genetic mutation will eventually develop symptoms. Studying genetic FTD is difficult due to the relative rarity of these conditions, and studies were initially limited by small sample sizes. In recent years, several large multi-site studies have been undertaken, including the genetic frontotemporal dementia initiative (GENFI) in Canada and Europe, and ARTFL/LEFFTDS in the United States. Several studies have shown MRI-based changes in presymptomatic and symptomatic gene carriers compared to non-carriers, most frequently in grey matter atrophy, but also in white matter alterations and functional activity.

2.6.1 Grey matter atrophy

Differing pattern of grey matter atrophy have been found in the three most common genetic variants of FTD, extending beyond the typical frontal/temporal pattern found in sporadic FTD (Figure 2.4A); C9orf72 expansion carriers show an especially widespread pattern of grey matter atrophy, encompassing noncortical regions including the thalamus and cerebellum, GRN mutation carriers show asymmetrical patterns of atrophy extending into the parietal lobe, and MAPT mutation carriers show a more focal pattern of temporal lobe atrophy (Fumagalli et al., 2018; Lee et al., 2014; Mahoney et al., 2012; Rohrer et al., 2010; Sha et al., 2012; Whitwell et al., 2012). Intersecting regions of atrophy have been found in the insula, orbitofrontal lobe, and anterior cingulate in all three groups (Cash et al., 2018). Fastest rates of atrophy have been found in GRN, while a very slow progressing group of C9orf72 has been observed (Whitwell et al., 2015).

Similar patterns were found to a lesser extent in presymptomatic gene carriers (Cash et al., 2018). Regional volume loss has been detected starting at least 10 years prior to the estimated onset of symptoms in the GENFI dataset (Rohrer et al., 2015) (Figure 2.4B). Earliest changes were

found in the C9orf72 expansion group; subcortical atrophy was detected up to 25 years before expected onset, followed by frontal and temporal lobe atrophy, and subsequently cerebellar atrophy. In GRN mutation carriers atrophy started in the insula, followed by the temporal and parietal lobes, and the striatum. In MAPT carriers atrophy began in the hippocampus and amygdala, followed by the temporal lobe and insula. In the ARTFL/LEFFTDS study, individual atrophy maps were able to separate presymptomatic from mild symptomatic subjects and predict conversion to symptomatic (Staffaroni, Cobigo, et al., 2020). Grey matter atrophy has been inconsistently detected in single site studies, with some studies detecting atrophy (Lee et al., 2017; Olm et al., 2018; Panman et al., 2019; Papma et al., 2017; Pievani et al., 2014) and others not (B. Borroni et al., 2008; Barbara Borroni et al., 2012; Dopper et al., 2014; Feis et al., 2019; Whitwell, Josephs, et al., 2011). Longitudinal studies have found atrophy over time, but again results are inconsistent (Caroppo et al., 2015; Le Blanc et al., 2020; Olm et al., 2018; Panman et al., 2019). A longitudinal analysis of subjects who converted from presymptomatic to symptomatic found steep grey matter volume loss near symptom onset in GRN and MAPT carriers (Jiskoot et al., 2019).

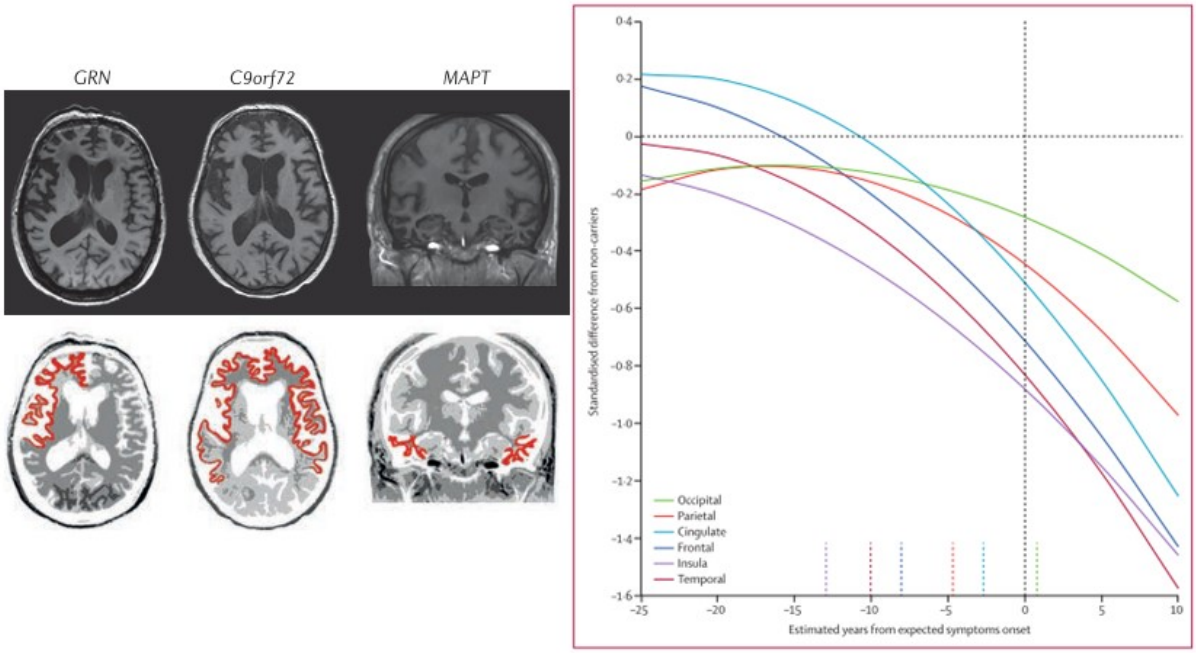

Figure 2.4: Grey matter atrophy patterns in genetic FTD. A) Characteristic patterns of grey matter atrophy (highlighted in red) in each genetic subtype. Patients with GRN mutations often exhibit asymmetrical frontotemporoparietal atrophy. Patients with a C9orf72 repeat expansion present mostly with a generalized symmetrical atrophy. Patients with MAPT mutations exhibit marked symmetrical temporal atrophy. **B)** Standardized difference between all (presymptomatic and symptomatic) mutation carriers and non-carriers in cortical grey matter volumes versus estimated years from expected symptoms onset. Dotted lines on the x-axis show the time at which the upper 95% confidence intervals for each curve crosses zero on the y-axis (i.e., the point at which a significant difference exists between mutation carriers and non-carriers). Figure and caption adapted with permission from (Rohrer et al., 2015) and (Meeter et al., 2017).

2.6.2 White matter changes

DTI metrics found early and widespread white matter alterations in presymptomatic carriers in GENFI up to 30 years prior to the estimated age of onset in the C9orf72 expansion group, primarily in posterior tracts including the posterior thalamic radiation, splenium of the corpus callosum, and posterior corona radiata. (Jiskoot, Bocchetta, et al., 2018). Differing patterns were again found for the three main mutations, with changes occurring later in those with GRN and MAPT mutations. Changes included the uncinate fasciculus and cingulum in MAPT and the

anterior and posterior internal capsule in GRN (Jiskoot, Bocchetta, et al., 2018). Similarly, multiple studies have found presymptomatic changes in DTI metrics, most commonly reduced FA, in each genetic group compared to non-carriers (B. Borroni et al., 2008; Dopper et al., 2014; Floeter et al., 2018; Jiskoot et al., 2019; Lee et al., 2017; Olm et al., 2018; Panman et al., 2019; Papma et al., 2017), although results are again inconsistent (Feis et al., 2019; Panman et al., 2019; Pievani et al., 2014).

2.6.3 Functional activity

Functional changes have been less frequently studied; several single-site studies reported altered functional connectivity in presymptomatic carriers compared to non-carriers most consistently in the salience network (Barbara Borroni et al., 2012; Dopper et al., 2014; Whitwell, Josephs, et al., 2011), with some evidence of gene specific patterns (Lee et al., 2017; Premi et al., 2014), while some studies detected no differences (Feis et al., 2019; Pievani et al., 2014). Others have found altered local activity measures including fALFF in GRN carriers (Premi et al., 2014, 2016).

2.6.4 Cognitive changes

Cognitive impairment has been reported in presymptomatic FTD (Cheran et al., 2019; Jiskoot, Panman, et al., 2018; Papma et al., 2017; Rohrer et al., 2015). Changes in cognitive, behavioural, and neuropsychological tests have been reported in GENFI up to five years prior to estimated onset (Rohrer et al., 2015), with differing patterns in each genetic group. In particular, language and memory decline has been observed in presymptomatic MAPT carriers (Cheran et al., 2019; Jiskoot, Panman, et al., 2018; Olney et al., 2020; Rohrer et al., 2015). In the ARTFL/LEFFTDS study, differences in executive function were found between asymptomatic

carriers and non-carriers (Staffaroni, Bajorek, et al., 2020), as well as some impairment in those with mild/questionable symptoms (Olney et al., 2020).

2.6.5 Suspected pattern/order of change based on these studies

Taken together, there is evidence of common affected regions across genetic variants, (those most commonly seen in symptomatic cases, such as the insula), while specific patterns are observed in each genetic mutation. These patterns frequently extend beyond frontal/temporal regions, (including posterior, subcortical involvement in C9orf72 and parietal involvement in GRN, while MAPT shows more focal temporal involvement). Differing rates of progression are also observed; earlier changes and slower progression observed in C9orf72 expansions, while GRN and MAPT mutations lead to steeper declines.

Several studies report alterations in fMRI and DTI metrics in the absence of grey matter atrophy (B. Borroni et al., 2008; Dopper et al., 2014; Papma et al., 2017; Whitwell, Josephs, et al., 2011), suggesting that these may be more sensitive biomarkers in the early disease stage. However, this is not a consistent finding (Feis et al., 2019; Lee et al., 2017; Pievani et al., 2014). These studies are limited by small sample sizes and variability in included subjects; they typically do not account for subject disease stage. Regression against the estimated years to symptom onset (EYO; calculated as the participant's age minus the mean age of symptom onset in their relatives) in the GENFI cohort suggests white matter changes preceding grey matter (Jiskoot, Bocchetta, et al., 2018; Rohrer et al., 2015), while grey matter atrophy was detected earlier than clinical changes (Rohrer et al., 2015). In another study asymptomatic mutation carriers performed similarly to non-carriers on all clinical measures but had decreased frontal and temporal lobe volumes (Olney et al., 2020). DTI metrics performed best at single subject classification of a combined group of gene carriers from non-carriers, over grey matter and fMRI changes (Feis et al., 2018).

Together these results indicate a potential sequence of degeneration, with functional connectivity and white matter integrity preceding grey matter atrophy, followed by cognitive decline, with differing patterns of disease progression in genetic variants. However, few studies have attempted to combine these various brain changes in an integrative model of disease progression.

2.7 Computational models of disease progression

2.7.1 Staging models

Numerous computational models have been developed that attempt to model the complex cerebral changes that are occurring throughout neurodegenerative disease progression (Oxtoby & Alexander, 2017). These models can integrate a variety of clinical and biological data in a data-driven way to estimate disease progression across the full disease time course. They have most frequently been studied in AD (Garbarino et al., 2019; Iturria-Medina et al., 2016; Jedynak et al., 2012; Venkatraghavan et al., 2019; Young et al., 2014). They typically attempt to integrate cross-sectional data from multiple biomarkers, making no a priori assumptions about the structure or relationship of the data (Oxtoby & Alexander, 2017). They usually consider each biomarker independently of one another and attempt to construct the typical trajectory of each over the disease course (Iturria-Medina et al., 2016; Jedynak et al., 2012). The event-based model is one commonly researched approach which estimates the sequence of biomarker changes during disease progression and the uncertainty associated with the ordering. It has been applied to a variety of biomarkers in sporadic and familial AD, Huntington's disease, and familial FTD (Fonteijn et al., 2012; Oxtoby et al., 2017, 2018; Panman et al., 2021; Venkatraghavan et al., 2019; Young et al., 2014). Data-driven models of disease staging have typically included a select number of

biomarkers, such as grey matter atrophy throughout the whole brain, or they include only a small number of brain regions previously shown to be implicated in the disease. Furthermore, they usually assume a single disease trajectory for all subjects.

Frequently, these models are then used to assign an individual stage, or disease severity score, to each subject in the analysis. As such, they provide a data-driven method for monitoring disease progression by combining multiple relevant biological measures into a single disease signature. For example, one study using a self-modelling framework to pool information from various biomarkers in AD found that the individual disease scores assigned by the model correlated strongly with the clinical classifications of AD (Jedynak et al., 2012). Individual subject staging derived from the event-based model has been used to classify individuals with AD from cognitively healthy individuals and to predict conversion to MCI or to AD, with high accuracy (Venkatraghavan et al., 2019; Young et al., 2014).

Few studies have applied data-driven disease progression modelling to FTD. Group-level temporal patterns have been found in grey matter and white matter by regressing against the EYO. This method is limited by the rough accuracy of this measure (Moore et al., 2020). A recent adaptation of the event-based model in GRN presymptomatic and symptomatic mutation carriers found early changes in language and neurofilament light chain, and white matter changes preceding grey matter alterations (Panman et al., 2021). Individual disease severity scores derived from this model could classify symptomatic individuals from presymptomatic individuals with high sensitivity (100%) and specificity (96%). Disease severity scores correlated strongly with EYO ($r=0.95$, $p=0.0003$) and the FTD clinical dementia rating (FTD-CDR: $r=0.84$, $p=0.0189$) for those with a diagnosis of nfvPPA, but not for those with bvFTD. A study combining a variation of the event-based model and clustering found data-driven subtypes that corresponded with genetic

FTD mutations and their temporal progression patterns using lobar grey matter volumes (Young et al., 2018). This study focuses on disease subtyping while accounting for the differing disease stage of each subject but does not analyze individual staging scores for its subjects.

2.7.2 Subtyping models

As mentioned, data-driven disease progression models typically assume a single disease trajectory for all subjects. While such models can lead to a better overall understanding of temporal progression, the assumption that all individuals have the same phenotype is a limitation, particularly in a highly heterogeneous disease like FTD. Studies typically deal with this heterogeneity by focusing on specific clinical or genetic variants, which have broadly distinct patterns of neurodegeneration. Studies of genetic FTD typically focus on the more homogeneous genetic variants individually, due to their predictable pathology. However, patterns overlap and considerable variability exists within groups. One study noted significant variability within genetic groups via analysis of the proportion of subjects with declining grey matter volume in the same voxels, indicating that no one region captures all subjects well (Olney et al., 2020). Differing patterns are also found within genetic groups when all subjects are diagnosed with the same clinical syndrome (Lee et al., 2014; Sha et al., 2012; Whitwell et al., 2012). Those diagnosed with the same clinical syndrome can have different pathological and genetic causes, while those with genetic FTD causing mutations will develop different clinical syndromes, complicating the development of biomarkers of the presymptomatic stage.

The assumption of a single disease trajectory limits the utility of disease progression models for patient stratification. Few studies have attempted to disentangle phenotypical heterogeneity to identify individuals who follow a similar disease trajectory. This would allow for targeting individuals who would potentially respond to similar treatment. It also offers the

possibility of challenging the traditional clinical-based classification of FTD and, even more broadly, dementia; data-driven subtypes may provide more biologically based categories by identifying individuals following a similar disease process, lending itself to more precision-based medicine in dementia.

Unsupervised machine learning, or clustering analyses, offer a data-driven method of subtyping diseases. This type of method has potential to uncover unknown subtypes with similar biological progression in heterogeneous diseases like FTD. Typical subtyping models assume all individuals are at the same disease stage, requiring the a priori staging and selection of subjects. Clustering analyses of bvFTD suggest at least four subtypes based on grey matter atrophy patterns (Ranasinghe et al., 2016; Whitwell et al., 2009). These models only include late-stage individuals who already have a clinical diagnosis, and do not account for disease stage.

A recent study used a combination of disease progression modelling and clustering analysis by iteratively fitting a mixture of staging models based on the event-based model to cluster presymptomatic and symptomatic genetic FTD subjects with different biomarker orderings. They detected four sub-trajectories with common temporal progression patterns based on grey matter lobar volumes. These sub-trajectories corresponded with the three main genetic variants. GRN and MAPT carriers primarily fell into single subtypes, and C9orf72 carriers fell into two subtypes, one with primarily frontotemporal atrophy and one with primarily subcortical atrophy (Young et al., 2018). The ability of this model to identify temporal patterns that map onto genetic groups provides validation of the method, due to the distinct patterns of neurodegeneration observed in these groups. It is further able to uncover individuals with more homogenous trajectories within a known genetic group. As well, it does not need to use a priori staging.

2.7.3 Network-based models

Network-based approaches to disease progression modeling consider the spreading of biological alterations through brain networks, thereby offering a different approach to the understanding of disease progression. These models are based on the network-degeneration hypothesis, which suggests that the disease process begins in one or a small number of brain regions, then spreads through network connections (Drzezga, 2018). Under this hypothesis, the spatial propagation of each neurodegenerative disease should relate to structural, metabolic, and functional neural networks. Misfolded proteins – proteins which do not configure correctly – are known to be associated with various neurodegenerative disease, included tau and TDP-43 in FTD. Neuropathological evidence supports the prion-like hypothesis, which suggests that transneuronal spreading of these misfolded proteins through anatomical networks is the principal cause of neurodegeneration in these diseases. (Frost et al., 2009; Song et al., 2014).

Network-propagation models typically estimate disease progression though either structural or functional networks. Structural connectivity refers to the white matter fiber tracks connecting brain regions, derived from diffusion-weighted imaging, via tractography, while functional connectivity typically refers to regions of correlated temporal activity, as measured by resting-state fMRI. Much of this work has focused on AD, although several studies have looked at FTD as well.

Raj et al. (2012) developed a Network Diffusion Model which modeled disease propagation though structural connections; the increase in diseased fibre tracts from an affected cortical region to another region is a product of the disease concentration in both regions and the strength of the structural connection between the regions (Raj et al., 2012). After application of this model to healthy structural connectivity data, the obtained dissociable connectivity patterns

were found to correspond to grey matter atrophy patterns in both bvFTD and AD.

Seeley et al. (2009) demonstrated that grey matter atrophy patterns of various neurodegenerative disorders, included the clinical syndromes of FTD, mirror distinct functional networks in healthy subjects, by deriving these functional networks from the peak atrophy region in each disease group (Seeley et al., 2009) (Figure 2.5). A follow-up study investigated all atrophied regions in each syndrome as the seed region to derive the functional network, and tested various hypotheses about the manner in which network-based disease patterns occur (Zhou et al., 2012). They identified "epicentres" for each syndrome as those regions whose functional network most resembled atrophy patterns, finding similar regions to the peak atrophied regions found in their previous work. Furthermore, they found the most support for a transneuronal spreading model of disease progression; regions with shorter functional distances to the epicentres had greater atrophy. A recent study identified epicentres as in (Zhou et al., 2012) on a individual level and predicted future atrophy patterns using healthy functional connectomes; they found similar epicentres as previous research and distinct patterns of atrophy in bvFTD and svPPA, but considerable variability across individuals (Brown et al., 2019).

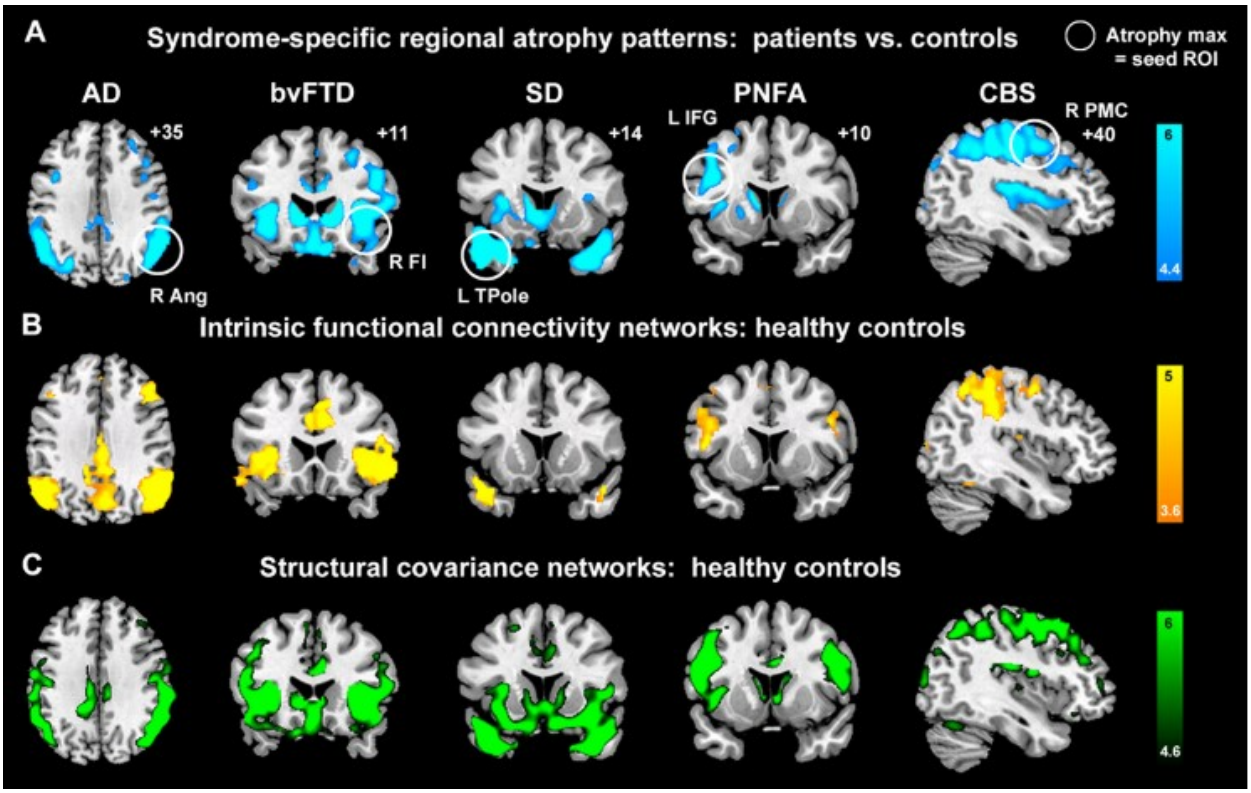

Figure 2.5: Clinical atrophy patterns mirror functional connectivity. A) Five distinct clinical syndromes showed dissociable atrophy patterns, whose peak atrophy regions (circled) provided seed regions for functional connectivity and structural covariance analyses. **B)** Functional connectivity in healthy individuals identified five distinct networks anchored by the five clinical atrophy seeds. **C)** Healthy subjects further showed grey matter volume covariance patterns that recapitulated results shown in (A) and (B). For visualization purposes, results are shown at $p < 0.00001$ uncorrected (A and C) and $p < 0.001$ corrected height and extent thresholds (B). Colour bars indicate t-scores. ANG = angular gyrus; FI = frontoinsula; IFGoper = inferior frontal gyrus, pars opercularis; PMC = premotor cortex; TPole = temporal pole. SD = semantic variant PPA; nfvPPA = nonaffluent PPA; CBS = cortical basal syndrome. Figure and caption adapted with permission from (Seeley et al., 2009).

The epicentres identified in this work correspond with previous research in the FTD clinical syndromes; bvFTD epicentres were identified in the right frontoinsula and the anterior cingulate cortex, regions which are atrophied in bvFTD and which make up parts of the salience network, involved in emotional processing. These regions are therefore hypothesized as initial onset regions of bvFTD; this is supported by evidence of selective loss of von economo neurons (VENs) and fork cells which are concentrated in these regions (Kim et al., 2012; A. F. Santillo et al., 2013;

Alexander F. Santillo & Englund, 2014; Seeley et al., 2006), as well as a higher proportion of TDP-43 inclusions in these cell types seen in bvFTD patients with TDP pathology, which correlates with atrophy in the salience network (Pasquini et al., 2020). However, these epicentres are based on the most atrophied regions in symptomatic disease; they do not necessarily represent the site of initial injury. The identified epicentres of the insula and anterior cingulate cortex correspond with research in genetic FTD, which suggests that these regions show early atrophy across genetic variants (Cash et al., 2018; Rohrer et al., 2015), however these studies also suggest differing patterns across variants, with other regions becoming altered first.

Unlike the data-driven disease progression models discussed in the previous section, network propagation models of disease progression have focused on single factors. They typically attempt to make inferences of an overall disease progression mechanism rather than obtain a disease signature which aims to support diagnosis or staging (Oxtoby & Alexander, 2017). These models have also typically used healthy brain networks and compared them to atrophy patterns in symptomatic individuals (i.e., end stage atrophy patterns), instead of comparing the diseased individuals brain networks to atrophy patterns across the whole disease time course.

While these studies support the spread of neuropathologic effect through network connections, it is unclear whether atrophy patterns are caused by misfolded protein toxicity, or if other factors are involved (Iturria-Medina & Evans, 2015). The current lack of multi-factorial models means that little is known about how various brain changes interact with each other in a causal manner, to influence disease progression.

2.7.4 Disease progression models in combination

The different models discussed in these sections have various purposes. While staging models aim to combine multiple biomarkers to determine the order of changes and obtain individual disease signatures that have direct applications to disease diagnosis and monitoring, network-based models aim more to describe the mechanisms by which disease progression occurs.

Each type of model provides complementary information that, when combined, can provide an integrative picture of disease progression. For example, individual disease staging models can be used with network-based models that require a priori staging. Mechanistic network-based models can also be used with data-driven subtypes to identify underlying biological patterns in more homogeneous groups of individuals. In these ways, disease staging and subtyping models can inform mechanistic network-based models to obtain fully data-driven modelling frameworks.

Chapter 3

Morphometric MRI as a diagnostic biomarker of frontotemporal dementia: a systematic review to determine clinical applicability

This chapter is modified with permission from the published article in *Neuroimage: Clinical* (McCarthy et al., 2018).

3.1 Overview and rationale

Specific patterns of frontal and temporal grey matter and white matter changes have been studied on a group level in clinical FTD. A high discriminative power is needed to differentiate between diseases on an individual level, to be useful in clinical practice. However, with improving methods of morphometric analysis and the use of multivariate statistics and machine learning methods, it is becoming increasingly feasible to improve diagnosis at the individual level. Supervised machine learning methods can use labeled data to differentiate individuals who have a certain disease from those who do not, typically then testing the results in unseen data. An extensive body of literature exists classifying AD in this way. These studies have found overall high accuracy levels when comparing AD to controls (often > 90% accuracy) (Falahati et al., 2014; Rathore et al., 2017). In recent years several studies have attempted this type of classification for the diagnosis of FTD using a variety of MRI measures and machine learning algorithms.

The aim of this systematic review was to summarize the current literature studying the diagnostic classification of FTD utilizing morphometric MRI data on an individual level, with the aim of evaluating its potential usefulness and readiness for clinical practice.

3.2 Methods

This systematic review followed the recommendations of PRISMA (McInnes et al., 2018; Moher et al., 2009) as applicable. An initial search was conducted up to March 12, 2018, using PubMed and PsychINFO with the following search terms: (frontotemporal dementia OR frontotemporal lobar degeneration) AND MRI AND ((diagnostic OR diagnosis) AND (accuracy OR classification OR prediction)). The search was limited to peer-reviewed, full text articles, published in English within the last 10 years (2007 or later) to focus on the most advanced image processing methods. All resulting papers were screened by title and abstract to exclude irrelevant studies, and full texts of selected articles were reviewed. Studies were included if they meet the following criteria: (1) conducted a diagnostic classification of FTD (behavioral or language variant, or both variants combined) versus control subjects or versus other disorders on an individual subject level and (2) used classification features derived from structural MRI, either alone or in combination. In the case of studies which conducted classifications based on MRI morphometry alone and in combination with other methods, only those results pertaining to MRI morphometry were included in this review. Reference lists of included articles were also manually searched to identify other relevant articles. The risk of bias and applicability of each included study was assessed with the QUADAS-2 tool (Whiting et al., 2011).

3.3 Results

The search produced 151 articles. Of these, 25 relevant articles were identified. Cross-reference list searches of each relevant article yielded three additional papers, resulting in a total of 28 papers for inclusion in this review (Fig. 3.1).

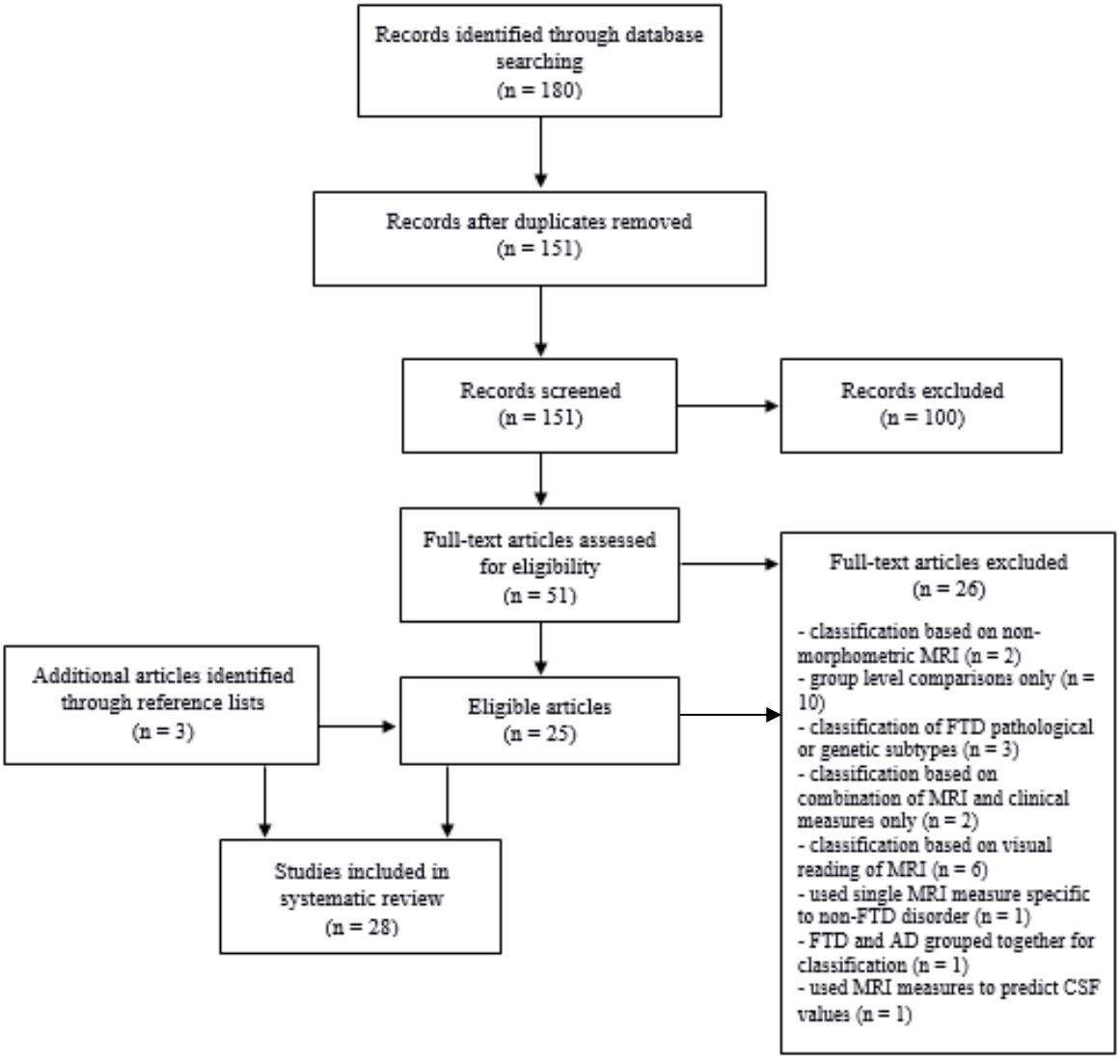

Figure 3.1. PRISMA flow chart of study selection.

3.3.1 Study characteristics

Eleven studies conducted a binary classification of FTD or specifically bvFTD from a control group. Seventeen studies conducted a binary classification of FTD or specifically bvFTD from AD. Six studies conducted a multi-class classification to differentiate FTD, AD and controls, while four studies conducted a multi-class classification between various dementia types and controls. Four studies conducted classifications of PPA; two studies differentiated PPA subtypes from each other and controls. One study classified PPA from controls. One study differentiated FTD subtypes (bvFTD and PPAs) from a combined group of all other subtypes and AD. Results are summarized in Tables 3.1 - 3.5. Accuracy, sensitivity, specificity, and/or area under the receiver operating characteristic curve (AUC) are reported, if provided. In cases where raw numbers were reported, applicable performance measures were calculated from these numbers. In this study we considered performance of 90% or greater as high, 70-90% as moderate, and less than 70% as low.

Studies varied considerably in methodology. The majority of studies looked at changes in grey matter structure, most commonly using voxel-based morphometry (VBM) to assess either grey matter concentration or volume. white matter integrity was commonly assessed using DTI measures. Studies used a variety of whole-brain and region of interest (ROI) based approaches, including a priori selection of ROIs and the use of ROIs that showed significant differences in group-level comparison. Studies also varied widely in classification methods. Machine learning classification techniques were utilized by most studies, the most common being support vector machines (SVM). Most studies used a k-fold cross validation (CV) approach, most commonly with a leave-one-out CV strategy. Only one study used independent subject data (from a different cohort) in a separate testing set (Klöppel et al., 2015).

Almost all studies used a clinically defined diagnosis as the reference standard. Six studies (Chow et al., 2008; Frings et al., 2014; Mahoney et al., 2014; Meyer et al., 2017; Muñoz-Ruiz et al., 2012; Wang et al., 2016) included a subset of patients with pathologically confirmed diagnosis or those with a known genetic mutation consistent with FTD. Three studies (Klöppel, Stonnington, Chu, et al., 2008; Lehmann et al., 2010; Vemuri et al., 2011) used pathologically defined dementia diagnosis as the gold standard. Two studies (Corey T. McMillan et al., 2014; Cory T. McMillan et al., 2012) grouped subjects as AD or FTD based on the presence or absence of CSF biomarkers consistent with AD. Studies also varied considerably in disease severity. Studies report a variety of methods for evaluating disease severity (Mini Mental State Exam, Clinical Dementia Rating, disease duration) making comparison difficult. Four studies used a control group consisting in part or entirely of those with subjective cognitive decline (Dukart et al., 2011; Koikkalainen et al., 2016; Möller et al., 2016; Tong et al., 2017). All others consisted of healthy, cognitively normal subjects. Studies also varied widely in their exclusion criteria. Some studies included FTD with concurrent motor symptoms while others excluded these subjects.

3.3.2 bvFTD vs controls

Five studies classified bvFTD from a control group (Chow et al., 2008; Mahoney et al., 2014; Meyer et al., 2017; Möller et al., 2016; Raamana et al., 2014) (Table 3.1 and Figure 3.2a). In general studies could distinguish FTD from controls with moderate to high accuracy, although results are heterogeneous. Two studies measured grey matter concentration with VBM using a SVM classifier. Meyer et al. (2017) achieved highest accuracy, sensitivity and specificity when using a ROI approach (frontal and temporal lobes – 84.6%, 80.7% and 88.5%, respectively), while Möller et al. (2016) reported low sensitivity (60%) but high specificity (98%) with a whole-brain approach. Mahoney et al. (2014) achieved moderate results using radial diffusivity from DTI. The

highest result was reported by Raamana et al. (2014) using surface displacements of the left lateral ventricle as inputs to a SVM, using a train/test approach (AUC of 0.938, sensitivity of 100% and specificity of 88%) The result was somewhat lower when using leave-one-out CV (AUC of 0.826, sensitivity of 79, specificity of 87). These results contrast with this study's reported results for other regions (right lateral ventricle and left and right hippocampus) in which sensitivity is low. None of the studies classifying the bvFTD subtype from controls looked at different MRI metrics in combination.

3.3.3 FTD vs controls

Six studies classified a combined group of FTD clinical subtypes from a control group (Table 3.2 and Figure 3.2b), again with overall moderate to high accuracy (Bron et al., 2017; Davatzikos et al., 2008; Du et al., 2007; Dukart et al., 2011; Muñoz-Ruiz et al., 2012; Zhang et al., 2013). Davatzikos et al. (2008) reported 100% accuracy when using grey matter and white matter volumetric features derived from principle component analysis as inputs to an SVM, however this study was small (FTD n=12) and may not have used a completely independent test set. Very high results were also reported by Bron et al. (2017) when using grey matter, white matter, or supratentorial brain volume with an SVM (AUC 0.95-0.96). This study did not report sensitivity and specificity numbers. In contrast, Zhang et al. (2013) reported poor results using grey matter or white matter volumes and logistic regression in a ROI approach extracted from group differences, but achieved best results using radial diffusivity (accuracy, sensitivity, specificity, and AUC of 81.4%, 80.7%, 80.5%, 0.877, respectively). Two other studies reported moderately high results using various measures of grey matter structure alone (tensor-based morphometry, volumetry, VBM, cortical thickness) (Du et al., 2007; Muñoz-Ruiz et al., 2012). Only one study (Bron et al.,

2017) assessed a multimodal approach (white matter volume and fractional anisotropy), which achieved a similar result to that by white matter volume alone (AUC 0.95).

3.3.4 bvFTD vs AD

Six studies classified bvFTD from AD (Canu et al., 2017; Frings et al., 2014; Mahoney et al., 2014; Möller et al., 2016; Raamana et al., 2014; Wang et al., 2016) (Table 3.1 and Figure 3.2c). In general, results indicate that this is a much harder task than distinguishing from controls and results are highly variable. Canu et al. (2017) achieved moderately high results using cortical thickness in a random forest approach to distinguish bvFTD from AD (accuracy, sensitivity, and specificity of 82%, 80%, and 87% respectively). These results were not majorly improved when combined with DTI measures. No other study looked at the accuracy of combined MRI metrics. Other studies reported low to moderate accuracy in classifying bvFTD from AD using a range of single metrics including DTI, grey matter concentration, volumetry, and surface displacements (Frings et al., 2014; Mahoney et al., 2014; Möller et al., 2016; Raamana et al., 2014; Wang et al., 2016).

bvFTD					**vs Controls**				**vs AD**			
Name	*Sample*	*Classification*	*Measure*	*ROIs*	*Acc*	*SS*	*SP*	*AUC*	*Acc*	*SS*	*SP*	*AUC*
Canu et al., 2017	27 bvFTD 62 AD	Random forest	Cortical thickness	L inferior parietal Best 5 (L inferior parietal, R temporal pole, L isthmus cingulate, R inferior parietal, R precuneus)					78 82	76 80	83 87	
			DWI	R uncinate, AD Best 5 (R uncinate; AD, RD, MD, FA, Genu of CC; FA)					81 81	96 89	43 61	
			Combination	5 CT + 5 WM tract Best 5 (L inferior parietal, R temporal pole, R precuneus, L isthmus cingulate, L superior parietal)					82 84	76 79	96 81	
Chow et al., 2008	16 bvFTD 30 C	Logistic regression	Volumes	L medial middle frontal parenchymal	87	68.8	96.6					
Frings et al., 2014	15 bvFTD 14 AD	Logistic regression	Volume	caudate caudate + gyrus rectus GM					79 83			
Mahoney et al., 2014	27 bvFTD 25 AD 20 C		DTI-RD	Whole-brain CC L uncinate fasciculus L cingulum bundle		82 93 82 74	80 75 75 70	0.82 0.85 0.82 0.83				0.67
			DTI-FA	Whole-brain L uncinate fasciculus L cingulum bundle CC				0.73		78 77 63 56	68 68 80 80	0.74 0.76 0.67 0.73
			DTI-TD DTI-AD	Whole-brain Whole-brain				0.80 0.74				0.66 0.59
Meyer et al, 2017	52 bvFTD 52 C	SVM LOOCV	VBM-GM density	Whole-brain Frontal lobe Frontal + Basal ganglia & insula Temporal lobe Frontal & temporal lobe Frontal + Temporal + Basal Ganglia & insula	81.7 80.7 82.7 78.8 84.6 84.6	78.9 76.9 80.7 76.9 80.7 80.7	84.6 84.6 84.6 80.8 88.5 88.5					
Möller et al, 2016	26 bvFTD 42 AD 47 C	SVM Training Set LOOCV	VBM-GM density	Whole-brain	75	62	83		81	69	88	

	25 bvFTD 42 AD 47 C		Test Set			85	60	98	0.87	82	64	93	0.81
Raamana et al, 2014	30 bvFTD 34 AD 14 C	SVM	LOOCV	Surface displacements	L Hippocampus R Hippocampus L lateral ventricle R lateral ventricle		14 43 79 64	83 83 87 87	0.488 0.631 0.826 0.755		37 50 60 63	62 41 82 79	0.492 0.456 0.712 0.714
			Train/Test		L Hippocampus R Hippocampus L lateral ventricle R lateral ventricle		50 25 100 75	62 75 88 100	0.562 0.5 0.938 0.875		50 0 75 62	56 1 56 67	0.528 0.5 0.653 0.646
Wang et al., 2016	55 bvFTD 54 AD	Naïve Bayes 10-fold CV		VBM-GM volume	Amygdale, hippocampus, MTL, temporal pole, DLPFC, VMPFC, striatum and insula					51.4	36.4	66.7	

Table 3.1: Classifications of bvFTD versus Controls or AD.

For FTD vs AD classifications, sensitivity is defined as the proportion of correctly classified FTD subjects and specificity as the proportion of correctly classified AD subjects.

bvFTD = behavioral variant frontotemporal dementia, AD = Alzheimer's disease, C = Controls, SVM = support vector machines, CV = cross-validation, LOOCV = leave-one-out cross-validation, VBM = voxel-based morphometry, DWI = diffusion weighted imaging, DTI = diffusion tensor imaging, GM = grey matter, WM = white matter, ROI = region of interest, Acc = accuracy, SS = sensitivity, SP = specificity, AUC = Area under a receiver operator characteristic curve, L = left, R = right, RD = radial diffusivity, FA = fractional anisotropy, MD = mean diffusivity, AD = axial diffusivity, TD = trace diffusivity, MTL = medial temporal lobe, DLPFC = dorsolateral prefrontal cortex, VMPFC = ventromedial prefrontal cortex, CT = cortical thickness, CC = corpus collosum.

3.3.5 FTD vs AD

Eleven studies classified FTD (combined clinical subtypes, pathological subtypes, or CSF-defined) from AD (Bron et al., 2017; Davatzikos et al., 2008; Du et al., 2007; Dukart et al., 2011; Klöppel et al., 2015; Klöppel, Stonnington, Chu, et al., 2008; Lehmann et al., 2010; Corey T. McMillan et al., 2014; Cory T. McMillan et al., 2012; Muñoz-Ruiz et al., 2012; Whitwell, Jack, et al., 2011) (Table 3.2 and Figure 3.2d). Again, results are highly variable. McMillan et al. (2012) reported highest accuracy when using a combination of grey matter density and fractional anisotropy (sensitivity, specificity, and AUC of 87%, 83%, and 0.938 respectively) when distinguishing CSF-defined FTD and AD using regression, although this study did not use an independent testing set. McMillan et al. (2014) also reported moderately high sensitivity, specificity, and AUC (89%, 89%, and 0.874 respectively) to classify CSF-defined FTD and AD when using a combination of cortical thickness and fractional anisotropy in a data-driven approach. In contrast Klöppel, Stonnington, Chu, et al. (2008) reported similar numbers using grey matter volume alone, in a whole-brain approach with an SVM (accuracy, sensitivity, and specificity of 89.2%, 94.7%, and 83.3% respectively), while Whitwell et al. (2011) reported high AUC (0.93) using grey matter volumes of the temporoparietal cortex and hippocampus. Other studies again reported low to moderate accuracy in classifying FTD from AD with a range of different metrics (Bron et al., 2017; Davatzikos et al., 2008; Du et al., 2007; Dukart et al., 2011; Klöppel et al., 2015; Lehmann et al., 2010; Muñoz-Ruiz et al., 2012).

FTD					**vs Controls**				**vs AD**			
Name	*Sample*	*Classification*	*Measure*	*ROIs*	*Acc*	*SS*	*SP*	*AUC*	*Acc*	*SS*	*SP*	*AUC*
Bron et al, 2017	33 FTD 24 AD 34 C	SVM 4-fold CV	VBM-GM volume VBM-WM volume VBM-Supratentorial brain volume DTI-FA VBM-WM volume + DTI-FA	Whole-brain				0.95 0.96 0.95 0.91 0.95				0.78 0.76 0.72 0.80 0.81
Davatzikos et al., 2008	12 FTD 37 AD 12 C	SVM LOOCV	RAVENS-GM and WM volume	PCA	100				84.3			
		Fisher's discriminant Analysis	Volume	hippocampal, ventricular, total brain	75				70.9			
Du et al., 2007	19 FTD 22 AD 23 C	Logistic regression LOOCV	Volume	Frontal Parietal Temporal	89 81 85				79			
			Cortical thickness	Frontal Parietal Temporal	88 82 85				82			
Dukart et al., 2011	14 FTD 21 AD 13 C	SVM LOOCV	GM WM	Whole brain	77.8 77.8				80 74.3			
			GM	ROI (a priori)	85.2				60			
Klöppel et al., 2008	19 FTD 18 AD	SVM LOOCV	GM volume	Whole brain					89.2	94.7	83.3	
Klöppel et al., 2015	12 FTD 122 AD	SVM Separate test set	VBM-GM volume	Whole-brain								0.78
Lehmann et al., 2010	23 FTD 17 AD	SVM 2-level CV	Cortical Thickness	Whole-brain					79.4	91.3	54.5	0.87
McMillan et al., 2012	38 FTD 29 AD	Logistic regression	GM density	Precuneus Posterior cingulated Anterior temporal						82 87 79	79 66 69	0.883 0.890 0.792
			DTI-FA	Corpus callosum						79	59	0.795
			Combination	Corpus callosum, precuneus, posterior cingulated						87	83	0.938
McMillan et al, 2014	72 FTD 21 AD	Linear regression Train/test	Cortical thickness	Data-driven Anatomical						89 100	81 54	0.778 0.802
			Volume	Global GM Global ventricles						65 100	100 65	0.820 0.826

			DTI-FA	Data-driven Anatomical						100 56	46 78	0.808 0.649
			Combination	Data-driven Anatomical						89 78	89 70	0.874 0.742
Muñoz-Ruiz et al, 2012	37 FTD 46 AD 26 C	Regression Train/Test	Volume	Hippocampus	83	80	84		55	55	55	
			TBM	Hippocampus, amygdala, posterior temporal lobe, lateral ventricle in frontal horn, central part and occipital horn, lateral ventricle in temporal horn, gyri hippocampalis et ambiens, anterior cingulate gyrus and superior frontal gyrus.	82	90	77		62	67	56	
			VBM-GM concentration		83	91	77		72	76	67	
			VBM-GM volume		85	89	82		69	71	66	
Whitwell et al., 2011	14 FTD 14 AD	Logistic regression	GM volume	Temporoparietal cortex Hippocampus Temporoparietal cortex + hippocampus								0.81 0.74 0.93
Zhang et al, 2013	25 FTD 19 C	Logistic regression 4-fold CV	VBM-GM volume	ROI1 (B frontotemporal, anterior callosal)	65.7	80.1	48.7	0.665				
				ROI2 (L temporal)	63.9	77.0	46.6	0.722				
				ROI3 (L dorsal frontal)	45.7	74.2	5.4	0.566				
			VBM-WM volume	ROI1	59.2	77.2	34.6	0.627				
				ROI2	58.1	71.5	36.4	0.657				
				ROI3	47.4	79.8	5.3	0.606				
			DTI-RD	ROI1	76.0	79.9	72.3	0.853				
				ROI2	81.4	80.7	80.5	0.877				
				ROI3	67.6	73.3	58.6	0.722				

Table 3.2: Classifications of FTD vs Controls or AD. For FTD vs AD classifications, sensitivity is defined as the proportion of correctly classified FTD subjects and specificity as the proportion of correctly classified AD subjects.

FTD = frontotemporal dementia, AD = Alzheimer's disease, C = Controls, SVM = support vector machines, CV = cross-validation, LOOCV = leave-one-out cross-validation, VBM = voxel-based morphometry, DTI = diffusion tensor imaging, GM = grey matter, WM = white matter, ROI = region of interest, Acc = accuracy, SS = sensitivity, SP = specificity, AUC = Area under a receiver operator characteristic curve, TBM = tensor-based morphometry, PCA = principle component analysis, L = left, R = right, B = bilateral, RD = radial diffusivity, FA = fractional anisotropy.

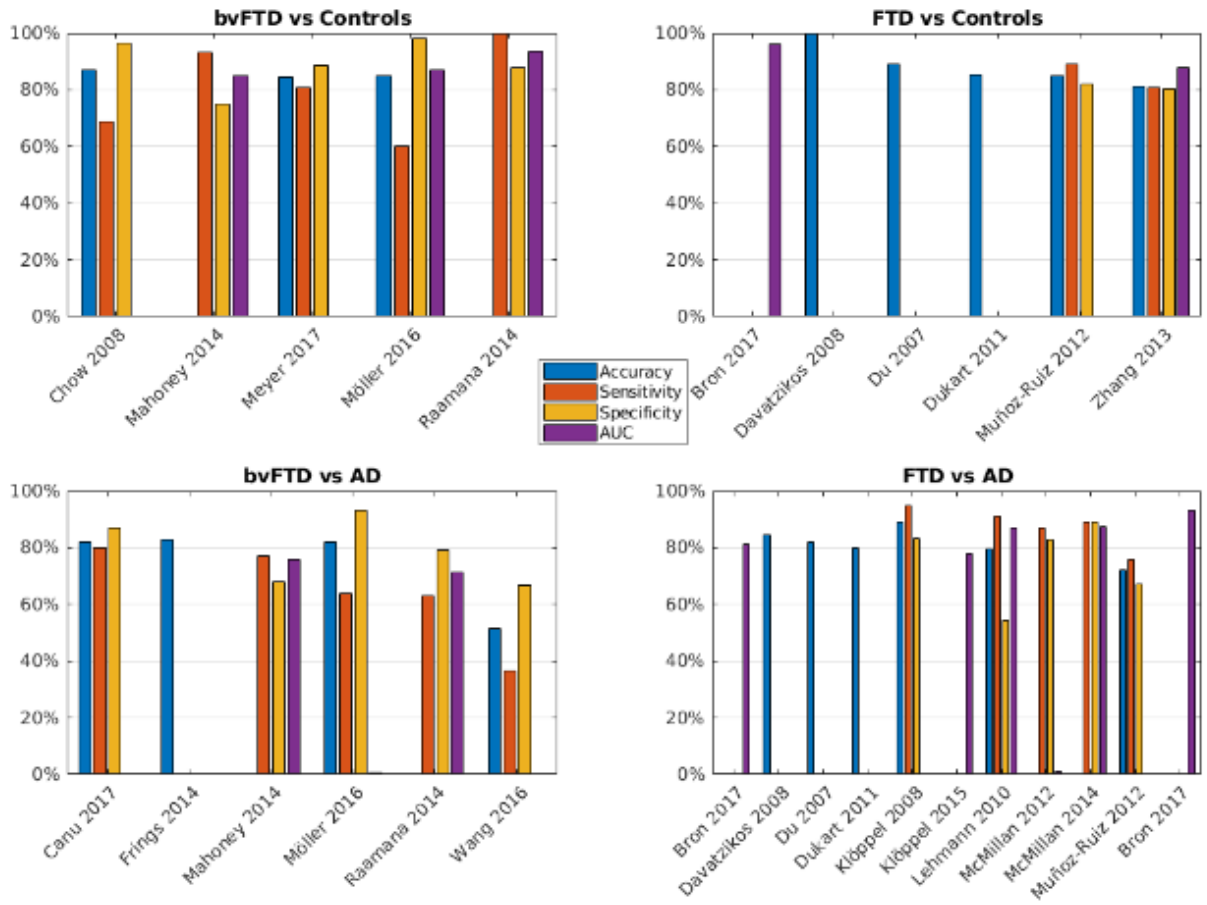

Figure 3.2: Visual representation of the classification accuracy for the different comparisons (for studies which conducted more than one classification, the best result is shown): behavioral variant frontotemporal dementia (bvFTD) vs Controls, frontotemporal dementia (any subtype - FTD) vs Controls, bvFTD vs Alzheimer's disease (AD), FTD (any subtype) vs AD.

3.3.6 Multi-class classifications

Several studies attempted a multi-class classification with varying accuracy. Six studies included a three-way classification between FTD, AD, and controls (Bron et al., 2017; Dukart et al., 2011; Kuceyeski et al., 2012; Möller et al., 2015; Raamana et al., 2014; Wang et al., 2016) (Table 3.3). Kuceyeski et al. (2012) reported the highest accuracy using radial diffusivity, with accuracy and sensitivity of 89.09% and 97.3% but lower specificity (72.22%) using linear discriminant analysis. Results were similar using the LoCo metric, a measurement of the amount

of structural network disruption incurred by a grey matter region for a particular pattern of white matter integrity loss (accuracy, sensitivity, and specificity of 87.27%, 91.89%, 77.78% respectively). Four studies conducted a multi-class classification between various dementias and controls (Klöppel et al., 2015; Koikkalainen et al., 2016; Tong et al., 2017; Vemuri et al., 2011) (Table 3.4). Vemuri et al. (2011) reported moderate sensitivity (84.4%) and high specificity (93.8%) for FTD classification versus all others using whole brain grey matter density approach and a novel classification approach (referred to as differential-STAND), however they did not have a completely independent test set. Results were considerably lower for other studies (Klöppel et al., 2015; Koikkalainen et al., 2016; Tong et al., 2017).

FTD, AD and controls								
Name	*Sample*	*Classification*	*Measure*	*ROIs*	*Acc*	*SS (FTD)*	*SP (FTD)*	*AUC*
Bron et al, 2017	33 FTD 24 AD 34 C	SVM 4-fold CV	VBM-GM volume VBM-WM volume VBM-Supratentorial brain volume DTI-FA VBM-WM volume + DTI-FA	Whole brain				0.85 0.83 0.84 0.83 0.87
Dukart et al., 2011	14 FTD 21 AD 13 C	SVM LOOCV	GM WM	Whole brain	72.9 66.7			
			GM	a priori ROIs	56.3			
Kuceyeski et al, 2012	18 FTD 18 AD 19 C	Linear discriminant analysis LOOCV	GM volume DWI-FA DWI-RD DWI-LD Combination GM + DWI LoCo	Whole-brain parcellation	76.36 76.36 89.09 85.45 83.64 87.27	81.08 72.97 97.30 89.19 91.89 91.89	66.67 83.33 72.22 77.78 66.67 77.78	
Möller et al, 2015	30 bvFTD 39 AD 41 C	Discriminant function analyses LOOCV	1st analysis: VBM-GM volume, Subcortical volumes, DWI-FA	Significant voxels/regions from paired group comparisons	91.4	66.7		
			2nd analysis: VBM-GM volume, subcortical volumes, DWI- AD, DWI-RD		86	75		
Raamana et al, 2014	30 bvFTD 34 AD 14 C	SVM Train/Test	Volumes	L Hippocampus R Hippocampus L lateral ventricle R lateral ventricle				0.5 0.54 0.5 0.5
			Laplacian invariants	L Hippocampus R Hippocampus L lateral ventricle R lateral ventricle				0.5 0.49 0.5 0.59
			Surface displacements	L Hippocampus R Hippocampus L lateral ventricle R lateral ventricle				0.66 0.56 0.76 0.77
Wang et al., 2016	55 bvFTD 54 AD 57 C	Naïve Bayes 10-fold CV	VBM-GM volume	amygdale, hippocampus, MTL, temporal pole, DLPFC, VMPFC, striatum and insula	54.2			

Table 3.3: Multi-class Classifications of FTD, AD, and Controls

FTD = frontotemporal dementia, AD = Alzheimer's disease, C = Controls, SVM = support vector machines, CV = cross-validation, LOOCV = leave-one-out cross-validation, VBM = voxel-based morphometry, DWI = diffusion weighted imaging, DTI = diffusion tensor imaging, GM = grey matter, WM = white matter, ROI = region of interest, Acc = accuracy, SS = sensitivity, SP = specificity, AUC = Area under a receiver operator characteristic curve, L = left, R = right, RD = radial diffusivity, FA = fractional anisotropy, AD = axial diffusivity, LD = longitudinal diffusivity, MTL = medial temporal lobe, DLPFC = dorsolateral prefrontal cortex, VMPFC = ventromedial prefrontal cortex, LoCo = Loss in Connectivity (the percent of WM tracts out of the total connecting to a GM region in a normal control that pass through voxels identified in a WM "injury" map ((Kuceyeski, Zhang, & Raj, 2012).

Multi Dementia Types								
Name	*Sample*	*Classification*	*Measures*	*ROIs*	*Acc*	*SS (FTD)*	*SP (FTD)*	*AUC (FTD)*
Klöppel et al., 2015	12 FTD 122 AD 4 LBD 18 C	SVM Separate test cohort	VBM-GM volume	Whole brain				0.78
Koikkalainen et al, 2016	92 FTD 223 AD 47 LBD 24 VaD 118 C	Disease State Index (DSI) 10-fold CV	Volumes VBM-GM concentration TBM Manifold learning ROI-based grading Vascular burden- WMH, cortical and lacunar infarcts volumes All features	Whole-brain parcellation hippocampus and frontotemporal lobe 	50.4 65.1 64.3 50.4 58.3 32.7 70.6	 62	 95	
Tong et al., 2017	92 FTD 219 AD 47 DLB 24 VaD 118 C	RUSBoost 10-fold CV	Volumes Grading Combination	Whole-brain parcellation	58.6 66.6 70			
Vemuri et al., 2011	47 FTD 48 AD 20 DLB 21 C	Differential-STAND LOOCV	GM density	Whole brain		84.4	93.8	

Table 3.4: Multi-class Classifications of Dementia

FTD = frontotemporal dementia, AD = Alzheimer's disease, C = Controls, LBD = Lewy body dementia, VaD = vascular dementia, CV = cross-validation, VBM = voxel-based morphometry, DWI = diffusion weighted imaging, DTI = diffusion tensor imaging, GM = grey matter, ROI = region of interest, Acc = accuracy, SS = sensitivity, SP = specificity, AUC = Area under a receiver operator characteristic curve, TBM = tensor-based morphometry, WMH = white matter hyperintensities, Differential-STAND = Differential Diagnosis Based on Structural Abnormality due to Neurodegeneration (Vemuri et al., 2011).

3.3.7 PPA subtypes

Four studies included classifications of PPA (Bisenius et al., 2017; Chow et al., 2008; Tahmasian et al., 2016; Wilson et al., 2009) (Table 3.5). Two studies classified each PPA subtype against controls using SVM of grey matter atrophy, with moderate to high accuracy across studies (accuracy ranged from 84-100%) (Bisenius et al., 2017; Wilson et al., 2009). Both studies also classified subtypes against each other, with varying results. Wilson et al. (2009) reported highest accuracy, sensitivity, and specificity (89.1%, 84.4%, 93.8% respectively, AUC of 0.964) to distinguish svPPA from nfvPPA using grey matter volume and a principal component analysis approach. Results were very high for both studies for lvPPA vs svPPA, while Wilson et al. (2009) achieved highest results for lvPPA vs nfvPPA (accuracy, sensitivity, specificity, AUC of 81.3%, 81.3%, 81.3% and 0.879 respectively). Tahmasian et al. (2016) classified each FTD subtype against a group of all others and AD using grey matter volume and SVM, resulting in high specificity (97.5% and 94.2%) but very poor sensitivity (50% and 0%) for both svPPA and nfvPPA vs others, while Chow et al. (2008) combined svPPA and nfvPPA subtypes together in a classification from a control group, achieving moderate sensitivity (78.6%) and high specificity (96.7%).

					nfvPPA vs Controls				**lvPPA vs Controls**				**svPPA vs Controls**			
Name	*Sample*	*Classification*	*Measures*	*ROIs*	*Acc*	*SS*	*SP*	*AUC*	*Acc*	*SS*	*SP*	*AUC*	*Acc*	*SS*	*SP*	*AUC*
Bisenius et al., 2017	16 nfvPPA 17 svPPA 11 lvPPA 20 C	SVM LOOCV	VBM-GM density	Whole-brain ROI (a priori from meta-analyses)	91 84	88 81	94 88	0.94 0.90	95 82	91 82	100 82	0.95 0.91	97 100	94 100	100 100	0.97 1
Wilson et al., 2009	32 nfvPPA 38 svPPA 16 lvPPA 115 C	SVM 2-level CV	GM volume	PCA	89.1	87.5	90.6	0.941	100	100	100	1	100	100	100	1
					svPPA vs nfvPPA				**lvPPA vs svPPA**				**lvPPA vs nfvPPA**			
Bisenius et al., 2017	16 nfvPPA 17 svPPA 11 lvPPA 20 C	SVM LOOCV	VBM-GM density	Whole-brain ROI (a priori from meta-analyses)	78 78	81 81	75 75	0.88 0.87	95 95	100 100	91 91	0.93 0.91	55 64	64 73	45 55	0.59 0.64
Wilson et al., 2009	32 nfvPPA 38 svPPA 16 lvPPA 115 C	SVM 2-level CV	GM volume	PCA	89.1	84.4	93.8	0.964	93.8	93.8	93.8	0.984	81.3	81.3	81.3	0.879
					PPA (svPPA and nfvPPA) vs Controls											
					Acc				*SS*				*SP*			
Chow et al., 2008	14 PPA 30 C	Logistic regression	Volumes	L anterior temporal	90.9				78.6				96.7			

					bvFTD vs others			**svPPA vs. others**			**nfvPPA vs others**		
					Acc	*SS*	*SP*	*Acc*	*SS*	*SP*	*Acc*	*SS*	*SP*
Tahmasian et al, 2015	11 bvFTD 4 svPPA 5 nfvPPA 20 AD	SVM LOOCV	VBM-GM volume	A priori based on the NDH	72.5	45.4	82.7	92.5	50	97.5	82.5	0	94.2

Table 3.5: PPA Classifications

bvFTD = behavioral variant frontotemporal dementia, AD = Alzheimer's disease, C = Controls, nfvPPA = progressive nonfluent aphasia, svPPA = semantic dementia, lvPPA = logopenic progressive aphasia, PPA = primary progressive aphasia, SVM = support vector machines, LOOCV = leave-one-out cross-validation, VBM = voxel-based morphometry, GM = grey matter, ROI = region of interest, Acc = accuracy, SS = sensitivity, SP = specificity, AUC = Area under a receiver operator characteristic curve, PCA = principle component analysis, NDH = Network Degeneration Hypothesis, L = left.

3.3.8 Risk of bias assessment

The results of the QUADAS-2 evaluation are given in Table 3.6. The patient selection domain was rated as high risk of bias in six studies that had inappropriate exclusion criteria (e.g., exclusion for subjects with abnormalities on structural MRI other than atrophy, such as white matter hyperintensities) combined with a case-control design. The index test was rated as high risk of bias in eight studies which did not use separate testing data or used all data to perform ROI selection or dimensionality reduction prior to classification. Two studies were given an unclear risk of bias on this domain. One study was rated as having applicability concerns on the index test domain as it only looked at the overall accuracy of multi-class classification of dementia types.

Study	**Risk of Bias**				**Applicability concerns**		
	Patient selection	*Index test*	*Reference standard*	*Flow and*	*Patient selection*	*Index test*	*Reference standard*
Bisenius 2017	Low	Low	Low	Low	Low	Low	Low
Bron 2017	Low	Low	Low	Low	Low	Low	Low
Canu 2017	High	Low	Low	Low	Low	Low	Low
Chow 2008	Low	High	Low	Low	Low	Low	Low
Davatzikos 2008	Low	Unclear	Low	Low	Low	Low	Low
Du 2007	Low	Low	Low	Low	Low	Low	Low
Dukart 2011	High	Low	Low	Low	Low	Low	Low
Frings 2014	Low	High	Low	Low	Low	Low	Low
Klöppel 2008	Low	Low	Low	Low	Low	Low	Low
Klöppel 2015	Low	Low	Low	Low	Low	Low	Low
Koikkalainen 2016	Low	Low	Low	Low	Low	Low	Low
Kuceyeski 2012	Low	Low	Low	Low	Low	Low	Low
Lehmann 2010	Low	Low	Low	Low	Low	Low	Low
Mahoney 2014	Low	High	Low	Low	Low	Low	Low
McMillan 2012	Low	High	Low	Low	Low	Low	Low
McMillan 2014	Low	Low	Low	Low	Low	Low	Low
Meyer 2017	Low	Low	Low	Low	Low	Low	Low
Möller 2015	High	High	Low	Low	Low	Low	Low
Möller 2016	Low	Low	Low	Low	Low	Low	Low
MuñozYRuiz 2012	High	Unclear	Low	Low	Low	Low	Low
Raamana 2014	Low	Low	Low	Low	Low	Low	Low
Tahmasian 2015	High	Low	Low	Low	Low	Low	Low
Tong 2017	Low	Low	Low	Low	Low	High	Low
Vemuri 2011	Low	High	Low	Low	Low	Low	Low
Wang 2016	Low	Low	Low	Low	Low	Low	Low
Whitwell 2011	Low	High	Low	Low	Low	Low	Low
Wilson 2009	Low	Low	Low	Low	Low	Low	Low
Zhang 2013	High	High	Low	Low	Low	Low	Low

Table 6: QUADAS-2 Evaluation

3.4 Discussion

3.4.1 Summary of results and implications

This systematic review provides a summary of studies attempting to classify FTD from non-FTD via morphometric MRI data with the aim to determine its potential for use as a diagnostic aide in clinical practice. Studies included in this review are highly heterogeneous in terms of subject selection, MRI methodology and classification methods, complicating the comparison of accuracy of results. However, overall studies report good levels of accuracy (see Table 3.7 for a summary of the best performance for each classification), indicating the potential value of MRI morphometry in the diagnosis of FTD.

	Name	Sample	Classification	Measures	ROIs	Acc	SS	SP	AUC
bvFTD vs Controls	Raamana et al, 2014	30 bvFTD 14 C	SVM Train/test	Surface displacements	L lateral ventricle		100	88	0.938
bvFTD vs AD	Canu et al., 2017	27 bvFTD 62 AD	Random forest	Cortical thickness	Best 5 (L inferior parietal, R temporal pole, L isthmus cingulate, R inferior parietal, R precuneus)	82	80	87	
FTD vs Controls	Davatzikos et al., 2008	12 FTD 12 C	SVM LOOCV	RAVENS-GM and WM volume	PCA	100			
FTD vs AD	McMillan et al, 2014	72 FTD 21 AD	Linear regression Train/test	Combination (Cortical thickness & DTI-FA)	Data-driven		89	89	0.874
FTD vs AD & Controls	Kuceyeski et al, 2012	18 FTD 18 AD 19 C	Linear discriminant analysis LOOCV	DWI-RD	Whole-brain parcellation	89.09	97.30	72.22	
FTD vs other dementias	Vemuri et al., 2011	7 FTD 48 AD 20 LBD 21 C4	Differential-STAND LOOCV	GM density	Whole brain		84.4	93.8	
nfvPPA vs Controls	Bisenius et al., 2017	6 nfvPPA 20 C	SVM LOOCV	VBM-GM density	Whole-brain	91	88	94	0.94
lvPPA vs Controls	Wilson et al., 2009	16 lvPPA 115 C	SVM 2-level CV	GM volume	PCA	100	100	100	1
svPPA vs Controls	Bisenius et al., 2017	17 svPPA 20 C	SVM LOOCV	VBM-GM density	ROI (a priori from meta-analyses)	100	100	100	1
	Wilson et al., 2009	38 svPPA 115 C	SVM 2-level CV	GM volume	PCA	100	100	100	1
svPPA vs nfvPPA	Wilson et al., 2009	32 nfvPPA 38 svPPA	SVM 2-level CV	GM volume	PCA	89.1	84.4	93.8	0.964
lvPPA vs svPPA	Bisenius et al., 2017	11 lvPPA 17 svPPA	SVM LOOCV	VBM-GM density	Whole-brain	95	100	91	0.93
lvPPA vs nfvPPA	Wilson et al., 2009	32 nfvPPA 16 lvPPA	SVM 2-level CV	GM volume	PCA	81.3	81.3	81.3	0.879

Table 3.7: Summary of studies with the best performance

For FTD vs AD classifications, sensitivity is defined as the proportion of correctly classified FTD subjects and specificity as the proportion of correctly classified AD subjects.

FTD = frontotemporal dementia, bvFTD = behavioral variant frontotemporal dementia, AD = Alzheimer's disease, C = Controls, nfvPPA = progressive nonfluent aphasia, svPPA = semantic dementia, lvPPA = logopenic progressive aphasia, LBD = Lewy body dementia, SVM = support vector machines, LOOCV = leave-one-out cross-validation, VBM = voxel-based morphometry, DTI = diffusion tensor imaging, GM = grey matter, WM = white matter, ROI = region of interest, Acc = accuracy, SS = sensitivity, SP = specificity, AUC = Area under a receiver operator characteristic curve, PCA = principle component analysis, L = left, R = right, RD = radial diffusivity, FA = fractional anisotropy, Differential-STAND = Differential Diagnosis Based on Structural Abnormality due to Neurodegeneration (Vemuri et al., 2011),

FTD could be diagnosed with high accuracy from control groups, with many studies finding accuracies of over 80% or 90% with good sensitivity and specificity. However, most studies include subjects with well characterized patients in which there is likely already significant atrophy, and therefore the added benefit of morphometry is uncertain. Results distinguishing FTD from AD were somewhat poorer. This is unsurprising given that minimal atrophy is expected in control subjects and that there exists overlap in atrophy patterns between FTD and AD (De Souza et al., 2013). Studies which conducted multi-class classifications did not all report specific sensitivity and specificity values for FTD, although Vemuri et al. (2011) reported good sensitivity and specificity (84.4% and 93.8%) in distinguishing FTD from other dementias. Only four studies specifically classified PPAs, generally with moderate to high accuracy. No studies attempted to distinguish bvFTD patients from those with psychiatric disorders, and these two disorders have been shown to be difficult to distinguish clinically (Woolley et al., 2011). However, it is likely that this distinction will be similar to that of control subjects as no atrophy is expected in most psychiatric disorders other than severe and persistent mental illness, such as schizophrenia with chronic psychotropic treatment, that have been linked to subtle volume loss over time (Andreasen et al., 2011).

Most studies have looked at grey matter atrophy. Fewer studies have used DTI measures, proving mixed results but with some studies suggesting DTI may be more sensitive in the early stages of the disease (Kuceyeski et al., 2012; Zhang et al., 2013). Most studies included in this review only looked at single MRI measures. Hypothetically a multimodal approach combining various MRI modalities such as grey matter structure and white matter integrity should produce more accurate classification than a single modality, as these modalities should provide complimentary information about different aspects of the disease. This is supported by some

studies (Corey T. McMillan et al., 2014; Cory T. McMillan et al., 2012) while others found no improvement when adding white matter to cortical metrics (Bron et al., 2017; Klöppel, Stonnington, Chu, et al., 2008). These differences are likely due to differing patient groups and methodology.

3.4.2 Comparison to visual MRI reading

Currently, FTD diagnosis is usually assisted via visual reading of MRI scans with or without semi-structured visual rating scales in clinical practice. It is therefore important that an effective MRI morphometry-based classification tool improves on current practices.

Klöppel, Stonnington, Barnes, et al. (2008) found that radiologists with different levels of experience varied widely in their ability to distinguish pathologically defined FTD from AD on visual reading of MRI (ranges for accuracy, sensitivity, and specificity were 56.8-83.8%, 55.6-83.8%, and 57.9-90.0% respectively) and generally performed poorer than an SVM classifier of grey matter volume on the same cohort (Klöppel, Stonnington, Chu, et al., 2008). Accuracy was positively correlated with the radiologist's level of experience. Koikkalainen et al. (2016) reported much poorer results (overall accuracy of 46.6%, with a sensitivity of 50% for FTD versus others) when using a disease state index classifier on multiple visual rating scales in the multi-class classification of dementia types compared to their morphometric results.

In a mixed neuropsychiatric population, visual reading of baseline MRIs by neuroradiologists using visual rating scales reported high specificity (93%) but only moderate sensitivity (70%) in distinguishing bvFTD from non-bvFTD, using clinical diagnosis at two-year follow-up as the gold standard (Vijverberg et al., 2016). In a cohort of pathologically defined dementia (Harper et al., 2016), unstructured visual assessment by experienced raters resulted in

moderate sensitivity (82%) and high specificity (99%) in distinguishing FTD from controls, while moderate sensitivity (74%) and specificity (81%) was achieved when distinguishing FTD from AD. These results are comparable with many of the results obtained from morphometry studies. Semi-structured visual rating scales were found to provide comparatively high sensitivity and specificity in distinguishing FTD from controls (82% and 89% using the medial temporal lobe atrophy (MTA) scale, and 89% and 97% when using an SVM on the results of multiple visual rating scales). Visual rating scales resulted in moderate specificity (81% for an orbito-frontal scale, and 88% when using an SVM on the results of multiple visual rating scales) but low sensitivity (55% and 56%) when distinguishing FTD from AD.

Overall, the results from visual radiologists' review appear generally poorer than the best reported results from MRI morphometry studies, indicating the potential usefulness of automated MRI morphometry for improving diagnosis of FTD. However, it is not proven at this point if morphometry outperforms semi-structures visual rating scales (Chow et al., 2011; Harper et al., 2016). It is possible that morphometric approaches could improve diagnostic accuracy in settings where clinicians have less experience in identifying FTD neuroradiological features (Klöppel, Stonnington, Barnes, et al., 2008). A middle ground approach, which provides quantitative morphometric data to clinicians (without applying a classifier) exists as commercial products but has little clinical penetration and the impact on diagnostic accuracy is unclear; this method may provide a more easily interpretable method of aiding clinician's diagnosis (as opposed to the typical black box approach of machine learning classifiers), but would be limited to a single, simple metric such as regional segmentations. Machine learning classification allows for the combination of a large number of morphometric features, which should improve accuracy.

Chapter 4

Disease progression modelling in genetic FTD: methodology

This chapter describes the methodology used in the processing of multi-model MRI data used in the analyses described in Chapters 5, 6, and 7. This chapter is modified with permission from the manuscript "Data-driven staging of genetic frontotemporal dementia using multi-modal MRI" which has been accepted for publication at *Human Brain Mapping*.

4.1 Dataset

These analyses used data from the Genetic FTD Initiative (GENFI; http://www.genfi.org.uk/). GENFI is a large international study gathering longitudinal data on individuals with genetic FTD (C9orf72 expansion, GRN, or MAPT mutations) and their first-degree relatives, which include an equal proportion of asymptomatic carriers and non-carriers. GENFI aims to develop markers which can identify FTD in its earliest stages as well as track disease progression. We used multimodal MRI (volumetric T1 and T2, resting state functional MRI, and diffusion weighted imaging) as well as demographic, clinical and neuropsychological data from the third data release of GENFI2, comprising 690 participants recruited from 23 sites in Canada and Europe. All participants were genotyped at their local site and underwent a standardized clinical assessment which consisted of a medical history, family history, and physical examination (Rohrer et al., 2015). Symptomatic status was based on this assessment, according to established diagnostic criteria (Gorno-Tempini et al., 2011; Rascovsky et al., 2011). Mutation carriers were defined a presymptomatic when clinical criteria were not fulfilled.

4.2 Image acquisition and processing

MRI scans were acquired using 3T scanners, or 1.5T at sites where 3T was not available. Protocols were designed to harmonize across scanners and sites as much as possible (Rohrer et al., 2015).

4.2.1 T1

Volumetric T1-weighted MRI were acquired for 643 subjects. Acquisition parameters (median and ranges) included: slice thickness 1.1 mm (1 to 1.2 mm), repetition time 2000 ms (6.6 to 2400), echo time 2.9 ms (2.2 to 9 ms), flip angle 8 (8 to 11), number of slices 208 (140 to 208). Images were processed following the steps described in (Iturria-Medina et al., 2017). In summary, images were segmented into grey matter, white matter, and CSF probabilistic maps using SPM12. The grey matter maps were normalized to MNI space using DARTEL (Ashburner, 2007) and modulated to preserve the total amount of signal.

4.2.2 T2

Volumetric T2-weighted MRI were acquired for all available subjects (n = 530). Acquisition parameters (median and ranges) included: repetition time 3200 ms (2200 to 3200 ms), echo time 401 mm (75 to 403 mm), slice thickness 1.1 mm (1 to 1.2 mm), flip angle 120 (90 to 120), number of slices 176 (156 to 196). All T2 images were normalized to MNI space using the parameters acquired for the T1 image with the closest acquisition date, using SPM12. T1/T2 ratios were calculated by dividing the T2 image from the T1 image with the closest acquisition date.

4.2.3 Resting-state functional MRI

Resting state fMRI data were acquired for all available subjects (n = 619) using an echo-planar imaging sequence. Acquisition parameters (median and ranges) included: slice thickness 3.5 mm (2.7 to 3.5 mm), repetition time 2500 ms (2200 to 3000 ms), echo time 30 ms (30 to 50 ms), flip angle 80 (80 to 90), number of timepoints 200 (140 to 200). Images were processed following steps outlined in (Iturria-Medina et al., 2017) using tools from SPM12, FSL, and the REST toolbox. Pre-processing steps included motion correction, slice timing correction, normalisation to MNI space using the parameters acquired for the T1 image with the closest acquisition date, and signal filtering to keep only low frequency fluctuations (0.01 – 0.08 Hz). Maps of fALFF (fractional amplitude of low frequency fluctuations), were calculated, to have a regional indicator of the brain's functional integrity (Zou et al., 2008).

4.2.4 Diffusion-weighted MRI

Diffusion-weighted images were acquired for all subjects who had the standard GENFI protocol (n = 483) which consisted of two sequences, with either four or five b0 images (no diffusion sensitization), and 64 diffusion-weighted images (b = 1000 s/mm^2). The second sequence was used when available. Additional acquisition parameters (median and ranges) included: slice thickness 2.5 mm (2 to 3 mm), repetition time 7300 ms (3742 to 10300 ms), echo time 90 ms (36 to 100 ms). Images were pre-processed using Mrtrix3 software (Tournier et al., 2019). Pre-processing steps included denoising, Gibbs ringing correction, eddy current distortions correction, and bias field correction. Diffusion tensor measures of fractional anisotropy (FA) and mean diffusivity (MD) were calculated using FSL. Images were normalized to MNI space using the

parameters acquired for the T1 image with the closest acquisition date using SPM12. All subsequent analyses of FA and MD refer to grey matter.

4.3 Quality control and data pre-processing

All modalities underwent visual inspection, and images of poor quality were excluded. Imaging data from 637 subjects was used in the subsequent analyses. All imaging data were processed using the NeuroPM-box (Iturria-Medina, Carbonell, et al., 2020) (available at neuropm-lab.com/neuropm-box.html) "organizing input for MCM" tool, consisting of regional grey matter parcellation of each image, outlier detection and correction, and imputation of missing modalities. The NeuroPM-box is currently designed for the analysis of grey matter. As such, all modalities in this study are measured in the grey matter. Mean grey matter density, fALFF, T1/T2 ratio, and grey matter FA and MD were calculated for cortical and subcortical regions, based on the Desikan–Killiany–Tourville (DKT) atlas (Klein & Tourville, 2012). All baseline data with missing modalities were imputed using the trimmed scores regression with internal principal component analysis algorithm, implemented in the Missing Data Imputation Toolbox for MATLAB, which considers the relationship between all subjects and variables to obtain imputed data by iteratively fitting PCA models to the data (Folch-Fortuny et al., 2016).

4.4 Data harmonization

We used ComBat to harmonize baseline data of each imaging metric by site and scanner type. ComBat, an empirical Bayesian method of harmonizing multi-site data originally used in genomics (Johnson et al., 2007), has been shown to be robust for multi-site imaging studies with small numbers of participants per site (Fortin et al., 2017, 2018). The biological variability in

genetic variants, disease status (non-carrier, presymptomatic carrier, symptomatic carrier), and the EYO was preserved, as well as age, sex, and years of education.

4.5 Demographics of included subjects

In all subsequent analyses, we analyzed cross-sectional data from 637 participants who had at least one useable T1 scan, including 269 presymptomatic carriers, 115 symptomatic carriers and 253 non-carriers (see Table 4.1 for demographic characteristics). Of the presymptomatic carriers, 92 had a C9orf72 expansion, 129 had a GRN mutation, and 48 had a MAPT mutation. Of the symptomatic subjects, 56 had a C9orf72 expansion, 40 had a GRN mutation, and 19 had a MAPT mutation. In terms of clinical diagnosis, 80 had a diagnosis of bvFTD (67 probable bvFTD (supported by imaging), 11 possible (based solely on clinical criteria), 2 unknown), 20 had a primary progressive aphasia (15 non fluent variant, 1 semantic variant, 4 non-specified), 4 had amyotrophic lateral sclerosis (ALS), 5 had FTD- ALS, 2 had corticobasal syndrome, 1 had progressive supranuclear palsy, and 3 had non-specified dementia.

	Presymptomatic	Symptomatic	Non-carriers
N	269	115	253
Mutation[c]			
C9orf72	92 (34.2)	56 (48.7)	87 (34.4)
GRN	129 (48.0)	40 (34.8)	126 (49.8)
MAPT	48 (17.8)	19 (16.5)	40 (15.8)
Age (years)[a]	44.9 ±11.9 (20.1 – 75.5)	63.0 ± 8.6 (32.9 – 78.7)	46.8 ± 13.7 (18.6 – 85.7)
Sex (female)[b]	170 (63.2)	50 (43.5)	142 (56.1)
Education (years)[a]	14.3 ± 3.3	11.9 ± 4.1	14.0 ± 3.5
CBI-R[a]	5.1 ± 9.1	61.2 ± 32.0	3.9 ± 6.3
MMSE[a]	29.3 ± 1.2	22.5 ± 6.3	29.4 ± 1.1
EYO[a]	-13.8 ± 11.5	3.4 ± 6.8	NA

Table 4.1. Demographics of included subjects**.**

Diagnoses in symptomatic subjects: 80 bvFTD (41 C9orf72, 20 GRN, 19 MAPT), 5 FTD-ALS (all C9orf72), 4 ALS (C9orf72), 15 nonfluent variant PPA (2 C9orf72, 13 GRN), 1 semantic variant PPA (C9orf72), 2 corticobasal syndrome (GRN), 4 dementia – not otherwise specified (GRN), 1 progressive supranuclear palsy (C9orf72).

Data are n (%) or mean ± standard deviation (range).

[a] $p < 0.001$ (1-way ANOVA), significant differences between symptomatic and presymptomatic, as well as non-carriers ($p < 0.001$, Tukey tests).

[b] $p < 0.001$ (chi-square), difference in distribution across groups.

[c] genetic mutation status in non-carriers refers to the mutation carried in family members

bvFTD = behavioural variant frontotemporal dementia, ALS = amyotrophic lateral sclerosis, PPA = primary progressive aphasia, MMSE = Mini Mental State Examination, CBI-R = Cambridge Behavioural Inventory Revised version, EYO = estimated years to symptom onset.

Chapter 5

Data-driven staging of genetic frontotemporal dementia using multi-modal MRI

This chapter is modified with permission from the manuscript "Data-driven staging of genetic frontotemporal dementia using multi-modal MRI" which has been accepted for publication at *Human Brain Mapping*.

5.1 Overview and rationale

Data-driven models of disease staging have been infrequently applied to FTD; those that have typically order a select number of biomarkers, either from a single modality or from select brain regions, or they look at a single genetic variant. Disease staging is complicated in FTD due to the substantial clinical, genetic, and pathological variations. To optimize therapeutic opportunities, staging biomarkers need to accurately track disease progression despite this heterogeneity, both in symptomatic FTD and in the long presymptomatic period. There are several disease-modifying treatments under development for genetic FTD variants (Tsai & Boxer, 2016). The near to full penetrance of FTD-causing gene mutations means that asymptomatic carriers could eventually be included in clinical trials, however, trials are impeded by the variation in age at onset and clinical presentation observed within gene mutations given that presymptomatic mutation carriers will develop different phenotypes. In the context of a relatively rare disease, phase 3 trials will need to merge presymptomatic carriers with symptomatic subjects into a single

study with unified outcome measures. It is therefore necessary to find unifying ways to stage the disease during both the presymptomatic and symptomatic phases.

The contrastive trajectory inference (cTI) is a recent unsupervised machine learning algorithm for staging disease, which uses multi-dimensional data to order and score individuals along sub-trajectories of disease progression. When applied to gene expression data from individuals with Alzheimer's and Huntington's diseases, cTI-identified individual disease scores were significantly associated with clinical and neuropathological disease severity (Iturria-Medina, Khan, et al., 2020).

The aim of this analysis was to create a unified disease staging system using multi-modal neuroimaging features from presymptomatic and symptomatic carriers of FTD-causing mutations using the cTI. We compared the cTI obtained disease scores to existing measures of disease severity and clinical performance as a proof of concept of cTI scores for staging disease in a heterogeneous dataset of genetic FTD.

5.2 Methods

Details of the dataset, imaging acquisition and processing, quality control, and data pre-processing and harmonization are described in Chapter 4.

5.2.1 cTI method

The contrastive Trajectory Inference algorithm (cTI, implemented in the *NeuroPM-box* software (Iturria-Medina, Khan, et al., 2020))) is an unsupervised machine learning method to analyze temporal patterns in multi-dimensional populational datasets. Data can first be adjusted for confounding variables using robust additive linear regression modeling with pair-wise

interactions. The cTI method then consists of unsupervised feature selection (for high dimensional datasets), dimensionality reduction via contrastive principal component analysis, and subject ordering to obtain individual disease scores (Iturria-Medina, Khan, et al., 2020).

Contrastive principal component analysis (cPCA) (Abid et al., 2018) is an unsupervised method of data exploration and visualization which identifies patterns in a target population (i.e., a diseased population) by controlling against patterns in a background population (a control group). By adjusting for patterns identified in the background population, such as aging effects or noise, cPCA has be found to be more sensitive to disease progression, by identifying trends in the population of interest that may be missed using standard methods of dimensionality reduction (i.e., PCA). The model then automatically chooses the contrasted principal component space which best optimizes the enriched trends in the target population. Each subject's position in the contrasted principal component space therefore reflects their disease state, with further distance from the background indicating more advanced disease.

Subjects are ordered and assigned an individual "pseudo-time" score according to their proximity to the background, standardized to be between 0 and 1. Low scores indicate proximity to the background population while high scores indicate proximity to the most diseased subjects. In the context of neurodegeneration, the pseudo-time score can be interpreted as a personalized index of disease stage (from the continuum of young subjects that are decades away from symptoms up to the more advanced dementia cases).

The cTI also estimates the specific contribution of each feature on the obtained disease scores. Individual weights of each feature reflect how much that feature contributed to the contrasted principal component space from which the subject ordering and disease scores were

obtained. A larger weight value therefore indicates a greater influence on the cTI-obtained disease scores.

5.2.2 cTI analysis

In this analysis we considered baseline data from five MRI-derived biomarkers in the grey matter (grey matter density, fALFF, T1/T2 ratio, FA, and MD). The cTI was run using all features due to the relatively small number of included features (5 modalities x 78 brain regions = 390 features). Data was first linearly adjusted by age, sex, and years of education. Parameters of the linear regression were obtained in non-carriers only, in order to obtain estimates of healthy aging. Parameters were then applied to all subjects. All non-carriers were used as the background population. As opposed to including all gene mutation carriers in the target population, we choose to include symptomatic carriers only. Therefore, the symptomatic subjects only were used in the data exploration and visualization via cPCA, in contrast to the non-carriers, and the corresponding transformations of the data to the disease-associated space (contrastive principal component space) were then applied to all subjects. We used symptomatic subjects as the target population due to their more advanced disease state which should allow for better determination of the disease-associated patterns by the cTI (as only subtle changes are expected in the presymptomatic participants), and due to the much larger number of presymptomatic carriers compared to symptomatic (many of whom are young and likely far from symptom onset) which would likely bias the model towards early presymptomatic cases, increasing the difficulty of finding underlying disease-associated trends. The cTI was run using the combination of all five-imaging metrics, as well as each metric individually.

5.2.3 Post-hoc statistical analysis

We compared the cTI obtained disease scores to the EYO, clinical assessment, and neuropsychological test scores using Pearson's correlation. Tests included the Mini Mental State Examination (MMSE) for cognition, the Cambridge Behavioural Inventory Revised version (CBI-R) for behavioural symptoms, and a neuropsychological battery measuring cognition, attention, memory, language, and executive function (Digit Span forwards and backwards from the Wechsler Memory Scale-Revised, a Digit Symbol Task, Parts A and B of the Trail Making Test, the short version of the Boston Naming Test, Category Fluency (animals), Letter Fluency and the Wechsler Abbreviated Scale of Intelligence Block Design task). Z-scores were calculated for all neuropsychological tests based on language-specific norms (Rohrer et al., 2015). Differences in disease status were tested using one-way ANOVAs. Post hoc pairwise differences between groups were analyzed using Tukey's test.

5.2.4 Sensitivity Analysis

To assess the impact of missing data and the subsequent imputation of this missing data on the analyses, the cTI was run, with all five modalities in combination, using only those individuals with all imaging modalities at their baseline visit (n = 282) and the above analyses repeated in this subgroup.

5.3 Results

5.3.1 cTI-identified disease scores

The cTI identified disease scores, obtained using all imaging metrics in combination, were significantly correlated with MMSE ($r = -0.273$, $p < 0.001$, Figure 5.1A), CBI-R ($r = 0.516$, $p <$

0.001, Figure 5.1B), and each neuropsychological test (all |r| 0.276 – 0.468, $p < 0.001$, Figure 5.2) for all gene mutation carriers. A higher disease score was associated with greater impairment on all tests and clinical scales. Correlations were not significant in presymptomatic carriers or symptomatic carriers alone ($p > 0.05$, Table 5.1), except for the MMSE which showed a significant positive correlation with disease scores in the symptomatic group ($p < 0.05$, Table 5.1). Correlations between cTI scores in the full group (including non-carriers) were similar to those in the gene mutation carriers (all $p < 0.001$, Table 5.1).

Significant differences in disease scores were found for disease status ($F = 270.9$, $p < 0.001$), with symptomatic subjects having higher disease scores than both asymptomatic carriers and non-carriers and asymptomatic carriers having higher disease scores than non-carriers ($p < 0.001$, Figure 5.1C). Differences were not driven by a single genetic group. Disease scores were also significantly correlated with the EYO for all gene mutation carriers, with a higher disease score associated with a shorter expected time to symptom onset ($r = 0.334$, $p < 0.001$, Figure 5.1D). See Table 5.1 for all correlations. Figure 5.3 shows the association between disease scores and age, by disease status.

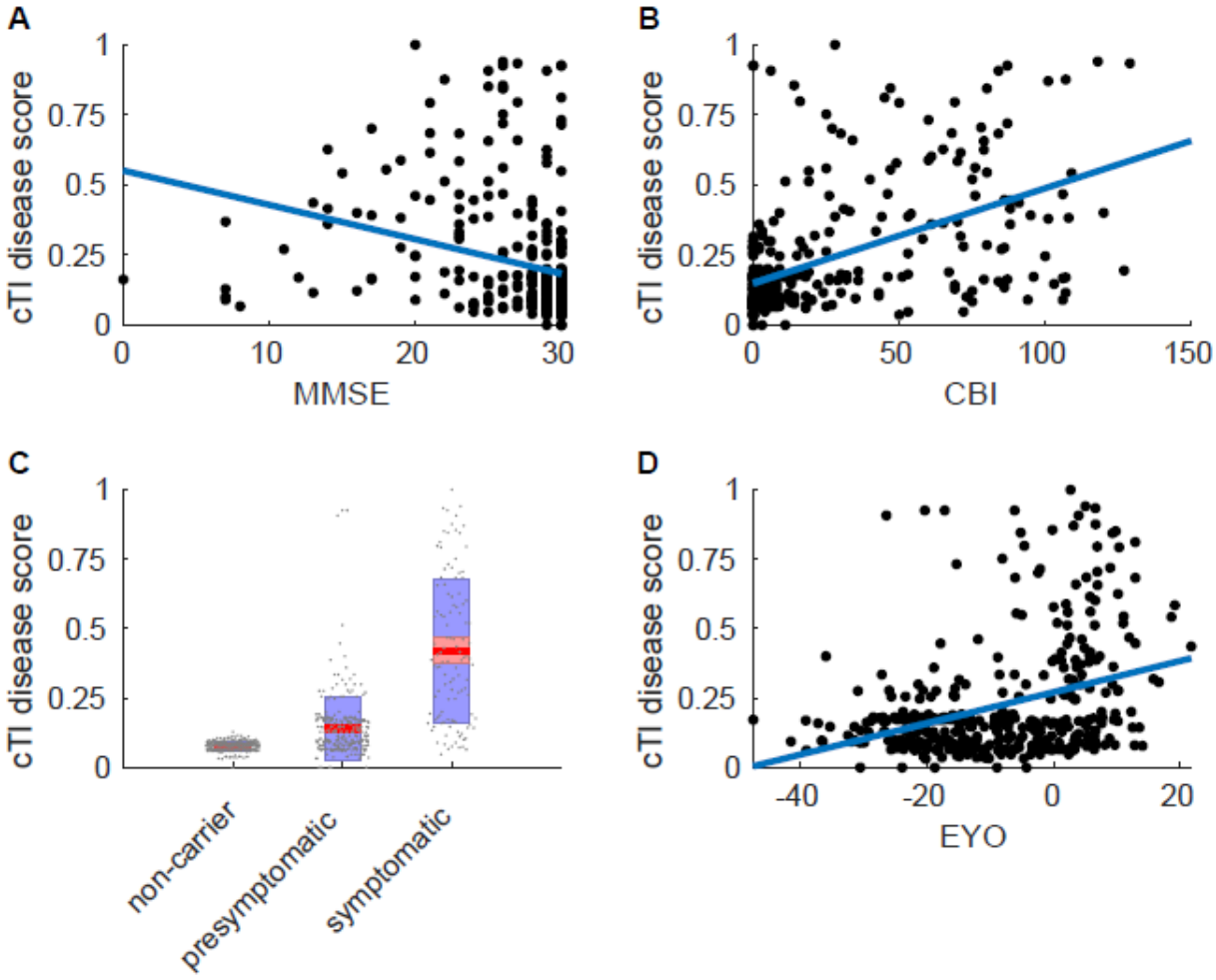

Figure 5.1: Association between cTI identified disease scores and **A)** MMSE, **B)** CBI-R, **C)** Disease status, and **D)** EYO. In C, points are laid over a 1.96 SEM (95% confidence interval) in red and at 1 SD in blue.

MMSE=Mini Mental State Examination, CBI=Cambridge Behavioural Inventory, EYO=estimated years to symptom onset.

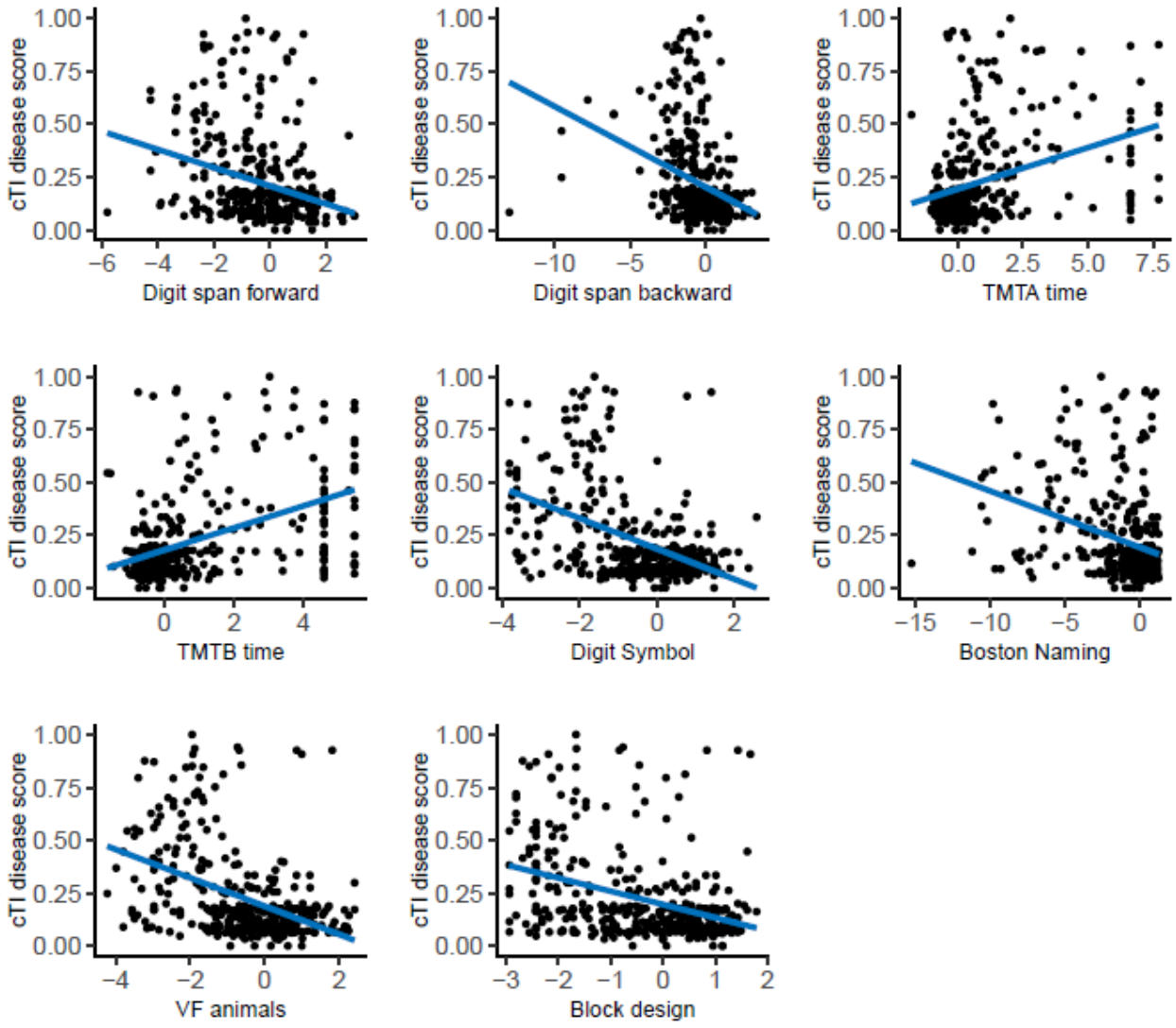

Figure 5.2: Association between cTI identified disease scores and neuropsychological tests.

TMTA = Trail Making Test Part A, TMTB = Trail Making Test Part B, VF = Verbal Fluency

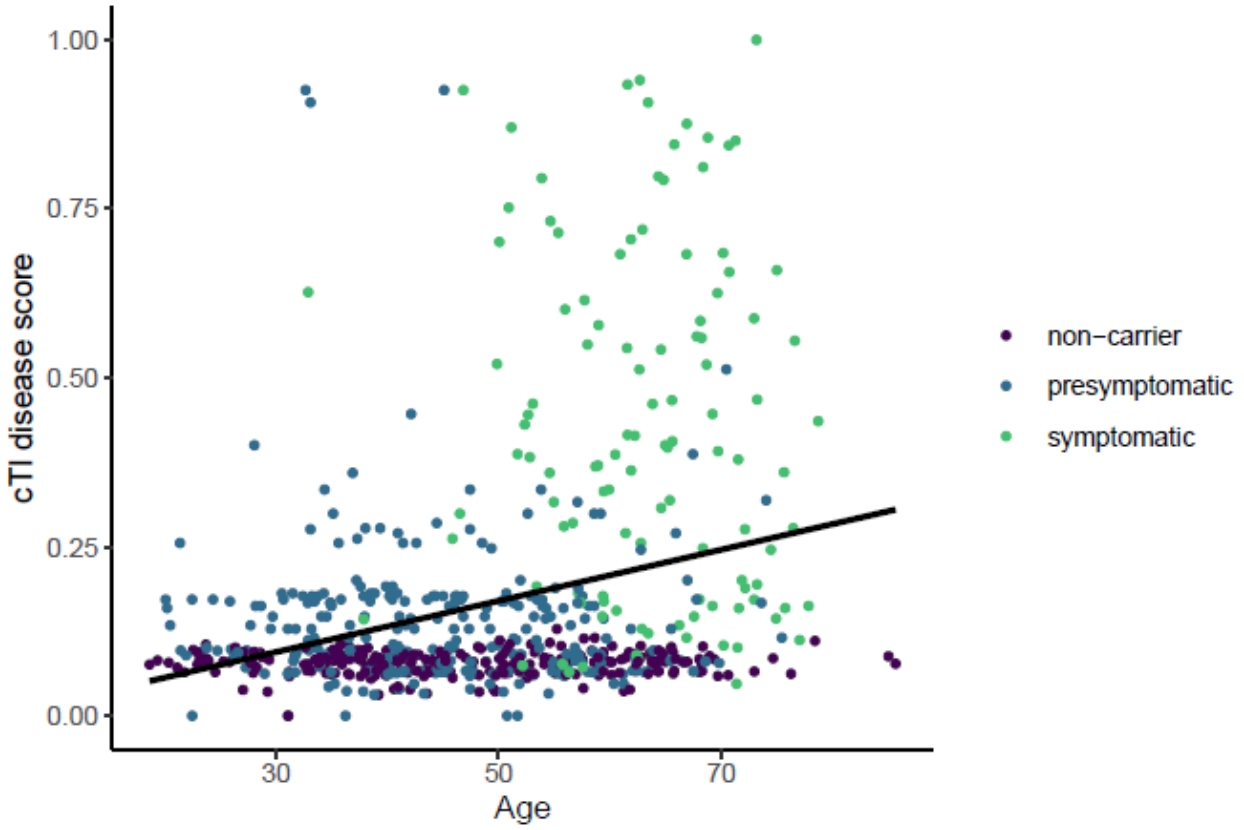

Figure 5.3: Association between cTI identified disease scores and age, by disease status.

	Carriers	Presymptomatic	Symptomatic	All
MMSE	-0.273*	-0.014	0.237**	-0.337*
CBI-R	0.516*	0.017	0.109	0.573*
DS F score	-0.276*	0.008	0.087	-0.269*
DS B score	-0.292*	-0.017	0.091	-0.295*
TMTA time	0.357*	0.019	-0.072	0.392*
TMTB time	0.466*	0.061	0.015	0.490*
Digit symbol	-0.468*	0.025	-0.026	-0.461*
Boston naming	-0.334*	0.015	0.132	-0.385*
VF animals	-0.436*	0.043	0.057	-0.424*
VF F	-0.406*	-0.007	-0.062	-0.387*
VF A	-0.386*	-0.064	0.023	-0.374*
VF S	-0.398*	-0.037	-0.021	-0.389*
Block design	-0.370*	0.090	0.069	-0.371*
EYO	0.343*	-0.089	0.026	0.298*

Table 5.1: Correlation (r) between cTI disease scores (all modalities) and each clinical/neuropsychological test for all gene carriers, presymptomatic carriers only, symptomatic carriers only, and the full group (included non-carriers).

MMSE = Mini Mental State Examination, CBI-R = Cambridge Behavioural Inventory Revised version, DS F = Digit Span forwards, DS B = Digit Span, TMTA = Trail Making Test Part A, TMTB = Trail Making Test Part B, VF = Verbal Fluency, EYO = estimated years to symptom onset.

* indicates significant correlation ($p < 0.001$).

** indicates at significant correlation ($p < 0.05$).

5.3.2 Feature contributions

We summed the feature weights across modalities and regions to determine the total contribution of each modality (Figure 5.4) and the total contribution of each brain region (Figure 5.5) to the obtained disease scores. DTI metrics provided the highest contribution (MD followed by FA), while fALFF provided the lowest. Grey matter density and T1/T2 ratio had similar contributions. Total regional contributions indicate highest values for frontal, temporal, and subcortical regions.

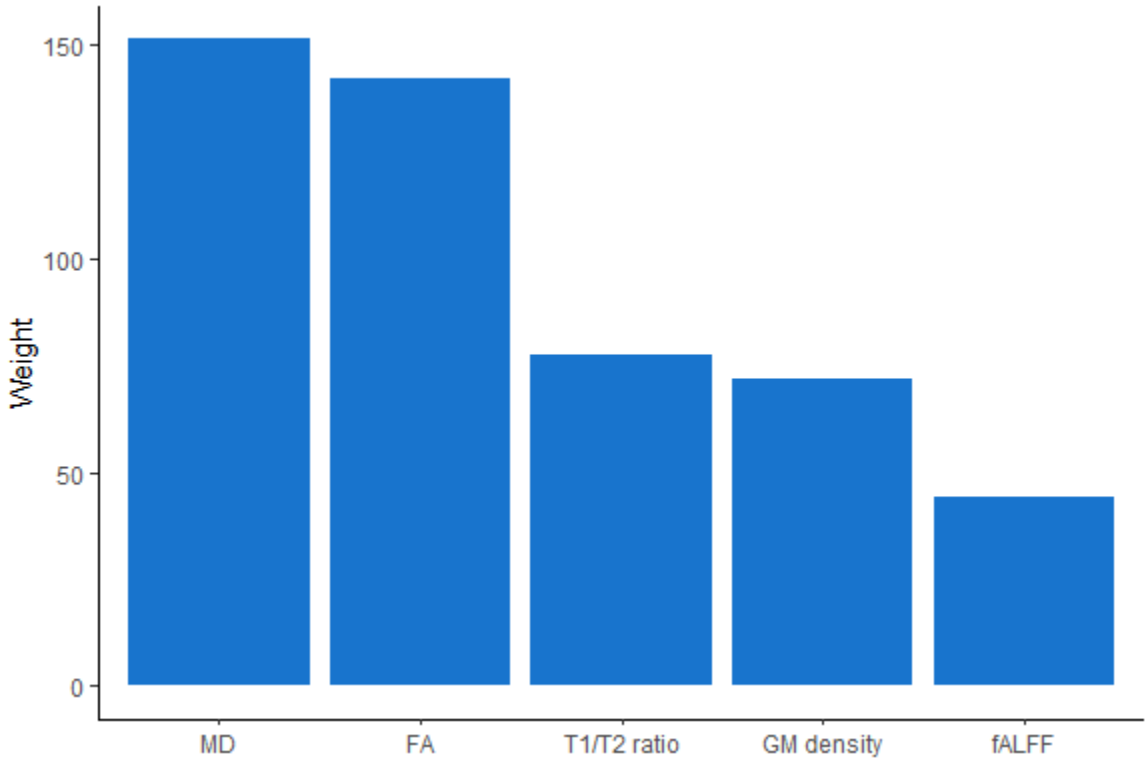

Figure 5.4: Total contribution of each modality to the cTI identified disease scores.

GM = grey matter, fALFF = fractional Amplitude of Low Frequency Fluctuations, FA = fractional anisotropy, MD = mean diffusivity.

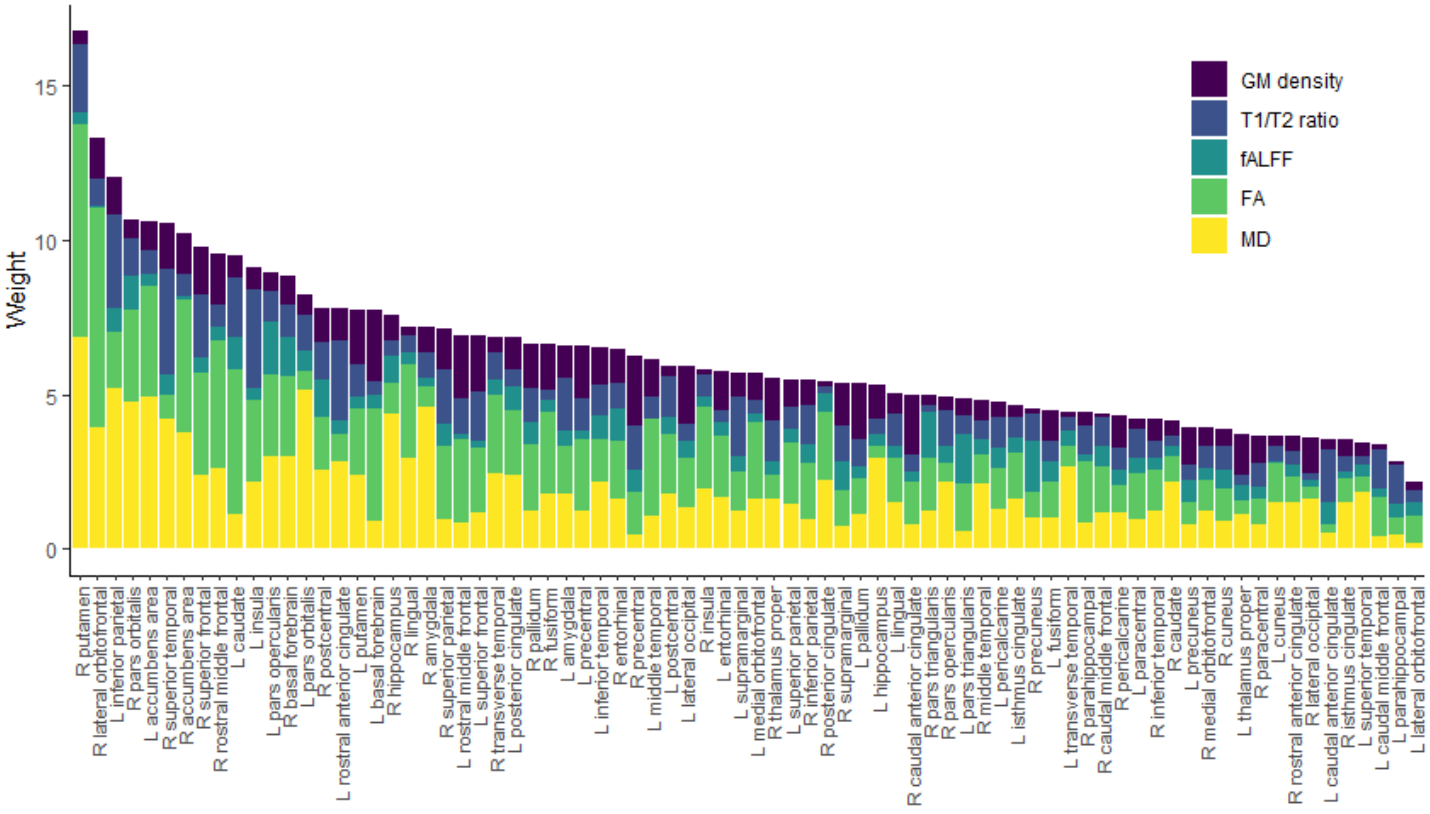

Figure 5.5: Total contribution of each brain region to the cTI identified disease scores.

GM = grey matter, fALFF = fractional Amplitude of Low Frequency Fluctuations, FA = fractional anisotropy, MD = mean diffusivity, L = left, R = right.

5.3.3 Individual modalities

When obtained using each imaging metric individually, the cTI identified disease scores in all gene mutation carriers were significantly correlated with CBI-R (Table 5.2; grey matter density: $r = 0.391$, fALFF: $r = 0.377$, T1/T2 ratio: $r = 0.373$, $p < 0.001$), and all neuropsychological tests for all modalities (Table 5.2; grey matter density: $|r|$ 0.281 – 0.447, fALFF $|r|$ 0.277 – 0.442, $p < 0.001$), and with the MMSE for all modalities except FA (Table 5.2; grey matter density: $r = -0.368$, fALFF: $r = -0.355$, $p < 0.001$). A higher disease score was associated with greater

impairment on all tests. Significant differences in disease scores were found for disease status, with symptomatic subjects having higher disease scores than both asymptomatic carriers and non-carriers ($p < 0.001$). Differences between asymptomatic carriers and non-carriers were not significant (fALFF, $p = 0.15$, FA, $p = 0.1$, T1/T2 ratio, $p = 0.07$; MD, $p = 0.06$; grey matter density, $p = 0.97$). A significant correlation was found with the EYO for all modalities (Table 5.2; $|r|$ 0.107 – 0.353, $p < 0.05$), with a higher disease score associated with a shorter time to symptom onset among gene carriers.

	GM Density	T1/T2 ratio	fALFF	FA	MD
MMSE	-0.368	-0.188	-0.355	-0.093ǂ	-0.24
CBI-R	0.391	0.373	0.377	0.28	0.261
DS F score	-0.306	-0.237	-0.277	-0.107	-0.258
DS B score	-0.281	-0.258	-0.289	-0.177	-0.243
TMTA time	0.358	0.160	0.376	0.210	0.238
TMTB time	0.447	0.275	0.442	0.225	0.265
Digit symbol	-0.442	-0.261	-0.372	-0.264	-0.237
Boston naming	-0.415	-0.244	-0.362	-0.247	-0.216
VF animals	-0.433	-0.296	-0.355	-0.210	-0.239
VF F	-0.358	-0.285	-0.374	-0.248	-0.266
VF A	-0.336	-0.269	-0.322	-0.229	-0.258
VF S	-0.357	-0.236	-0.318	-0.220	-0.269
Block design	-0.360	-0.217	-0.350	-0.211	-0.233
EYO	0.353	0.225	0.286	0.205	0.107

Table 5.2: Correlation (r) between cTI disease scores for each modality and each clinical/neuropsychological test (in all gene carriers).

MMSE = Mini Mental State Examination, CBI-R = Cambridge Behavioural Inventory Revised version, DS F = Digit Span forwards, DS B = Digit Span, TMTA = Trail Making Test Part A, TMTB = Trail Making Test Part B, VF = Verbal Fluency, EYO = estimated years to symptom onset, GM = grey matter, fALFF = fractional Amplitude of Low Frequency Fluctuations, FA = fractional anisotropy, MD = mean diffusivity.

ǂ indicates non-significant correlation ($p > 0.05$). All other correlations are statistically significant for all modalities ($p < 0.05$).

5.3.4 Sensitivity Analysis

Overall results of the analysis in the subset of subjects with full baseline imaging are similar to those in the full dataset; cTI disease scores were significantly correlated with all clinical and neuropsychological tests, and with the EYO ($p < 0.001$). All correlations were equal to or stronger than in the full analysis. Significant differences in disease scores were found for disease status ($F = 318.6$, $p < 0.001$). Symptomatic subjects had higher disease scores than both asymptomatic carriers and non-carriers ($p < 0.001$), but differences between asymptomatic carriers and non-carriers were not significant ($p = 0.15$). The feature contribution analysis indicated a higher contribution of grey matter density. The ordering of regional contributions was also somewhat altered but highest values were again found for frontal, temporal, and subcortical regions.

5.4 Discussion

In this analysis we show that the cTI, a data-driven staging model, can identify the cross-sectional progression of disease in a heterogeneous sample of genetic FTD using only neuroimaging metrics without clinical information. As a proof of validity, significant correlations were found between the data-driven cTI identified disease scores and the estimated years to symptom onset and to all the tested measures of clinical performance. In addition, higher mean cTI scores were found in presymptomatic carriers compared to non-carriers, showing that the staging system may be able to detect subtle pre-dementia changes in mutation carriers, although this change was not replicated in a subset of subjects with complete data. Grey matter DTI measures, particularly MD, provided the largest contribution to the model. Disease scores derived from individual metrics were also significantly correlated with clinical performance. Differences in disease scores between presymptomatic carriers and noncarriers did not reach statistical

significance in individual metrics, suggesting a combination of metrics may be important to differentiate presymptomatic carriers from asymptomatic subjects.

This study is a proof of concept that it is possible to generate a data-driven unified staging system across genetic and phenotypical variations that correlates strongly with the most relevant clinical and cognitive measures in FTD. Previous application of the cTI model has shown strong associations between the model derived disease scores and clinical and neuropathological disease severity in both Alzheimer's and Huntington's diseases, as well as a cohort encompassing the spectrum of both diseases (Iturria-Medina, Khan, et al., 2020). Our results corroborate the use of cTI-derived disease scores as a marker of neurodegenerative diseases, showing that the individual scores reflect a combination of subtle clinical differences in the presymptomatic period and disease severity in symptomatic patients. We further show that the model can accurately produce a disease staging score in a heterogeneous population including the wide variety of clinical presentations and genetic mutations found in genetic FTD, factoring the presymptomatic and symptomatic spectrum. This association is found despite the large number of subjects in the early presymptomatic stage (i.e., more than 30-40 years prior to probable symptom onset). The association was largely driven by differences between the presymptomatic and symptomatic periods, as correlations in the individual subgroups were not significant; this is likely because most presymptomatic subjects will have normal to very mild impairment on these tests, while symptomatic subjects are impaired. It also may reflect the inability of the clinical and cognitive scales to reflect specific aspects of each individual's subtle clinical decline.

The cTI has previously been applied to gene expression data. This analysis shows the utility of this model derived using neuroimaging features. The feature contributions analysis indicates that DTI metrics, in particular MD, are the biggest contributors to the model. These measures have

rarely been studied in grey matter, although increases in MD have been reported in symptomatic FTD (Whitwell et al., 2010). This finding may warrant further investigation of grey matter microstructural changes. Of note, both DTI metrics indicate strong contributions to the model from similar brain regions. FA and MD attempt to measure different processes; FA is a measure of directional tissue coherence (in grey matter, a potential measure of neuron orientations) and MD is a measure of the amount of total local diffusion (in grey matter, a potential measure of extracellular space). However, it is likely that these measures are picking up on multiple inter-related microstructural changes occurring in the same brain regions.

Our results indicate moderate association between disease scores derived individually from grey matter atrophy, fALFF and T1/T2 ratio and clinical performance. Grey matter atrophy is the most frequently studied imaging biomarker in FTD, and atrophy has been consistently reported across phenotypes and genetics, symptomatically and presymptomatically (Cash et al., 2018; Rohrer et al., 2015; Staffaroni, Cobigo, et al., 2020). T1/T2 ratio and fALFF have been much less frequently studied. fALFF contributed the least to the combined model, a somewhat surprising finding given functional alterations are hypothesized to be an earlier feature of FTD than structural grey matter changes. Alterations in functional connectivity have been reported in both presymptomatic and symptomatic FTD (Dopper et al., 2014; Lee et al., 2017; Premi et al., 2016), however results suggesting early functional changes are inconsistent. T1/T2 ratio, as a marker of intracortical myelin, has not been investigated in FTD to our knowledge; results here indicate a change in myelin content along FTD progression. We obtained the highest correlations with clinical measures when using a combination of all modalities, and all modalities providing some level of contribution to the model, indicating an added benefit of combining information from multiple modalities which provide complementary information. Our results suggest that the

combination of metrics may be particularly important to differentiate presymptomatic carriers from controls.

The regional contributions analysis indicated that along with frontal and temporal regions, subcortical involvement was an important contributor to the model, while the left inferior parietal region also showed a high contribution. Subcortical regions have traditionally received less attention in FTD research, however recent research suggests subcortical regions may play a key role in FTD (Bocchetta, Malpetti, et al., 2021). Subcortical involvement has also been reported in genetic FTD, including presymptomatically (Bocchetta, Todd, et al., 2021; Rohrer et al., 2015). Parietal involvement has been reported most commonly in GRN mutations (Rohrer et al., 2015). Overall, there appears to be a higher contribution from regions in the right hemisphere. This may be due to the asymmetric atrophy pattern typically found in GRN carriers (Rohrer et al., 2015), who are the largest group in this analysis.

The sensitivity analysis suggests that the observed associations between disease scores and the estimated years to symptom onset and to all the tested measures of clinical performance are fairly robust, while the differences between presymptomatic carriers and controls, the contribution of grey matter density to the disease scores are more sensitive to missing data. These findings should therefore be validated in a larger dataset with more complete data.

While further validation work is required, this study provides initial evidence for the development of unifying, biologically based staging to monitor disease progression and treatment outcomes in heterogeneous neurodegenerative disorders.

Chapter 6

Data-driven subtyping of genetic frontotemporal dementia using multimodal MRI

6.1 Overview and rationale

Most disease progression models assume a single disease trajectory for all individuals, which limits the utility of these models for patient stratification. Previous subtyping studies have focused on identifying distinct groupings from subjects at a similar disease stage (typically symptomatic individuals). One study to date has combined these two methods to obtain subtypes of individuals who follow similar temporal trajectories in genetic FTD (Young et al., 2018). Similar to other disease progression models, this model only used a small number of features (grey matter lobar volumes). However, it was able to identify genetic subtypes in the GENFI dataset, providing initial validation for this type of method, given that genetic variants have specific pathology and group-level differences in neuroimaging found in these groups.

The cTI method of disease progression modelling described in Chapter 5 was able to identify disease stage in the heterogenous GENFI dataset using a combination of MRI-derived features. A recent extension of this model combines disease staging with subtyping. In an initial analysis, the cTI was able to distinguish between control subjects, Alzheimer's and Huntington's diseases using gene expression data. 87% of controls was assigned to subtype 1, 71% of those with AD were assigned to subtype 2, and 89% of those with Huntington's disease were assigned to subtype 3 (Iturria-Medina et al., 2021).

The aim of this analysis was to obtain data-driven sub-trajectories in a heterogenous group of presymptomatic and symptomatic genetic FTD cases, based on MRI-derived metrics, using the cTI method. We validated cTI-obtained sub-trajectories against genetic groups. As well, we compared clinical diagnoses of symptomatic participants across subtypes.

6.2 Methods

Details of the dataset, imaging acquisition and processing, quality control, and data pre-processing and harmonization are described in Chapter 4.

6.2.1 cTI subtyping method

This chapter describes an extension to the original cTI method described in Chapter 5 (Iturria-Medina et al., 2021). Dimensionality reduction is performed via contrastive principal component analysis as described in Chapter 5, and each subject is projected onto the resulting disease-associated space. Each subject is then assigned to a sub-trajectory, consisting of subjects that cluster together in the disease-associated space. Each sub-trajectory therefore consists of a subgroup of subjects potentially following a common disease progression pattern. The number of trajectories is determined automatically, up to a previously indicated maximum number. Each subject may be assigned to more than one sub-trajectory, indicating that these sub-trajectories may overlap, especially near their beginning, where the cTI may not distinguish between these paths. In these cases, possible subtypes assignments are ranked from most to least probable.

6.2.2 cTI subtyping analysis

The cTI was run as described in Chapter 5. Data was first linearly adjusted by covariables (age, sex, and years of education). All non-carriers were used as the background population, and

all symptomatic carriers were used as the target population. A maximum of four clusters was indicated, representing the three genetic variants (*C9orf72, GRN, MAPT*) and the control group of non-carriers. Baseline data from grey matter density, fALFF, T1/T2 ratio and grey matter FA and MD were used.

6.2.3 Post-hoc statistical analysis

For each data-driven cTI subtype, we looked at the percentage make-up of subjects from each genetic group, as gene variants have specific pathology and group-level differences in neuroimaging. cTI subtypes were also compared to the clinical diagnoses in symptomatic subjects in the same manner.

6.3 Results

6.3.1 cTI-identified sub-trajectories

Using all modalities in combination, the cTI, identified four sub-trajectories. 9.6% of subjects were assigned to more than one subtype. Based on the most probable assignment for each of these subjects, subtype 1 contained 51 subjects, subtype 2 contained 25 subjects, subtype 3 contained 55 subjects, and subtype 4 contained 506 subjects. The cTI did not recover the three genetic variants, instead assigning most gene carriers (≥ 65%) to subtype 4, as well as 88% of non-carriers (Figure 6.1A). All presymptomatic carriers, of all gene variants, are assigned to subtype 4 (Figure 6.1B). Symptomatic carriers are found in all four subtypes; while C9orf72 and especially GRN carriers are both primarily found in subtype 3, MAPT carriers are more evenly spread out across subtypes 2-4 (Figure 6.1C). cTI identified subtypes also do not distinguish between clinical

diagnosis (Figure 6.1D); subjects of varying diagnoses are assigned primarily to subtype 3 (42% of bvFTD; 87% of nfvPPA, 100% of PPA-NOS).

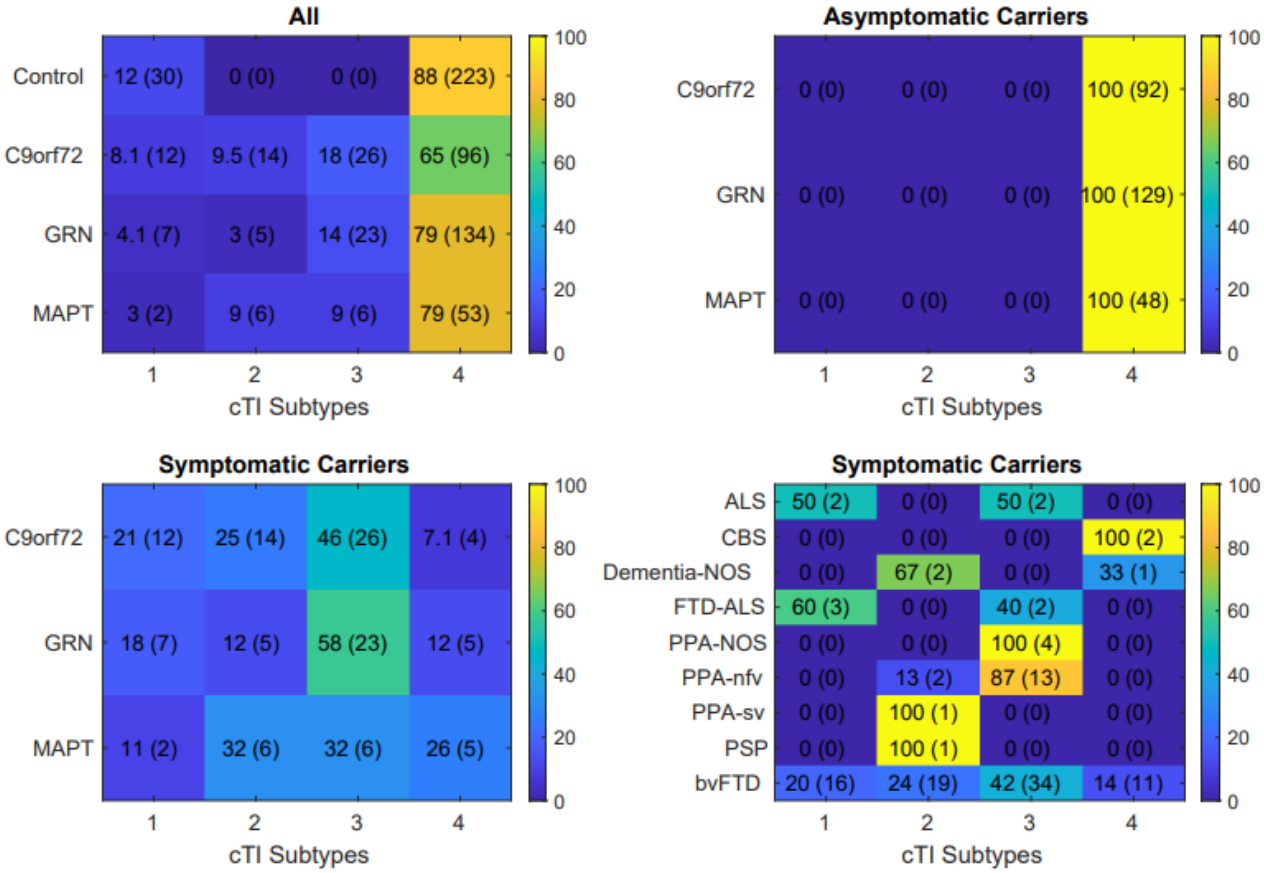

Figure 6.1: Confusion matrices comparing cTI subtyping to gene variants and non-carriers, asymptomatic carriers by gene variant, symptomatic carriers by gene variant, and symptomatic carriers by clinical diagnosis. Numbers are percentages (number of subjects).

bvFTD = behavioural variant frontotemporal dementia, ALS = amyotrophic lateral sclerosis, PPA = primary progressive aphasia, PPA-nfv = nonfluent variant PPA, PPA-sv = semantic variant PPA, CBS = corticobasal syndrome, Dementia-NOS = dementia - not otherwise specified, PSP = progressive supranuclear palsy.

6.4 Discussion

The subtyping analysis did not lead to the identification of clear genetic or clinical categorizations. The cTI has previously recovered subtypes in a cohort containing multiple diseases (Alzheimer's and Huntington's (Iturria-Medina, Carbonell, et al., 2020)). Recovering genetic subtypes in FTD is a more difficult task. The inability to uncover genetic variants suggests that genetic variants have significantly overlapping neuroimaging features at early presymptomatic stages. Neurodegeneration is expected to be subtle in early disease stages; there are likely not clear distinctions between non-carriers and early presymptomatic carriers of each gene variant. Subtyping may therefore require a wider variety of imaging markers, or the addition of non-imaging biological markers.

The subtyping results are in contrast to the previous study which recovered genetic FTD variants using an unsupervised machine learning algorithm and lobar grey matter volumes (Young et al., 2018). That study found four subtypes which corresponded to the three genetic variants (including two subtypes in C9orf72). This difference may be due to the different methods used by the model. The cTI conducts dimensionality reduction via contrastive principal component analysis, then clusters subjects in the dimensionally reduced space; the model employed in (Young et al., 2018) iteratively fits a mixture of staging models based on the event-based model (Fonteijn et al., 2012) to cluster subjects with different biomarker orderings. It is possible that this method is better able to detect subtypes of genetic FTD. Unlike the cTI however, this model is unable to handle multi-model, high dimensional data.

The cTI also did not identify subtypes based on clinical presentation, indicating that it is unable to predict which phenotype a presymptomatic individual will develop. The majority of

symptomatic subjects included in this study have been diagnosed with bvFTD, while only a small number of symptomatic subjects have a diagnosis other than bvFTD. It is therefore likely that there are not enough subjects in the non-bvFTD groups for the model to distinguish common patterns of these presentations.

Overall, the cTI was unable to accurately obtain sub-trajectories of genetic FTD in this dataset. Predicting genetic and clinical subtypes will likely require larger datasets, as well as a wider variety of biological markers including serum or CSF measures such as Neurofilament Light Chain.

Chapter 7

Multifactorial causal model of disease progression in genetic frontotemporal dementia

7.1 Overview and rationale

In contrast to the models described in the previous chapters, which aim to provide staging and subtyping as tools for clinical applications, particularly in clinical trials, network-based models of neurodegenerative disease progression are mechanistic in nature; they typically aim to describe the underlying mechanisms by which disease progression occurs. Most existing models study the propagation of a single factor through structural or functional networks and typically look at advanced stage disease (i.e., symptomatic individuals). Existing multi-factorial models of disease progression typically measure changes in magnitude of each factor independently of one another, reflecting sensitivity of each factor to disease progression.

The multifactorial causal model (MCM) (Iturria-Medina et al., 2017) is a multifactorial network-based model which estimates disease progression by considering how multiple imaging-based biological factors directly interact and spread throughout brain networks. The MCM considers that once a change occurs in a given biological factor in one region of the brain, said factor can directly alter the state of other factors in the same region as well as propagate through physical brain networks to influence factors in other regions. For example, changes in neural activity may directly influence grey matter atrophy, and vice versa. Concurrently, these changes may propagate through axonal connections to other brain areas. Similar factor-factor interaction and propagation mechanisms can occur in these other regions in a continuous cycle. This model

considers that small changes in a factor in one region can have large effects on interconnected factors (Iturria-Medina et al., 2016).

The MCM can be applied on a group-level using cross-sectional data from individuals across the full disease course to estimate typical patterns of progression, starting from the estimated initial disease onset. Specifically, the MCM can characterize the initial perturbations occurring at the estimated onset of the biological disease process and which factors and brain regions are altered at this stage, as well as the direct factor-factor interactions and the tendency of each factor to spread through brain networks.

The application of this model in AD on a group level has increased understanding of the neurobiological changes occurring in the preclinical stages, including an early causal role for vascular perfusion changes. It also suggests that AD is not caused by one dominant modality, highlighting the importance of considering multiple factors, each playing an importance role in disease development (Iturria-Medina et al., 2017). Application of this model in genetic FTD can therefore provide a more integrative understanding of disease progression, and consequently aide in the development of sensitive, early-stage biomarkers.

The aims of this analysis were to apply the MCM to MRI-based biomarkers of genetic presymptomatic and symptomatic FTD, to characterize biomarker interactions and propagation and estimate initial alterations in the disease process.

7.2 Method

Details of the dataset, imaging acquisition and processing, quality control, and data pre-processing and harmonization are described in Chapter 4.

7.2.1 Structural connectome processing

Structural connectomes were obtained from each preprocessed diffusion-weighted image using Mrtrix3. Processing steps included registration of T1 image to the average B0 image, T1 tissue segmentation, estimation of orientation distribution functions via constrained spherical deconvolution (Jeurissen et al., 2014; Tournier et al., 2007), probabilistic fibre tractography using anatomically constrained tractography (Smith et al., 2012), spherical deconvolution informed filtering of tractograms (SIFT) to improve the biological plausibility of tractograms (Smith et al., 2015), T1 parcellation using Freesurfer into 76 cortical and subcortical regions based on the DKT atlas (Klein & Tourville, 2012), and connectome construction to obtain region-region connections. Average connectomes were calculated for each combination of genetic group and disease status (non-carriers, presymptomatic, symptomatic). For those subjects that did not have a diffusion-weighted image which passed quality control, the average connectome for the corresponding gene mutation and disease status was used.

7.2.2 MCM method

The MCM is described in detail in (Iturria-Medina et al., 2017). The model considers the brain to be a dynamic multifactorial causal system. Each node in this system models the change in a given biological factor at a given brain region, over time (or disease progression). Each node is characterized by the current state of the biological factor, determined as the level of alteration from the initial state of the node (increase, decrease, or no change with regard to the baseline state). Therefore, at a given time the state of the system is described by a vector of the state space representing the alteration of each factor at each brain region. In the absence of external inputs, the change in state over time is characterised by (1) the direct interactions between each biological

factor, within each region, (2) the propagation of each factor alternation through physical networks (i.e., anatomical), and (3) the preservation of these changes. The model can take as input multiple biological factors derived from neuroimaging. When applied to a cross-sectional group analysis, the subjects first need to be staged according to disease severity. The subjects will then be ordered based on this staging, resulting in a pseudo-longitudinal dataset for MCM optimization. The resulting state space is therefore a vector of alteration levels from baseline (estimated from healthy control subjects), for each factor at each region, across disease stages.

7.2.3 MCM analysis

In this study the MCM was applied to the GENFI dataset cross-sectionally. As FTD is highly heterogeneous and distinct patterns of disease progression are expected in the three most common genetic mutations (Jiskoot, Bocchetta, et al., 2018; Rohrer et al., 2015; Young et al., 2018), separate models were computed for each mutation group (*C9orf72, GRN, MAPT*). In this analysis we considered five biological factors (grey matter atrophy, fALFF, T1/T2 ratio, grey matter FA and MD) measured at 76 cortical and subcortical regions, covering the brain's grey matter (Klein & Tourville, 2012). Data was first linearly adjusted by covariables (age, sex, and years of education). The model was first analysed using the original sample. Then, we used a bootstrapping procedure, creating 500 different datasets with replacement for each subtype (genetic group). The model optimization was repeated for each dataset.

7.2.4 Staging

In the initial model, all subjects were grouped into categorical stages based on commonly used measures of disease severity in previous research. All presymptomatic subjects were staged according to their EYO. Symptomatic subjects were staged based on relevant measures of clinical

symptoms. Non-carriers served as controls (stage 0). Presymptomatic subjects were staged into five groups based on 10 year intervals of the EYO (stage 1: more than 30 years away, stage 2: 30-20 years away, stage 3: 20-10 years away, stage 4: 10-0 years away, stage 5: past EYO). Symptomatic subjects were grouped into three stages based on the Clinical Dementia Rating Scale (CDR), when available: stage 6 (CDR below 1), stage 7 (CDR 1-2), stage 8 (CDR>= 2). If the CDR was not conducted, the same scoring was done using the mean CBI score, for those with a bvFTD diagnosis. Those with a PPA diagnosis were scored in the same manner based on tests of language fluency and grammar. The resulting matrix of the brain's alteration from baseline across regions and at each disease stage was then applied to the MCM (Iturria-Medina et al., 2017). In a second model, subjects were staged in a continuous manner using EYO for all presymptomatic subjects and length of disease duration (in years) for all symptomatic subjects. In a third model, all subjects were staged using the disease scores obtained from the cTI (as described in Chapter 5).

7.2.5 Statistical (post-hoc) analysis

The MCM calculates the accuracy of each subtype as the percent of the variance across the five imaging modalities that is accounted for by the model. First, we compared the accuracy across each of the three staging systems. We then calculated mean and 95% confidence intervals of the accuracy across all generated bootstrap samples.

The MCM estimates the initial system perturbation (i.e., the alteration of each modality at each brain region, at the estimated pathological disease onset). To estimate which modalities and brain regions are most altered at the initial disease onset, the absolute values of all factor-region pairs were compared.

The MCM also characterizes the underlying mechanisms of the disease process by estimating factor-factor interactions and factor spreading through physical networks. These processes are summarized in three measures: relative spreading, relative incoming influence, and relative outgoing influence (Iturria-Medina et al., 2017). Relative spreading measures the percent of the regional changes in each factor that are caused by alterations in that factor spreading from other brain regions through the brain's physical connections (i.e., the percent of regional changes in functional activity that can be attributed to functional alterations spreading from other brain regions). The relative incoming influence measures the percent of regional changes in each factor that are caused by the direct influences of all the other factors, excluding self-effects (i.e., the percent of functional alterations that are directly caused by interactions with the remaining four factors). This measure reflects which factors are the most vulnerable to influence by other factors during the disease process. The relative outgoing influence measures the percent of regional changes in all considered factors that are caused by the direct influence of a given factor, excluding self-effects (i.e., the percent of alterations in the other four factors that can be attributed to direct interactions with functional alterations). This measure reflects which factors are the most influential during the disease process.

7.3 Results

7.3.1 Accuracy

The accuracy of the categorical staging model was 2.46%, 0.97%, and 2.77% for C9orf72, GRN, and MAPT respectively, indicating that less than 5% of the variance in multifactorial regional abnormality patterns across all stages was captured by the model (Figure 7.1A). For the EYO/disease duration staging model accuracy was 3.11% for C9orf72, 3.41% for GRN, and

29.59% for MAPT (Figure 7.1B). For the cTI disease score staging model accuracy was 4.67% for C9orf72, 13.57% for GRN, 16.35% for MAPT (Figure 7.1C).

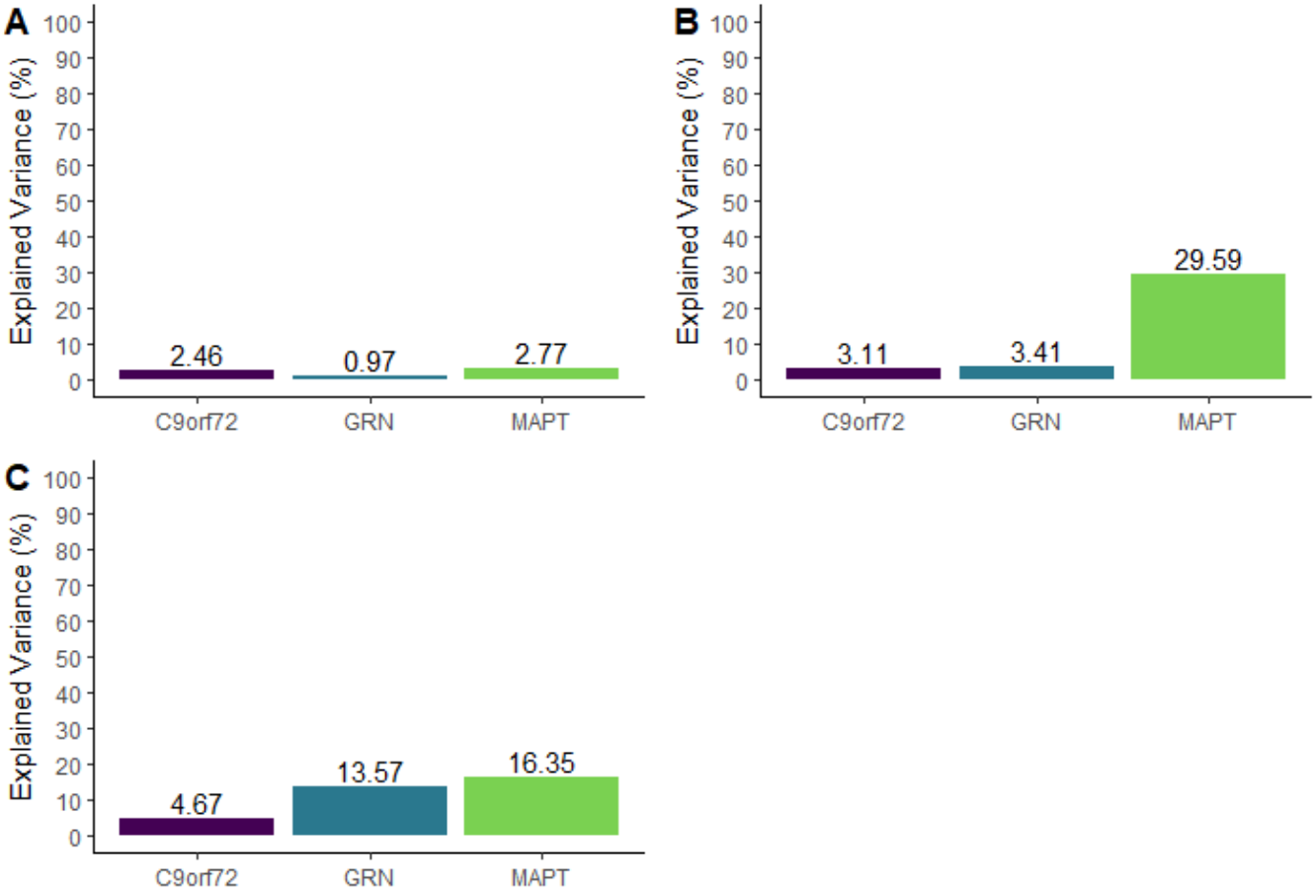

Figure 7.1: Explained variance of the MCM for each genetic subtype, for three different staging methods. **A)** categorical EYO/clinical stages. **B)** continuous EYO/disease duration staging. **C)** data-driven disease scores (cTI).

The remaining results are presented for the third staging system (cTI-derived disease scores), as this method provides a purely data-driven model of disease progression that is not based on any clinical information. Overall, this model had the best accuracy across all subtypes.

7.3.2 Initially altered factors and regions

Figure 7.2 shows the absolute alteration for the top 20 most altered factor-region pairs, at the estimated disease onset. In all three subtypes, subcortical regions are the most altered. Highest alterations are seen in FA, T1-T2 ratio, and grey matter density, again across all three subtypes.

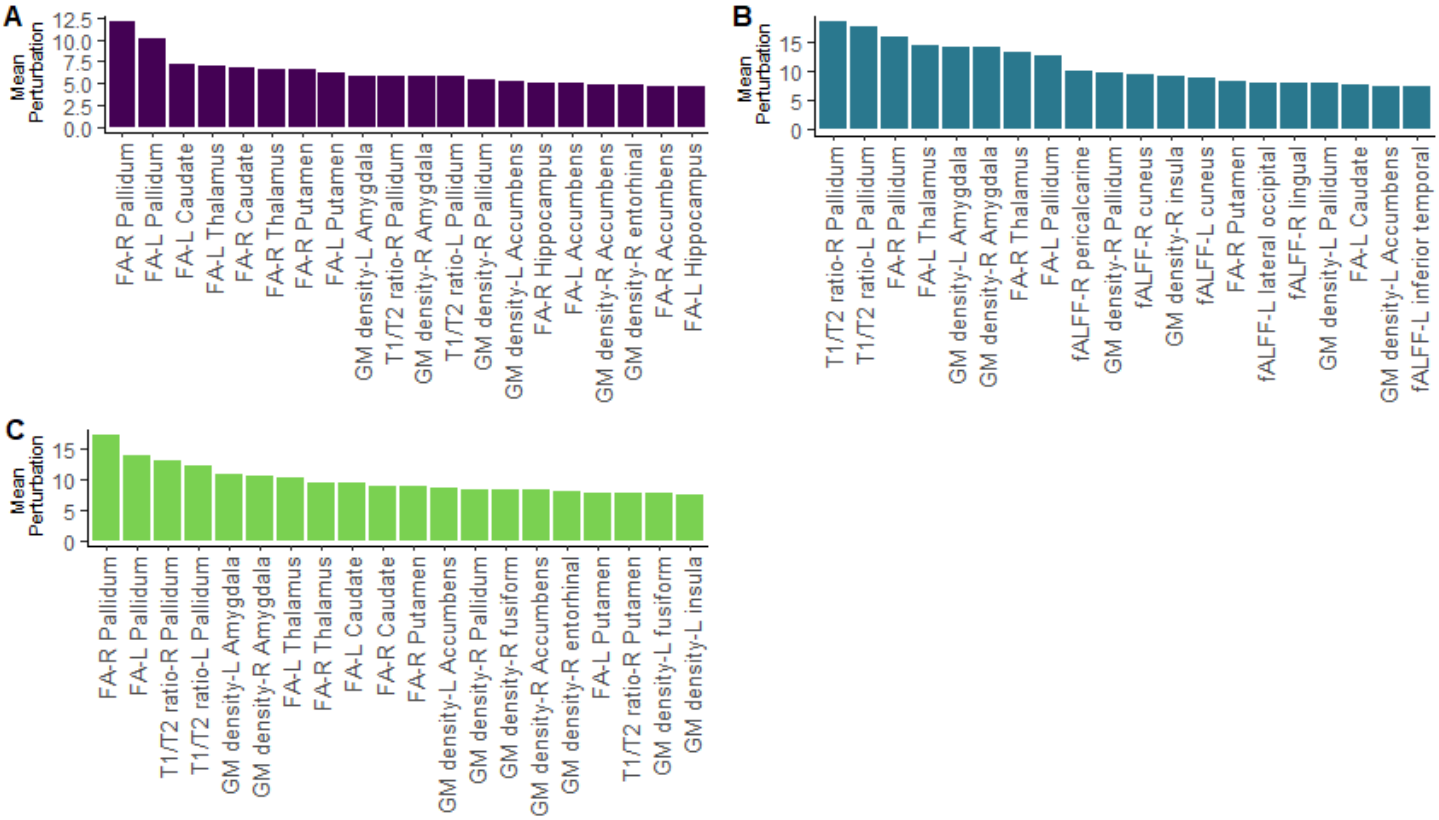

Figure 7.2: Absolute alteration in each factor-region at the estimated initial biological disease onset (Top 20 most altered factor-region pairs). **A)** C9orf72. **B)** GRN. **C)** MAPT.

7.3.3 Underlying mechanisms of disease process

Figure 7.3 shows the relative spreading, relative incoming, and relative outgoing influences. Relative spreading is generally low (ranging from 0 to 21% across factors and genetic subtypes), suggesting that spreading through structural networks is not a significant cause of factor alterations. Higher values are seen for C9orf72 and MAPT in fALFF, FA, and MD, while GRN values are low across all factors. Relative incoming and outgoing influences are slightly higher overall (ranging from 2.01 to 33.89), indicating that modalities may be more influenced by multifactorial interactions. Values are similar across factors for each subtype. fALFF is the most vulnerable, and least influential factor for both C9orf72 and MAPT, while values are again low across all factors for GRN.

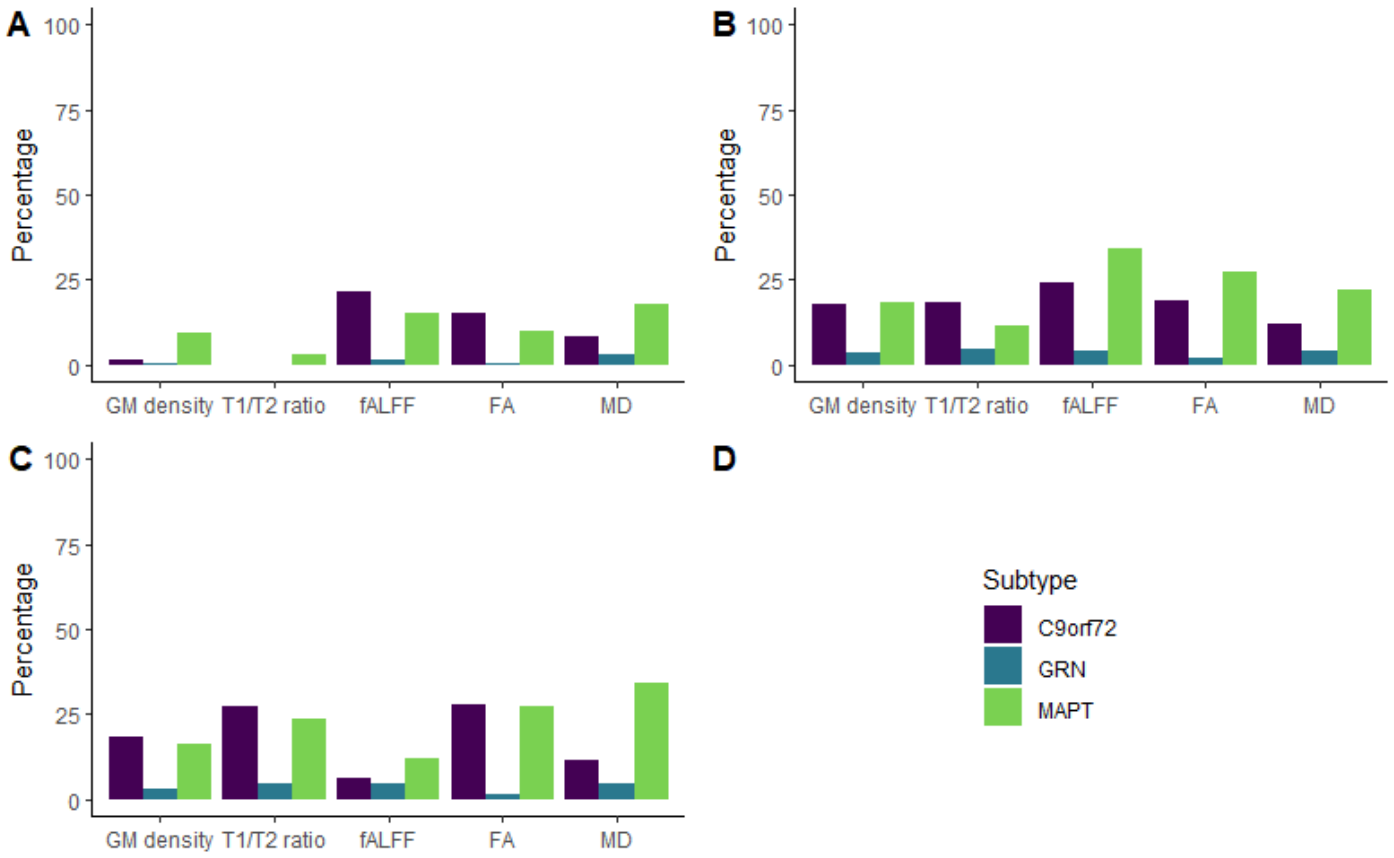

Figure 7.3. Underlying mechanisms of the disease process. **A)** Relative Spreading. **B)** Relative Incoming Influences. **C)** Relative Outgoing Influences.

7.3.4 Bootstrapping analysis

500 bootstrap repetitions were created (sampling with replacement) for each subtype. The MCM was repeated, using the cTI staging system, for each sample. Mean accuracies were slightly higher than in the original sample (approximately 17% for all subtypes; Figure 7.4A). 95% confidence intervals are wide, ranging from 0.75% to 58.32%. Histograms indicate a right-skewed distribution of the repetitions in all subtypes (Figure 7.4B-D), indicating the presence of subjects with outlier MRI values likely resulting in higher accuracy in some of the repetitions. Mean values

across repetitions for the initial perturbation and underlying mechanisms parameters were similar to values reported in the original sample.

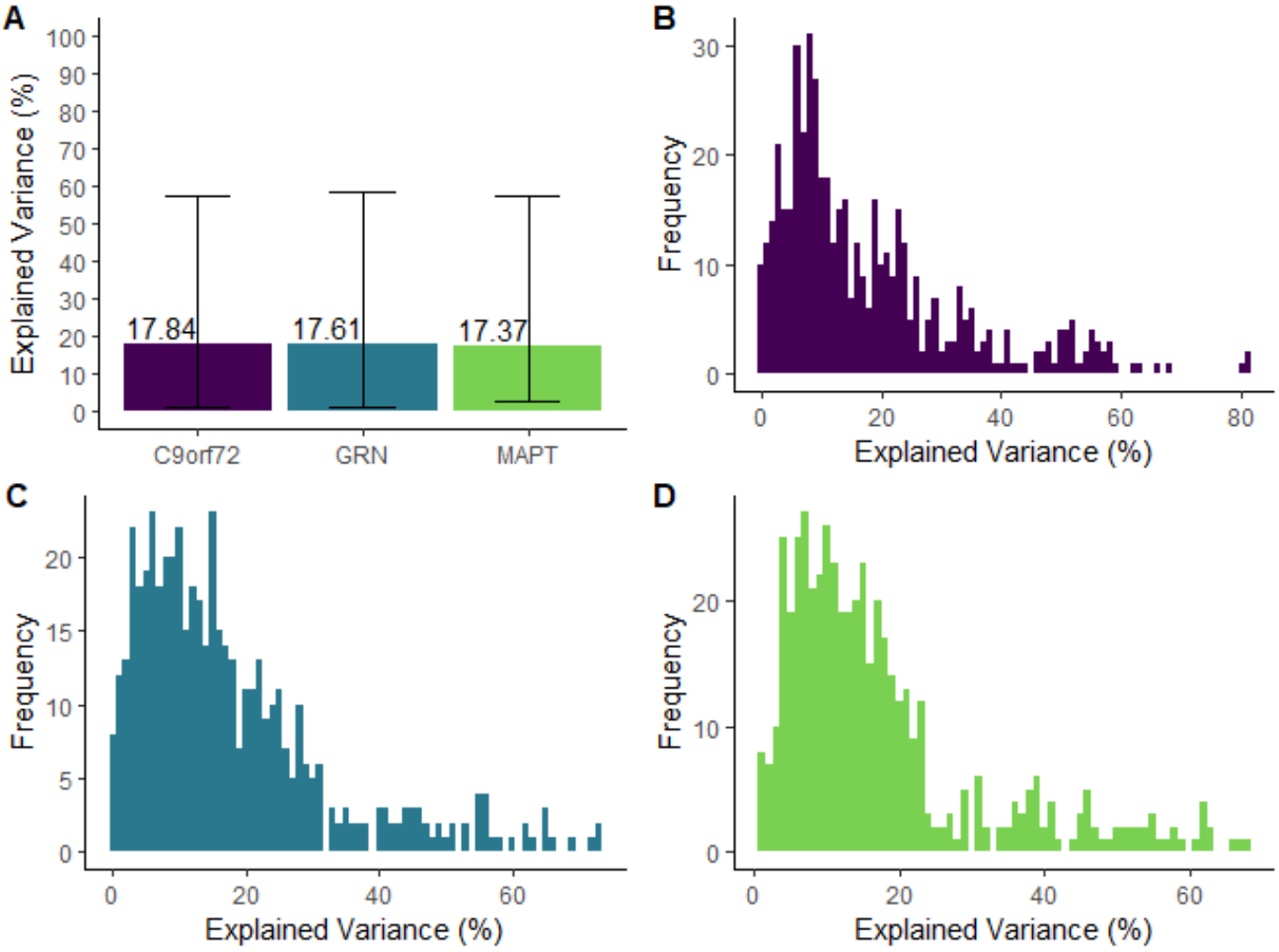

Figure 7.4: A) Mean explained variance of the MCM with 95% confidence intervals across 500 bootstrap repetitions for each genetic subtype. **B-D)** Distribution of explained variance across 500 bootstrap repetitions for **B)** C9orf72 **C)** GRN and **D)** MAPT.

7.4 Discussion

Overall, the MCM was unable to uncover specific patterns of disease onset and progression in genetic FTD subtypes. Accuracy was relatively low, indicating a poor model fit, with the

majority of the variance in the data not being accounted for by the model. This result contrasts with the application of the MCM in AD, which identified an early role for vascular perfusion changes. The poor model fit may be due to the relatively small number of subjects in each subtype, compared to the large number of features and parameters fit by the model. As well, this analysis included only metrics from structural and functional MRI, while the AD model was able to include a wider variety of factors including molecular markers of amyloid and tau. The bootstrapping analysis found wide confidence intervals in model fit, indicating high uncertainty in each subtype; results vary depending on which subjects are included in the sample. As noted, there is substantial heterogeneity in FTD (significantly more than in AD); differences in grey matter atrophy and functional activity has been previously observed within genetic groups (Lee et al., 2014; Olney et al., 2020; Sha et al., 2012; Whitwell et al., 2012), and individuals with the same genetic mutation can develop different clinical syndromes. Significantly, the model is based on cross-sectional data only; disease progression patterns are estimated using different individuals at different timepoints. It is likely that given the cross-sectional design, combined with the limited variety of MRI metrics, the relatively small sample sizes per subtype, and the heterogeneity in FTD, the MCM is unable to discern a clear average pattern of disease progression for each genetic group.

The categorical staging had the lowest accuracy, accounting for less than 5% of the variance seen in the MRI metrics in all subtypes. Continuous methods should provide a more informative staging to the MCM, while the discrete staging obscures information into arbitrary categories. The first two staging systems used here rely on the EYO, which is known to be a imprecise measure of symptom onset in FTD (Moore et al., 2020). For symptomatic subjects, they rely either on measures of clinical performance or the number of years since disease onset. The use of this information to stage subjects prevents the model from being purely data-driven, based

on biological information. In contrast, the third model uses the disease scores derived from the cTI model as applied to MRI metrics for all subjects, which we have shown are significantly correlated with EYO and clinical performance in Chapter 5. This provides a method for biologically based modelling, by combining the cTI with the MCM. In all cases however, accuracy was relatively low, with the majority of the variance in the data not being accounted for by the model.

In all three genetic groups, subcortical regions were the most altered at the estimated biological disease onset. Subcortical changes have previously been found in genetic FTD, including in presymptomatic individuals (Bocchetta, Todd, et al., 2021; Rohrer et al., 2015). These alterations were seen in FA, T1-T2 ratio, and grey matter density. As noted in Chapter 5, grey matter atrophy has been consistently reported in genetic FTD (Cash et al., 2018; Rohrer et al., 2015; Staffaroni, Cobigo, et al., 2020), while T1/T2 ratio and grey matter FA have been much less frequently studied. The analysis of the underlying mechanisms of disease progression indicates higher influence of factor-factor interactions on the disease progression than through the propagation of specific factor alterations through structural brain networks. However, percentages are relatively low across factors and genetic groups.

Overall, the model is unable to account for most of the variance in the data, limiting any conclusions which could be drawn regarding the initial disease onset and underlying mechanisms of genetic FTD progression. A larger sample size and wider variety of biological metrics may be able to provide a better fitting model.

7.5 Supplementary Figure

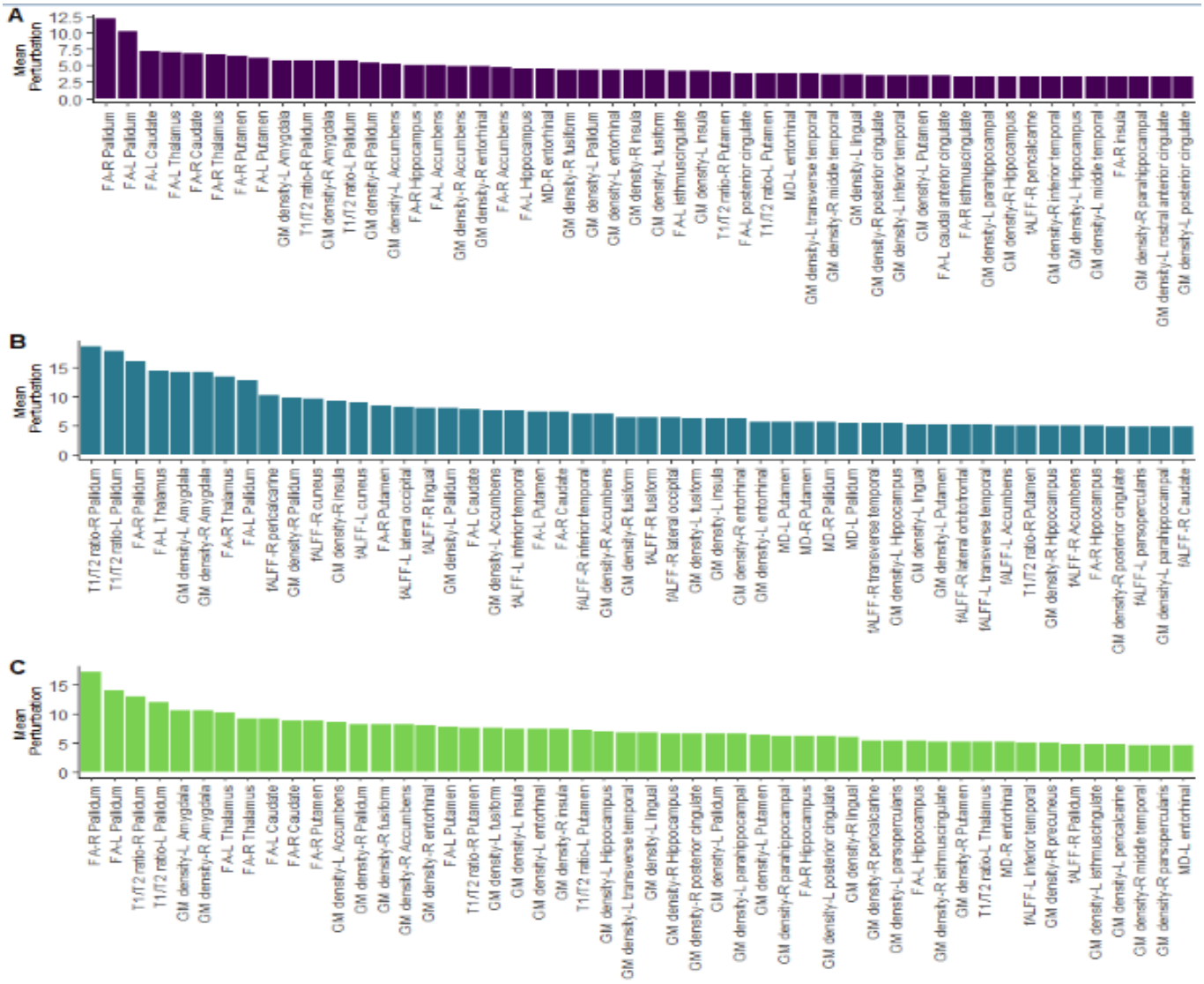

Supplementary Figure 7.1: Absolute alteration in each factor-region at the estimated initial biological disease onset (Top 50 most altered factor-region pairs). **A)** C9orf72. **B)** GRN. **C)** MAPT.

Chapter 8

Discussion

8.1 Summary of main findings and implications

This thesis aimed to explore MRI-based biomarkers in early stage FTD using computational modelling; specifically, to explore the application of machine learning and disease progression modelling with MRI-derived metrics in the diagnosis, staging, subtyping, and underlying mechanisms of FTD. We showed that morphometric MRI can accurately distinguish individuals with FTD from cognitively healthy individuals and from those with other forms of dementia in well defined datasets using machine learning techniques, giving promise to this method as an aide in FTD diagnosis (Chapter 3). Focusing on genetic FTD, we then applied two recently developed models of disease progression (cTI and MCM) to MRI-based metrics. Using the cTI, we showed that presymptomatic and symptomatic gene carriers can be staged using only MRI-based measures, obtaining biologically based disease scores that correlate with estimated disease onset and clinical performance (Chapter 5). Using the same model, we showed that MRI metrics alone were insufficient to distinguish between genetic subtypes (Chapter 6) and to identify distinct patterns of disease onset and mechanisms of progression using the MCM (Chapter 7) in presymptomatic and symptomatic gene carriers.

Overall, the analyses presented in this thesis indicate the potential of machine learning and disease progression modelling to improve understanding of FTD and indicate the potential benefits of MRI-based measures as effective biomarkers. They present good evidence for the continuing development of MRI-based computational methods for early FTD diagnosis, staging and disease monitoring.

The systematic review of FTD diagnostic classification found grey matter volumetric measures could accurately detect FTD, while indicating white matter DTI changes may be a sensitive biomarker in early stage FTD. The cTI staging model suggests that grey matter mean diffusivity is an important measure which may warrant further investigation of grey matter microstructural changes, which have been little investigated to date. Furthermore, the cTI staging model found that while single biomarkers may perform reasonably well on their own and have high clinical feasibility, the inclusion of other advanced imaging metrics increases precision, particularly in presymptomatic subjects and therefore could be valuable in a clinical trial setting. The systematic review did not find a proven benefit of a multimodal approach over single modalities in the few studies that did it (Bron et al., 2017; Klöppel, Stonnington, Chu, et al., 2008; Corey T. McMillan et al., 2014; Cory T. McMillan et al., 2012). More research is needed to confirm that a combination of complementary biomarkers would provide the best results in these analyses, although inclusion of more complex imaging metrics needs to be balanced with feasibility, especially in a clinical setting.

The analyses presented in this thesis also showcase some of the difficulties in applying computational models to complex heterogeneous diseases, and the limitations of the dataset used here, which contains primarily presymptomatic subjects, many of whom are far (20 – 30 years) from probable symptom onset. Brain changes in these individuals are expected to be subtle, and therefore difficult to detect. Importantly, we were able to obtain disease scores which reflect disease progression despite these limitations. Data-driven subtyping and mechanistic modelling would likely benefit from the inclusion of a larger number of subjects across the full disease course and more diverse biological factors.

8.2 Advantages of the current data-driven approach

There are several advantages to the current computational approach taken in this thesis. The chosen models are data-driven and based solely on biological information as opposed to clinical scales that introduce a component of subjective judgment. They are also able to combine information from various biomarkers, and therefore should be able to provide information above and beyond what clinical tests and individual biomarkers can provide. Importantly they have the potential to provide good biomarkers that can detect subtle changes in the earliest disease stages, before existing validated methods including visual reading of structural MRI and FDG-PET.

Discriminative modelling, such as supervised machine learning models used in classifications tasks, should be able to pick up on differences that can't be easily observed in very early-stage disease. Our systematic review shows that a wide variety of methods have been employed to study this task; it therefore remains to be seen what method may be the most appropriate to aid clinicians in early diagnosis.

The cTI is a data-driven model which does not rely on any a priori phenotypical information. It is able to obtain disease staging and subtyping from cross-sectional data. Furthermore, it can incorporate various features from high dimensional data, and data-driven feature selection, eliminating the necessity of choosing select biomarkers or brain regions, seen in existing models (Panman et al., 2021; Young et al., 2018). It therefore provides unbiased biomarkers based solely on biological metrics. Further work will be needed to evaluate the usefulness of this type of measure as a validated outcome for clinical trials. It would be particularly useful for trials of potential FTD-modifying therapies which would include genetic carriers who

are at various disease stages, including a combination of presymptomatic and symptomatic individuals.

The MCM is the first model to my knowledge which attempts to combine various biological factors and network-based spreading, to determine causal inference. It is also able to estimate the onset of the biological disease process, estimating the biological factors and brain regions that are most likely to be implicated in the disease origin. This is in contrast to previous research which has estimated epicentres based on the atrophy patterns of those with a clinical FTD diagnosis (Seeley et al., 2009; Zhou et al., 2012), an approach which does not necessarily indicate disease origin, as the most atrophied regions at late stage disease are not necessarily the regions where the disease originated. The MCM also uses biomarker and structural connectivity data from the full disease course, unlike previous models which have correlated healthy network connectivity patterns to end stage disease.

When applied on a group level the MCM requires a priori staging of subjects based on disease severity. The model is therefore only as good as the staging used. Stages based on clinical data or EYO may not necessarily be indicative of underlying biological processes. Previous research into genetic FTD has often used EYO to study disease progression, however the age of symptom onset can be highly variable, with wide variations sometimes found within family members. This variability is larger for C9orf72 and GRN mutations than for MAPT mutations (Moore et al., 2020), meaning that using EYO can lead to larger errors in estimating the timing of disease changes, especially in C9orf72 and GRN (Rohrer et al., 2015). However, when used in combination with the cTI staging and subtyping the MCM becomes as purely data-driven model (the cTI was in fact designed with this purpose in mind).

8.3 Limitations

8.3.1 Systematic review

Studies included in the systematic review are highly heterogeneous in terms of population demographics and methodology. These issues are similar to those regarding the diagnostic classification of AD (Falahati et al., 2014; Rathore et al., 2017).

Studies varied considerably on the subjects they included. Studies using small homogenous samples may result in the overfitting of data. A major issue with studies is the inclusion of well-characterized subjects that tend to be at a later disease stage and therefore may find higher accuracy because brain changes are more substantial and easier to differentiate. Ideally studies need to include patients in the earliest stages of the disease when diagnoses are ambiguous, such as the naturalistic symptom-based inclusion approach taken by the Late-Onset Frontal lobe study (Krudop et al., 2014). Many studies grouped FTD clinical variants together in analysis. Others have indicated that this may lead to the language variants driving the classification, resulting in higher performance (Möller et al., 2016). Several studies conducted a group-level analysis and then used the significant regions from this analysis in their classification. This will reduce the generalizability of the results as the regions used may be biased to the specific group of patients included in the study. For these reasons, results reported in these studies may be artificially high. Most studies utilized a cross-validation approach, where *k* subjects are sequentially left out of the training group, while others split the subjects into separate training and testing sets. Ideally studies should also validate classifiers on a separate independent cohort. It is likely that this would result in lower accuracy than the numbers reported in several of the studies included in the systematic review, given the methodology used.

Studies also differed in the metrics used to report results. We reported the most common metrics across studies (accuracy, sensitivity, specificity, and AUC). Some studies did not report sensitivity/specificity but only accuracy or AUC. While useful, these metrics are not sufficient on their own. As only a small number of studies reported balanced accuracy those numbers were not reported.

Limitations of the systematic review also include the possibility of incomplete retrieval of relevant papers, however more than one search engine was used and reference lists of included papers were reviewed for additional relevant papers, so this should be minimal. As only published studies were included in this review there is the potential for publication bias. The main biases identified in the included studies were the exclusion of subjects with abnormalities other than atrophy on structural MRI and the lack of an independent testing set.

Finally, while there has been major improvement in automated structural MRI processing pipelines over the years, there remains significant methodological challenges to its application at the single-subject level. One of the main limitations to the clinical validity of such methods is the variability with regards to sites, scanners, and repeated image acquisitions. This variability leads to inconsistency in measurements that reduce the accuracy of diagnostic classifications based on subtle differences in atrophy or other morphometric measures. The ideal MRI processing pipeline needs to perform robust registration and precise cortical and subcortical segmentation across different scanners. It should further be able to perform intra-subject registration to measure subtle brain changes over time. Being able to compare subjects to a large database of healthy controls across ages, sex and education level is also of significant benefit.

8.3.2 Data-driven analyses of genetic FTD

Data-driven models are always limited by the data in which they utilize; the ability of the models to give an accurate picture of disease progression depends on how well the data represent the underlying biological processes (Iturria-Medina, Sotero, Toussaint, Mateos-Perez, & Evans, 2016). Our analyses in this thesis were limited to cross-sectional, group level analyses. Models which can use purely cross-sectional data are important and useful especially as longitudinal dataset are much less common. The cTI is an example of this type of model which is able to uncover temporal patterns and provide accurate staging from cross-sectional data.

However, group-level studies inevitably mask some of the heterogeneity of FTD. Inferences from cross-sectional models make the assumption that biomarker trajectories are similar across all individuals. In the MCM analysis, subjects were grouped according to genetic mutation, meaning symptomatic subjects with different phenotypes were grouped together, while we do not know which clinical syndrome the presymptomatic subjects will eventually develop. This means that, while subjects were grouped with similar underlying pathology, the onset of biomarker changes and affected brain regions may be highly variable across individuals. In the MCM analysis, while we were able to use the cTI staging scores, the cTI was unable to find accurate subtypes; subjects were therefore only grouped according to gene mutation. With improvements in the cTI subtyping, it may be possible to observe data-driven subtypes within each genetic group, which may allow for an average disease trajectory to be obtained from the MCM for each data-driven subtype.

The current MCM analysis was limited by the number of subjects with longitudinal data available. As such, although the MCM has been formulated for individual analysis, it was not

possible to apply the model on an individual level here. Therefore, the data-driven model as applied to genetic FTD is not causal in nature, although the generative model itself is.

A limitation of these analyses is the modalities used. All neuroimaging features used in the genetic FTD disease progression models are structural and functional MRI features derived from the grey matter. This is because the MCM is currently only able to be applied to grey matter metrics. Furthermore, we were unable to include cerebral blood flow (CBF) measures from arterial spin labelling (ASL) MRI, as there is currently a wide variety of ASL acquisition protocols used across GENFI sites, which made processing this data unfeasible. Several of the included measures provide similar, inter-related information to the models, and while each included metric is used as a proxy for a different underlying biological process, the precision of these measures may be limited, reducing the effectiveness of these methods.

We were unable to use the FTD-CDR as a measure of disease severity for all subjects in the clinical staging in MCM and for the validation of cTI scores as it was not available in the majority of individuals. Finally, we used EYO as a measure of disease severity, both in the first two staging systems for the MCM, as well as to validate the cTI disease scores. EYO, as discussed, has been shown to be imprecise as a predictor of actual onset (Moore et al., 2020). Furthermore, it is likely affected by varied interpretations of the timing of symptom onset. Given the known diagnostic delays in bvFTD (Woolley et al., 2011), the accuracy of symptom onset may vary across clinical syndromes. However, EYO remains the only predictive estimate of time to symptom onset other than age.

8.4 Future directions

8.4.1 Potential biomarkers

This thesis focuses on MRI-based biomarkers, and primarily on structural changes. The systematic review in Chapter 3 focuses on morphometric MRI measures as the majority of studies published in this area have focused on morphometry. A few recent studies have looked at the added benefit of ASL or fMRI, and suggest that they may provide additional discriminative power. (Bron et al., 2017; Tahmasian et al., 2016).

As mentioned, the disease progression modelling in genetic FTD analyses focused only on MRI-based grey matter changes. They would benefit from the addition of other biomarkers, providing a wider variety of biological processes. ASL-derived CBF has been shown to be decreased in presymptomatic gene carriers (Dopper et al., 2016; Mutsaerts et al., 2019). A crucial step in implementing ASL is the harmonization of protocols across centres. While the MCM currently includes grey matter metrics only, the cTI allows for the inclusion of all types of biomarkers. Including DWI metrics from white matter in future models may provide increased benefit to the model. White matter microstructure changes may be an early feature of FTD (Feis et al., 2018; Jiskoot, Bocchetta, et al., 2018), and have shown to have high discriminative power in the systematic review. The implementation of more advanced DWI acquisitions would allow for the inclusion of newer DWI-based white matter metrics, such as fixel analysis, which should provide more precise measures of underlying microstructure compared to DTI measures (Dhollander et al., 2021).

Future models would likely also benefit from non-MRI and non-imaging biomarkers. FDG-PET, measuring glucose metabolism, is a measure which is already used clinically;

hypometabolism has also been observed in presymptomatic mutation carriers (Caroppo et al., 2015; Clarke et al., 2021; Jacova et al., 2013; Popuri et al., 2021). Neurofilament light chain, increased levels of which are thought to reflect axonal damage, has good potential as a prognostic biomarker in clinical FTD (Benussi et al., 2020; Rohrer et al., 2016) and presymptomatic mutation carriers (Meeter et al., 2016; Rojas et al., 2021; van der Ende et al., 2019). As well, increased levels of glial fibrillary acidic protein, a marker of astrocytic damage, have been found in GRN mutation carriers as well as in individuals with clinical FTD (Heller et al., 2020; Zhu et al., 2021).

In including a variety of biomarkers, it is important to balance benefit with clinical feasibility, especially for use in clinical settings. Additional MRI sequences can be performed in the same session. However, while the addition of more complex imaging metrics may improve accuracy in a research context, this would be harder to translate into clinical settings in which long MRI acquisition and a stringent quality control process in image processing are not feasible. Fluid biomarkers which can be measured from blood samples, such as neurofilament light chain, would be highly feasible and minimally invasive. Ultimately, a select number of biomarkers providing distinct information to the models, such as a combination of imaging and non-imaging metrics may provide the best results.

The current MCM analysis uses DWI-derived structural connectivity networks. The model allows for the inclusion of additional networks. The previous application of this model to AD included both structural networks and vascular networks derived from ASL (Iturria-Medina et al., 2017). It is also possible to include functional networks in the MCM; with the limitation being that these networks have an unknown underlying biological basis, unlike structural connectivity, which estimates physical connections between brain regions. For this reason, a structural network was used in the current analysis. Currently, the MCM can incorporate only grey matter derived

neuroimaging measures. Future versions are incorporating the effects of gene expression data and molecular data into the model (Adewale et al., 2021). The inclusion of more biological variables, from imaging to protein and genes, will constitute a truly integrative mechanistic model of disease progression.

8.4.2 Longitudinal, single-subject level studies

Individual level studies will be important to help understand some of the complexity that is masked by group level analysis, with the availability of more longitudinal datasets. GENFI is an ongoing study which continues to collect longitudinal data from participants. This data will allow for individual subject MCM analysis. The model has been applied in this manner to AD (Iturria-Medina et al., 2018). This will allow for the estimation of the variation in disease progression patterns in different genetic groups and disease stages.

Furthermore, individual subject models can be used to predict the time of symptom onset in each individual, based on the predicted future trajectories of the included biological and clinical markers. Also, on an individual level it is possible to model the influence of external effects, such as medications or lifestyle factors, and their effect on the individual's disease process. Finally, the MCM equations can be reversed to estimate which biomarker(s) a potential treatment would need to target in each individual (Iturria-Medina et al., 2018).

8.4.3 Real-life clinical cohorts

Disease progression models currently remain largely within the research domain. Further work is needed to evaluate the usefulness of these types of measures clinically and as validated outcomes for clinical trials.

Discriminative models need to be feasible for use in clinical practice; a straight-forward process that is not time consuming and is easy to interpret is needed, and it needs to be applicable across scanner types and centres. This type of method may be especially helpful for those clinicians with less experience diagnosing FTD, such as community hospitals and primary care physicians that do not have easy access to specialty FTD clinics.

Significantly, few published studies have attempted to apply machine learning derived diagnostic classifiers to real-life clinical settings at the individual level. This is a crucial step given that clinical populations are more heterogenous than well-characterize cohorts from large-scale imaging studies. For instance, pre-existing brain changes (e.g., past cerebro-vascular accident) and co-morbidities (e.g., alcohol use disorder) are commonly seen in memory clinics but are often not represented by the training sets of these studies. Only one study identified in the systematic review attempted to replicate the typical population of a memory clinic (Klöppel et al., 2015). Although this comes with significant challenges and lower accuracy than in the training set (Klöppel et al., 2015), it is an essential step before recommending the clinical use of these algorithms. In order to translate morphometric tools for FTD in clinical practice, it will be crucial to validate the use of automated morphometric MRI methods in a naturalistic mixed neuropsychiatric population, such as the distinction of those presenting with FTD-like symptoms at baseline into those ultimately diagnosed with FTD versus those not. Future studies should validate MRI automated morphometry methods in a mixed cohort of early disease stage patients, using final diagnosis (and ideally when available proven pathology at autopsy) as a gold standard.

Biomarkers of the presymptomatic and early symptomatic stage of genetic FTD would be a great benefit for future disease-modifying clinical trials, including the development of data-driven biologically based staging and subtyping. These models could potentially improve patient

selection and reduce required sample sizes in clinical trials (Pankov et al., 2016), which would accelerate drug discovery. Clear performance measures will also be needed for these applications; the model output needs to be easily understandable for users, including the model assumptions and the subsequent biases in the model's predictions, so that the results are not misinterpreted (Oxtoby & Alexander, 2017).

Studies included in the systematic review in Chapter 3 focused predominantly on sporadic FTD. This has been rarely studied in genetic FTD, although a recent study conducted single-subject multimodal MRI classification in presymptomatic mutation carriers compared to non-carriers, finding DTI metrics outperformed grey matter density and fMRI (Feis et al., 2018). It remains to be determined how FTD MRI biomarkers developed with sporadic FTD cohorts would fare in a population of genetic FTD given their less typical atrophy patterns extending beyond frontal and anterior temporal areas (Rohrer et al., 2015; Whitwell et al., 2012, 2015). Similarly, biomarkers developed in genetic FTD will require validation for use in sporadic cases of FTD.

8.5 Conclusions

In summary, this thesis sought to explore the use of computational methods in the application of MRI techniques as early-stage biomarkers in FTD. The analyses presented here demonstrate the potential for data-driven methods to develop accurate biomarkers of early-stage disease processes, while also showcasing some of the limitations and further work required to implement these methods most effectively.

We showed that current evidence provides good support for the ongoing development of automated morphometric MRI to improve the diagnosis and prognosis of early stage FTD in clinical practice. The inclusion of 3D-T1 MRI sequences in clinical imaging protocols would

facilitate the development of these tools, and eventually the integration of these methods in practice. However, more studies that use rigorous methodology and prospectively validate findings in independent real-life cohorts are needed before this method could be recommended in clinical practice.

We also find promising evidence for the development of unifying staging of heterogeneous neurodegenerative disorders using data-driven, unsupervised methods. Neuroimaging features show promise as potential biomarkers of disease progression but would most likely benefit from being combined with complementary clinical and biological information for optimal staging. While further validation work is required, biologically based staging systems are a promising tool to monitor monitoring disease progression and treatment outcomes in future clinical trials of genetic FTD.

We are unable to validate data-driven subtypes or uncover average trajectories of disease initiation and progression in genetic FTD based on MRI measures alone. A larger dataset and wider variety of biomarkers, as well as MCM application on an individual level, will likely lead to improved subtyping and understanding of causal mechanisms in future studies.

Overall, these results contribute to an improved understanding of MRI-based biomarkers in early stage FTD, lending themselves to the development of improved biomarkers and clinical applications.

Bibliography

Abid, A., Zhang, M. J., Bagaria, V. K., & Zou, J. (2018). Exploring patterns enriched in a dataset with contrastive principal component analysis. *Nature Communications*, *9*(1), 2134. https://doi.org/10.1038/s41467-018-04608-8

Adewale, Q., Khan, A. F., Carbonell, F., & Iturria-Medina, Y. (2021). Integrated transcriptomic and neuroimaging brain model decodes biological mechanisms in aging and Alzheimer's disease. *ELife*, *10*, 1–22. https://doi.org/10.7554/eLife.62589

Agosta, F., Galantucci, S., Magnani, G., Marcone, A., Martinelli, D., Antonietta Volontè, M., Riva, N., Iannaccone, S., Ferraro, P. M., Caso, F., Chiò, A., Comi, G., Falini, A., & Filippi, M. (2015). MRI signatures of the frontotemporal lobar degeneration continuum. *Human Brain Mapping*, *36*(7), 2602–2614. https://doi.org/10.1002/hbm.22794

Agosta, F., Scola, E., Canu, E., Marcone, A., Magnani, G., Sarro, L., Copetti, M., Caso, F., Cerami, C., Comi, G., Cappa, S. F., Falini, A., & Filippi, M. (2012). White matter damage in frontotemporal lobar degeneration spectrum. *Cerebral Cortex*, *22*(12), 2705–2714. https://doi.org/10.1093/cercor/bhr288

Andreasen, N. C., Nopoulos, P., Magnotta, V., Pierson, R., Ziebell, S., & Ho, B.-C. C. (2011). Progressive brain change in schizophrenia: A prospective longitudinal study of first-episode schizophrenia. *Biological Psychiatry*, *70*(7), 672–679. https://doi.org/10.1016/j.biopsych.2011.05.017

Ashburner, J. (2007). A fast diffeomorphic image registration algorithm. *NeuroImage*, *38*, 95–113. https://doi.org/10.1016/j.neuroimage.2007.07.007

Bateman, R. J., Xiong, C., Benzinger, T. L. S., Fagan, A. M., Goate, A., Fox, N. C., Marcus, D. S., Cairns, N. J., Xie, X., Blazey, T. M., Holtzman, D. M., Santacruz, A., Buckles, V., Oliver, A., Moulder, K., Aisen, P. S., Ghetti, B., Klunk, W. E., McDade, E., … Morris, J. C. (2012). Clinical and biomarker changes in dominantly inherited Alzheimer's disease. *New England Journal of Medicine*, *367*(9), 795–804. https://doi.org/10.1056/NEJMoa1202753

Benussi, A., Karikari, T. K., Ashton, N., Gazzina, S., Premi, E., Benussi, L., Ghidoni, R., Rodriguez, J. L., Emeršič, A., Simrén, J., Binetti, G., Fostinelli, S., Giunta, M., Gasparotti, R., Zetterberg, H., Blennow, K., & Borroni, B. (2020). Diagnostic and prognostic value of serum NfL and p-Tau 181 in frontotemporal lobar degeneration. *Journal of Neurology, Neurosurgery and Psychiatry*, *91*, 960–967. https://doi.org/10.1136/jnnp-2020-323487

Bertoux, M., De Souza, L. C., Corlier, F., Lamari, F., Bottlaender, M., Dubois, B., & Sarazin, M. (2014). Two distinct amnesic profiles in behavioral variant frontotemporal dementia. *Biological Psychiatry*, *75*(7), 582–588. https://doi.org/10.1016/j.biopsych.2013.08.017

Bisenius, S., Mueller, K., Diehl-Schmid, J., Fassbender, K., Grimmer, T., Jessen, F., Kassubek, J., Kornhuber, J., Landwehrmeyer, B., Ludolph, A., Schneider, A., Anderl-Straub, S., Stuke, K., Danek, A., Otto, M., Schroeter, M. L., & FTLDc study group. (2017). Predicting primary progressive aphasias with support vector machine approaches in structural MRI data. *NeuroImage: Clinical*, *14*, 334–343. https://doi.org/10.1016/j.nicl.2017.02.003

Bisenius, S., Neumann, J., & Schroeter, M. L. (2016). Validating new diagnostic imaging criteria for primary progressive aphasia via anatomical likelihood estimation meta-analyses. *European Journal of Neurology*, *23*, 704–712. https://doi.org/10.1111/ene.12902

Bocchetta, M., Malpetti, M., Todd, E. G., Rowe, J. B., & Rohrer, J. D. (2021). Looking beneath

the surface: the importance of subcortical structures in frontotemporal dementia. *Brain Communications*, *3*(3). https://doi.org/10.1093/BRAINCOMMS/FCAB158

Bocchetta, M., Todd, E. G., Peakman, G., Cash, D. M., Convery, R. S., Russell, L. L., Thomas, D. L., Iglesias, J. E., van Swieten, J. C., Jiskoot, L. C., Seelaar, H., Borroni, B., Galimberti, D., Sanchez-Valle, R., Laforce, R., Moreno, F., Synofzik, M., Graff, C., Masellis, M., … Zulaica, M. (2021). Differential early subcortical involvement in genetic FTD within the GENFI cohort. *NeuroImage. Clinical*, *30*. https://doi.org/10.1016/J.NICL.2021.102646

Borroni, B., Alberici, A., Premi, E., Archetti, S., Garibotto, V., Agosti, C., Gasparotti, R., Di Luca, M., Perani, D., & Padovani, A. (2008). Brain magnetic resonance imaging structural changes in a pedigree of asymptomatic progranulin mutation carriers. *Rejuvenation Research*, *11*(3), 585–595. https://doi.org/10.1089/rej.2007.0623

Borroni, Barbara, Alberici, A., Cercignani, M., Premi, E., Serra, L., Cerini, C., Cosseddu, M., Pettenati, C., Turla, M., Archetti, S., Gasparotti, R., Caltagirone, C., Padovani, A., & Bozzali, M. (2012). Granulin mutation drives brain damage and reorganization from preclinical to symptomatic FTLD. *Neurobiology of Aging*, *33*(10), 2506–2520. https://doi.org/10.1016/j.neurobiolaging.2011.10.031

Bron, E. E., Smits, M., Papma, J. M., Steketee, R. M. E., Meijboom, R., de Groot, M., van Swieten, J. C., Niessen, W. J., & Klein, S. (2017). Multiparametric computer-aided differential diagnosis of Alzheimer's disease and frontotemporal dementia using structural and advanced MRI. *European Radiology*, *27*(8), 3372–3382. https://doi.org/10.1007/s00330-016-4691-x

Brown, J. A., Deng, J., Neuhaus, J., Sible, I. J., Sias, A. C., Lee, S. E., Kornak, J., Marx, G. A., Karydas, A. M., Spina, S., Grinberg, L. T., Coppola, G., Geschwind, D. H., Kramer, J. H.,

Gorno-Tempini, M. L., Miller, B. L., Rosen, H. J., & Seeley, W. W. (2019). Patient-Tailored, Connectivity-Based Forecasts of Spreading Brain Atrophy. *Neuron*, *104*(5), 856-868.e5. https://doi.org/10.1016/j.neuron.2019.08.037

Canu, E., Agosta, F., Mandic-Stojmenovic, G., Stojković, T., Stefanova, E., Inuggi, A., Imperiale, F., Copetti, M., Kostic, V. S., & Filippi, M. (2017). Multiparametric MRI to distinguish early onset Alzheimer's disease and behavioural variant of frontotemporal dementia. *NeuroImage: Clinical*, *15*, 428–438. https://doi.org/10.1016/j.nicl.2017.05.018

Caroppo, P., Habert, M. O., Durrleman, S., Funkiewiez, A., Perlbarg, V., Hahn, V., Bertin, H., Gaubert, M., Routier, A., Hannequin, D., Deramecourt, V., Pasquier, F., Rivaud-Pechoux, S., Vercelletto, M., Edouart, G., Valabregue, R., Lejeune, P., Didic, M., Corvol, J. C., … Le Ber, I. (2015). Lateral Temporal Lobe: An Early Imaging Marker of the Presymptomatic GRN Disease? *Journal of Alzheimer's Disease*, *47*(3), 751–759. https://doi.org/10.3233/JAD-150270

Cash, D. M., Bocchetta, M., Thomas, D. L., Dick, K. M., van Swieten, J. C., Borroni, B., Galimberti, D., Masellis, M., Tartaglia, M. C., Rowe, J. B., Graff, C., Tagliavini, F., Frisoni, G. B., Laforce, R., Finger, E., de Mendonça, A., Sorbi, S., Rossor, M. N., Ourselin, S., & Rohrer, J. D. (2018). Patterns of gray matter atrophy in genetic frontotemporal dementia: results from the GENFI study. *Neurobiology of Aging*, *62*, 191–196. https://doi.org/10.1016/j.neurobiolaging.2017.10.008

Cheran, G., Wu, L., Lee, S., Manoochehri, M., Cines, S., Fallon, E., Lynch, T., Heidebrink, J., Paulson, H., Goldman, J., Huey, E., & Cosentino, S. (2019). Cognitive Indicators of Preclinical Behavioral Variant Frontotemporal Dementia in MAPT Carriers. *Journal of the*

International Neuropsychological Society, *25*(2), 184–194. https://doi.org/10.1017/S1355617718001005

Chow, T. W., Binns, M. a, Freedman, M., Stuss, D. T., Ramirez, J., Scott, C. J. M., & Black, S. (2008). Overlap in frontotemporal atrophy between normal aging and patients with frontotemporal dementias. *Alzheimer Disease and Associated Disorders*, *22*(4), 327–335. https://doi.org/10.1097/WAD.0b013e31818026c4

Chow, T. W., Gao, F., Links, K. A., Ween, J. E., Tang-Wai, D. F., Ramirez, J., Scott, C. J. M., Freedman, M., Stuss, D. T., & Black, S. E. (2011). Visual rating versus volumetry to detect frontotemporal dementia. *Dementia and Geriatric Cognitive Disorders*, *31*(5), 371–378. https://doi.org/10.1159/000328415

Clarke, M. T. M., St-Onge, F., Beauregard, J. M., Bocchetta, M., Todd, E., Cash, D. M., Rohrer, J. D., & Laforce, R. (2021). Early anterior cingulate involvement is seen in presymptomatic MAPT P301L mutation carriers. *Alzheimer's Research and Therapy*, *13*(1). https://doi.org/10.1186/s13195-021-00777-9

Cohen, A. D., Landau, S. M., Snitz, B. E., Klunk, W. E., Blennow, K., & Zetterberg, H. (2019). Fluid and PET biomarkers for amyloid pathology in Alzheimer's disease. In *Molecular and Cellular Neuroscience* (Vol. 97, pp. 3–17). Academic Press Inc. https://doi.org/10.1016/j.mcn.2018.12.004

Davatzikos, C., Resnick, S. M., Wu, X., Parmpi, P., & Clark, C. M. (2008). Individual patient diagnosis of AD and FTD via high-dimensional pattern classification of MRI. *NeuroImage*, *41*(4), 1220–1227. https://doi.org/10.1016/j.neuroimage.2008.03.050

Day, G. S., Farb, N. A. S., Tang-Wai, D. F., Masellis, M., Black, S. E., Freedman, M., Pollock, B.

G., & Chow, T. W. (2013). Salience network resting-state activity prediction of frontotemporal dementia progression. *JAMA Neurology*, *70*(10), 1249–1253. https://doi.org/10.1001/jamaneurol.2013.3258

De Souza, L. C., Chupin, M., Bertoux, M., Lehéricy, S., Dubois, B., Lamari, F., Le Ber, I., Bottlaender, M., Colliot, O., & Sarazin, M. (2013). Is hippocampal volume a good marker to differentiate alzheimer's disease from frontotemporal dementia? *Journal of Alzheimer's Disease*, *36*(1), 57–66. https://doi.org/10.3233/JAD-122293

Dhollander, T., Clemente, A., Singh, M., Boonstra, F., Civier, O., Duque, J. D., Egorova, N., Enticott, P., Fuelscher, I., Gajamange, S., Genc, S., Gottlieb, E., Hyde, C., Imms, P., Kelly, C., Kirkovski, M., Kolbe, S., Liang, X., Malhotra, A., … Caeyenberghs, K. (2021). Fixel-based Analysis of Diffusion MRI: Methods, Applications, Challenges and Opportunities. *NeuroImage*, *241*, 118417. https://doi.org/10.1016/J.NEUROIMAGE.2021.118417

Dopper, E. G. P., Chalos, V., Ghariq, E., den Heijer, T., Hafkemeijer, A., Jiskoot, L. C., de Koning, I., Seelaar, H., van Minkelen, R., van Osch, M. J. P., Rombouts, S. A. R. B., & van Swieten, J. C. (2016). Cerebral blood flow in presymptomatic MAPT and GRN mutation carriers: A longitudinal arterial spin labeling study. *NeuroImage: Clinical*, *12*, 460–465. https://doi.org/10.1016/j.nicl.2016.08.001

Dopper, E. G. P., Rombouts, S. A. R. B., Jiskoot, L. C., Den Heijer, T., De Graaf, J. R. A., De Koning, I., Hammerschlag, A. R., Seelaar, H., Seeley, W. W., Veer, I. M., Van Buchem, M. A., Rizzu, P., & Van Swieten, J. C. (2014). Structural and functional brain connectivity in presymptomatic familial frontotemporal dementia. *Neurology*, *83*, e19–e26. https://doi.org/10.1212/WNL.0000000000000583

Drzezga, A. (2018). The network degeneration hypothesis: Spread of neurodegenerative patterns along neuronal brain networks. *Journal of Nuclear Medicine*, *59*(11), 1645–1648. https://doi.org/10.2967/jnumed.117.206300

Du, A.-T., Schuff, N., Kramer, J. H., Rosen, H. J., Gorno-Tempini, M. L., Rankin, K., Miller, B. L., & Weiner, M. W. (2007). Different regional patterns of cortical thinning in Alzheimer's disease and frontotemporal dementia. *Brain*, *130*(4), 1159–1166. https://doi.org/10.1093/brain/awm016

Ducharme, S., Price, B. H., Larvie, M., Dougherty, D. D., & Dickerson, B. C. (2015). Clinical approach to the differential diagnosis between behavioral variant frontotemporal dementia and primary psychiatric disorders. *The American Journal of Psychiatry*, *172*(9), 827–837. https://doi.org/10.1176/appi.ajp.2015.14101248

Dukart, J., Mueller, K., Horstmann, A., Barthel, H., Möller, H. E., Villringer, A., Sabri, O., & Schroeter, M. L. (2011). Combined evaluation of FDG-PET and MRI improves detection and differentiation of dementia. *PLoS ONE*, *6*(3). https://doi.org/10.1371/journal.pone.0018111

Falahati, F., Westman, E., & Simmons, A. (2014). Multivariate data analysis and machine learning in Alzheimer's disease with a focus on structural magnetic resonance imaging. *Journal of Alzheimer's Disease*, *41*(3), 685–708. https://doi.org/10.3233/JAD-131928

Farb, N. A. S., Grady, C. L., Strother, S., Tang-Wai, D. F., Masellis, M., Black, S., Freedman, M., Pollock, B. G., Campbell, K. L., Hasher, L., & Chow, T. W. (2013). Abnormal network connectivity in frontotemporal dementia: Evidence for prefrontal isolation. *Cortex*, *49*(7), 1856–1873. https://doi.org/10.1016/j.cortex.2012.09.008

Feis, R. A., Bouts, M. J. R. J., Dopper, E. G. P., Filippini, N., Heise, V., Trachtenberg, A. J., Van

Swieten, J. C., Van Buchem, M. A., Van Der Grond, J., Mackay, C. E., & Rombouts, S. A. R. B. (2019). Multimodal MRI of grey matter, white matter, and functional connectivity in cognitively healthy mutation carriers at risk for frontotemporal dementia and Alzheimer's disease. *BMC Neurology*, *19*(1). https://doi.org/10.1186/s12883-019-1567-0

Feis, R. A., Bouts, M. J. R. J., Panman, J. L., Jiskoot, L. C., Dopper, E. G. P., Schouten, T. M., de Vos, F., van der Grond, J., van Swieten, J. C., & Rombouts, S. A. R. B. (2018). Single-subject classification of presymptomatic frontotemporal dementia mutation carriers using multimodal MRI. *NeuroImage: Clinical*, *20*, 188–196. https://www.sciencedirect.com/science/article/pii/S2213158218302262?via%3Dihub

Filippi, M., Agosta, F., Scola, E., Canu, E., Magnani, G., Marcone, A., Valsasina, P., Caso, F., Copetti, M., Comi, G., Cappa, S. F., & Falini, A. (2013). Functional network connectivity in the behavioral variant of frontotemporal dementia. *Cortex*, *49*(9), 2389–2401. https://doi.org/10.1016/j.cortex.2012.09.017

Floeter, M. K., Danielian, L. E., Braun, L. E., & Wu, T. (2018). Longitudinal diffusion imaging across the C9orf72 clinical spectrum. *Journal of Neurology, Neurosurgery and Psychiatry*, *89*(1), 53–60. https://doi.org/10.1136/jnnp-2017-316799

Folch-Fortuny, A., Arteaga, F., & Ferrer, A. (2016). Missing Data Imputation Toolbox for MATLAB. *Chemometrics and Intelligent Laboratory Systems*, *154*, 93–100. https://doi.org/10.1016/j.chemolab.2016.03.019

Fonteijn, H. M., Modat, M., Clarkson, M. J., Barnes, J., Lehmann, M., Hobbs, N. Z., Scahill, R. I., Tabrizi, S. J., Ourselin, S., Fox, N. C., & Alexander, D. C. (2012). An event-based model for disease progression and its application in familial Alzheimer's disease and Huntington's

disease. *NeuroImage*, *60*(3), 1880–1889. https://doi.org/10.1016/j.neuroimage.2012.01.062

Fortin, J. P., Cullen, N., Sheline, Y. I., Taylor, W. D., Aselcioglu, I., Cook, P. A., Adams, P., Cooper, C., Fava, M., McGrath, P. J., McInnis, M., Phillips, M. L., Trivedi, M. H., Weissman, M. M., & Shinohara, R. T. (2018). Harmonization of cortical thickness measurements across scanners and sites. *NeuroImage*, *167*, 104–120. https://doi.org/10.1016/j.neuroimage.2017.11.024

Fortin, J. P., Parker, D., Tunç, B., Watanabe, T., Elliott, M. A., Ruparel, K., Roalf, D. R., Satterthwaite, T. D., Gur, R. C., Gur, R. E., Schultz, R. T., Verma, R., & Shinohara, R. T. (2017). Harmonization of multi-site diffusion tensor imaging data. *NeuroImage*, *161*, 149–170. https://doi.org/10.1016/j.neuroimage.2017.08.047

Frings, L., Yew, B., Flanagan, E., Lam, B. Y. K., Hull, M., Huppertz, H. J., Hodges, J. R., & Hornberger, M. (2014). Longitudinal grey and white matter changes in frontotemporal dementia and Alzheimer's disease. *PLoS ONE*, *9*(3), 1–8. https://doi.org/10.1371/journal.pone.0090814

Frost, B., Jacks, R. L., & Diamond, M. I. (2009). Propagation of Tau misfolding from the outside to the inside of a cell. *Journal of Biological Chemistry*, *284*(19), 12845–12852. https://doi.org/10.1074/jbc.M808759200

Fumagalli, G. G., Basilico, P., Arighi, A., Bocchetta, M., Dick, K. M., Cash, D. M., Harding, S., Mercurio, M., Fenoglio, C., Pietroboni, A. M., Ghezzi, L., van Swieten, J., Borroni, B., de Mendonça, A., Masellis, M., Tartaglia, M. C., Rowe, J. B., Graff, C., Tagliavini, F., … Galimberti, D. (2018). Distinct patterns of brain atrophy in Genetic Frontotemporal Dementia Initiative (GENFI) cohort revealed by visual rating scales. *Alzheimer's Research & Therapy*,

10(1), 46. https://doi.org/10.1186/s13195-018-0376-9

Galvin, J. E., Howard, D. H., Denny, S. S., Dickinson, S., & Tatton, N. (2017). The social and economic burden of frontotemporal degeneration. *Neurology*, *89*(20), 2049–2056. https://doi.org/10.1212/WNL.0000000000004614

Garbarino, S., Lorenzi, M., Oxtoby, N. P., Vinke, E. J., Marinescu, R. V., Eshaghi, A., Ikram, M. A., Niessen, W. J., Ciccarelli, O., Barkhof, F., Schott, J. M., Vernooij, M. W., & Alexander, D. C. (2019). Differences in topological progression profile among neurodegenerative diseases from imaging data. *ELife*, *8*, 1–27. https://doi.org/10.7554/eLife.49298

Garcin, B., Lillo, P., Hornberger, M., Piguet, O., Dawson, K., Nestor, P. J., & Hodges, J. R. (2009). Determinants of survival in behavioral variant frontotemporal dementia. *Neurology*, *73*(20), 1656–1661. https://doi.org/10.1212/WNL.0b013e3181c1dee7

Gordon, E., Rohrer, J. D., & Fox, N. C. (2016). Advances in neuroimaging in frontotemporal dementia. In *Journal of Neurochemistry* (Vol. 138, pp. 193–210). Wiley/Blackwell (10.1111). https://doi.org/10.1111/jnc.13656

Gorno-Tempini, M., Hillis, A., Weintraub, S., Kertesz, A., Mendez, M., Cappa, S., Ogar, J., Rohrer, J., Black, S., Boeve, B., Manes, F., Dronkers, N., Vandenberghe, R., Rascovsky, K., Patterson, K., Miller, B., Knopman, D., Hodges, J., Mesulam, M., & Grossman, M. (2011). Classification of primary progressive aphasia and its variants. *Neurology*, *76*, 1006–1014. https://doi.org/10.1212/WNL.0b013e31821103e6

Hafkemeijer, A., Möller, C., Dopper, E. G. P., Jiskoot, L. C., Schouten, T. M., van Swieten, J. C., van der Flier, W. M., Vrenken, H., Pijnenburg, Y. A. L., Barkhof, F., Scheltens, P., van der Grond, J., & Rombouts, S. A. R. B. (2015). Resting state functional connectivity differences

between behavioral variant frontotemporal dementia and Alzheimer's disease. *Frontiers in Human Neuroscience*, *9*(September). https://doi.org/10.3389/fnhum.2015.00474

Harper, L., Fumagalli, G. G., Barkhof, F., Scheltens, P., O'Brien, J. T., Bouwman, F., Burton, E. J., Rohrer, J. D., Fox, N. C., Ridgway, G. R., & Schott, J. M. (2016). MRI visual rating scales in the diagnosis of dementia: Evaluation in 184 post-mortem confirmed cases. *Brain*, *139*(4), 1211–1225. https://doi.org/10.1093/brain/aww005

Heller, C., Foiani, M. S., Moore, K., Convery, R., Bocchetta, M., Neason, M., Cash, D. M., Thomas, D., Greaves, C. V., Woollacott, I. O. C., Shafei, R., van Swieten, J. C., Moreno, F., Sanchez-Valle, R., Borroni, B., Laforce, R., Masellis, M., Tartaglia, M. C., Graff, C., … Bessi, V. (2020). Plasma glial fibrillary acidic protein is raised in progranulin-associated frontotemporal dementia. *Journal of Neurology, Neurosurgery & Psychiatry*, *91*(3), 263–270. https://doi.org/10.1136/JNNP-2019-321954

Ismail, Z., Agüera-Ortiz, L., Brodaty, H., Cieslak, A., Cummings, J., Fischer, C. E., Gauthier, S., Geda, Y. E., Herrmann, N., Kanji, J., Lanctôt, K. L., Miller, D. S., Mortby, M. E., Onyike, C. U., Rosenberg, P. B., Smith, E. E., Smith, G. S., Sultzer, D. L., & Lyketsos, C. (2017). The Mild Behavioral Impairment Checklist (MBI-C): A Rating Scale for Neuropsychiatric Symptoms in Pre-Dementia Populations. *Journal of Alzheimer's Disease*, *56*(3), 929–938. https://doi.org/10.3233/JAD-160979

Iturria-Medina, Y., Carbonell, F., Assadi, A., Adewale, Q., Khan, A. F., Baumeister, R., & Sanchez-Rodriguez, L. (2020). NeuroPM toolbox: integrating Molecular, Neuroimaging and Clinical data for Characterizing Neuropathological Progression and Individual Therapeutic Needs. *MedRxiv*, 2020.09.24.20200964. http://adni.loni.usc.edu/wp-

content/uploads/how_to_apply/ADNI_Acknowledgement_List.pdf

Iturria-Medina, Y., Carbonell, F., Assadi, A., Adewale, Q., Khan, A. F., Baumeister, T. R., & Sanchez-Rodriguez, L. (2021). Integrating molecular, histopathological, neuroimaging and clinical neuroscience data with NeuroPM-box. *Communications Biology*, *4*, 614. https://doi.org/10.1038/s42003-021-02133-x

Iturria-Medina, Y., Carbonell, F. M., & Evans, A. C. (2018). Multimodal imaging-based therapeutic fingerprints for optimizing personalized interventions: Application to neurodegeneration. *NeuroImage*, *179*, 40–50. https://doi.org/10.1016/J.NEUROIMAGE.2018.06.028

Iturria-Medina, Y., Carbonell, F. M., Sotero, R. C., Chouinard-Decorte, F., & Evans, A. C. (2017). Multifactorial causal model of brain (dis)organization and therapeutic intervention: Application to Alzheimer's disease. *NeuroImage*, *152*, 60–77. https://doi.org/10.1016/j.neuroimage.2017.02.058

Iturria-Medina, Y., & Evans, A. C. (2015). On the central role of brain connectivity in neurodegenerative disease progression. *Frontiers in Aging Neuroscience*, *7*(MAY), 90. https://doi.org/10.3389/fnagi.2015.00090

Iturria-Medina, Y., Khan, A. F., Adewale, Q., & Shirazi, A. H. (2020). Blood and brain gene expression trajectories mirror neuropathology and clinical deterioration in neurodegeneration. *Brain*, *143*(2), 661–673. https://doi.org/10.1093/brain/awz400

Iturria-Medina, Y., Sotero, R. C., Toussaint, P. J., Mateos-Pérez, J. M., Evans, A. C., Weiner, M. W., Aisen, P., Petersen, R., Jack, C. R., Jagust, W., Trojanowki, J. Q., Toga, A. W., Beckett, L., Green, R. C., Saykin, A. J., Morris, J., Shaw, L. M., Khachaturian, Z., Sorensen, G., …

Furst, A. J. (2016). Early role of vascular dysregulation on late-onset Alzheimer's disease based on multifactorial data-driven analysis. *Nature Communications*, *7*(May). https://doi.org/10.1038/ncomms11934

Jack, C. R., Knopman, D. S., Jagust, W. J., Petersen, R. C., Weiner, M. W., Aisen, P. S., Shaw, L. M., Vemuri, P., Wiste, H. J., Weigand, S. D., Lesnick, T. G., Pankratz, V. S., Donohue, M. C., & Trojanowski, J. Q. (2013). Tracking pathophysiological processes in Alzheimer's disease: an updated hypothetical model of dynamic biomarkers. *The Lancet. Neurology*, *12*(2), 207–216. https://doi.org/10.1016/S1474-4422(12)70291-0

Jacova, C., Hsiung, G. Y. R., Tawankanjanachot, I., Dinelle, K., McCormick, S., Gonzalez, M., Lee, H., Sengdy, P., Bouchard-Kerr, P., Baker, M., Rademakers, R., Sossi, V., Stoessl, A. J., Feldman, H. H., & Mackenzie, I. R. (2013). Anterior brain glucose hypometabolism predates dementia in progranulin mutation carriers. *Neurology*, *81*(15), 1322–1331. https://doi.org/10.1212/WNL.0b013e3182a8237e

Jedynak, B. M., Lang, A., Liu, B., Katz, E., Zhang, Y., Wyman, B. T., Raunig, D., Jedynak, C. P., Caffo, B., & Prince, J. L. (2012). A computational neurodegenerative disease progression score: Method and results with the Alzheimer's disease neuroimaging initiative cohort. *NeuroImage*, *63*(3), 1478–1486. https://doi.org/10.1016/j.neuroimage.2012.07.059

Jeurissen, B., Tournier, J. D., Dhollander, T., Connelly, A., & Sijbers, J. (2014). Multi-tissue constrained spherical deconvolution for improved analysis of multi-shell diffusion MRI data. *NeuroImage*, *103*, 411–426. https://doi.org/10.1016/j.neuroimage.2014.07.061

Jiskoot, L. C., Bocchetta, M., Nicholas, J. M., Cash, D. M., Thomas, D., Modat, M., Ourselin, S., Rombouts, S. A. R. B., Dopper, E. G. P., Meeter, L. H., Panman, J. L., van Minkelen, R., van

der Ende, E. L., Donker Kaat, L., Pijnenburg, Y. A. L., Borroni, B., Galimberti, D., Masellis, M., Tartaglia, M. C., … Rohrer, J. D. (2018). Presymptomatic white matter integrity loss in familial frontotemporal dementia in the GENFI cohort: A cross-sectional diffusion tensor imaging study. *Annals of Clinical and Translational Neurology*, *5*(9), 1025–1036. https://doi.org/10.1002/acn3.601

Jiskoot, L. C., Panman, J. L., Meeter, L. H., Dopper, E. G. P., Donker Kaat, L., Franzen, S., Van Der Ende, E. L., Van Minkelen, R., Rombouts, S. A. R. B., Papma, J. M., & Van Swieten, J. C. (2019). Longitudinal multimodal MRI as prognostic and diagnostic biomarker in presymptomatic familial frontotemporal dementia. *Brain*, *142*, 193–208. https://doi.org/10.1093/brain/awy288

Jiskoot, L. C., Panman, J. L., van Asseldonk, L., Franzen, S., Meeter, L. H. H., Donker Kaat, L., van der Ende, E. L., Dopper, E. G. P., Timman, R., van Minkelen, R., van Swieten, J. C., van den Berg, E., & Papma, J. M. (2018). Longitudinal cognitive biomarkers predicting symptom onset in presymptomatic frontotemporal dementia. *Journal of Neurology*, *265*(6), 1381–1392. https://doi.org/10.1007/s00415-018-8850-7

Johnson, W. E., Li, C., & Rabinovic, A. (2007). Adjusting batch effects in microarray expression data using empirical Bayes methods. *Biostatistics*, *8*(1), 118–127. https://doi.org/10.1093/biostatistics/kxj037

Josephs, K. A., Hodges, J. R., Snowden, J. S., MacKenzie, I. R., Neumann, M., Mann, D. M., & Dickson, D. W. (2011). Neuropathological background of phenotypical variability in frontotemporal dementia. In *Acta Neuropathologica* (Vol. 122, Issue 2, pp. 137–153). Springer. https://doi.org/10.1007/s00401-011-0839-6

Kim, E. J., Sidhu, M., Gaus, S. E., Huang, E. J., Hof, P. R., Miller, B. L., DeArmond, S. J., & Seeley, W. W. (2012). Selective frontoinsular von economo neuron and fork cell loss in early behavioral variant frontotemporal dementia. *Cerebral Cortex*, *22*(2), 251–259. https://doi.org/10.1093/cercor/bhr004

Klein, A., & Tourville, J. (2012). 101 labeled brain images and a consistent human cortical labeling protocol. *Frontiers in Neuroscience*, *6*, 171. https://doi.org/10.3389/fnins.2012.00171

Klöppel, S., Peter, J., Ludl, A., Pilatus, A., Maier, S., Mader, I., Heimbach, B., Frings, L., Egger, K., Dukart, J., Schroeter, M. L., Perneczky, R., Häussermann, P., Vach, W., Urbach, H., Teipel, S., Hüll, M., & Abdulkadir, A. (2015). Applying automated MR-based diagnostic methods to the memory clinic: A prospective study. *Journal of Alzheimer's Disease*, *47*(4), 939–954. https://doi.org/10.3233/JAD-150334

Klöppel, S., Stonnington, C. M., Barnes, J., Chen, F., Chu, C., Good, C. D., Mader, I., Mitchell, L. A., Patel, A. C., Roberts, C. C., Fox, N. C., Jack, C. R., Ashburner, J., & Frackowiak, R. S. J. (2008). Accuracy of dementia diagnosis - A direct comparison between radiologists and a computerized method. *Brain*, *131*(11), 2969–2974. https://doi.org/10.1093/brain/awn239

Klöppel, S., Stonnington, C. M., Chu, C., Draganski, B., Scahill, R. I., Rohrer, J. D., Fox, N. C., Jack, C. R., Ashburner, J., & Frackowiak, R. S. J. (2008). Automatic classification of MR scans in Alzheimer's disease. *Brain*, *131*(3), 681–689. https://doi.org/10.1093/brain/awm319

Koikkalainen, J., Rhodius-Meester, H., Tolonen, A., Barkhof, F., Tijms, B., Lemstra, A. W., Tong, T., Guerrero, R., Schuh, A., Ledig, C., Rueckert, D., Soininen, H., Remes, A. M., Waldemar, G., Hasselbalch, S., Mecocci, P., van der Flier, W., & Lötjönen, J. (2016). Differential diagnosis of neurodegenerative diseases using structural MRI data. *NeuroImage: Clinical*,

11, 435–449. http://linkinghub.elsevier.com/retrieve/pii/S2213158216300407

Krudop, W. A., Kerssens, C. J., Dols, A., Prins, N. D., Möller, C., Schouws, S., Barkhof, F., Van Berckel, B. N. M., Teunissen, C. E., Van Der Flier, W. M., Scheltens, P., Stek, M. L., & Pijnenburg, Y. A. L. (2014). Building a new paradigm for the early recognition of behavioral variant frontotemporal dementia: Late Onset Frontal Lobe Syndrome Study. *American Journal of Geriatric Psychiatry*, *22*(7), 735–740. https://doi.org/10.1016/j.jagp.2013.02.002

Kuceyeski, A., Zhang, Y., & Raj, A. (2012). Linking white matter integrity loss to associated cortical regions using structural connectivity information in Alzheimer's disease and fronto-temporal dementia: The Loss in Connectivity (LoCo) score. *NeuroImage*, *61*(4), 1311–1323. https://doi.org/10.1016/j.neuroimage.2012.03.039

Lam, B. Y. K., Halliday, G. M., Irish, M., Hodges, J. R., & Piguet, O. (2014). Longitudinal white matter changes in frontotemporal dementia subtypes. *Human Brain Mapping*, *35*, 3547–3557. https://doi.org/10.1002/hbm.22420

Lashley, T., Rohrer, J. D., Mead, S., & Revesz, T. (2015). Review: An update on clinical, genetic and pathological aspects of frontotemporal lobar degenerations. *Neuropathology and Applied Neurobiology*, *41*, 858–881. https://doi.org/10.1111/nan.12250

Le Blanc, G., Jetté Pomerleau, V., McCarthy, J., Borroni, B., van Swieten, J., Galimberti, D., Sanchez-Valle, R., LaForce, R., Moreno, F., Synofzik, M., Graff, C., Masellis, M., Tartaglia, M. C., Rowe, J. B., Vandenberghe, R., Finger, E., Tagliavini, F., de Mendonça, A., Santana, I., … Ducharme, S. (2020). Faster Cortical Thinning and Surface Area Loss in Presymptomatic and Symptomatic C9orf72 Repeat Expansion Adult Carriers. *Annals of Neurology*, 1–10. https://doi.org/10.1002/ana.25748

Lee, S. E., Khazenzon, A. M., Trujillo, A. J., Guo, C. C., Yokoyama, J. S., Sha, S. J., Takada, L. T., Karydas, A. M., Block, N. R., Coppola, G., Pribadi, M., Geschwind, D. H., Rademakers, R., Fong, J. C., Weiner, M. W., Boxer, A. L., Kramer, J. H., Rosen, H. J., Miller, B. L., & Seeley, W. W. (2014). Altered network connectivity in frontotemporal dementia with C9orf72 hexanucleotide repeat expansion. *Brain*, *137*(11), 3047–3060. https://doi.org/10.1093/brain/awu248

Lee, S. E., Sias, A. C., Mandelli, M. L., Brown, J. A., Brown, A. B., Khazenzon, A. M., Vidovszky, A. A., Zanto, T. P., Karydas, A. M., Pribadi, M., Dokuru, D., Coppola, G., Geschwind, D. H., Rademakers, R., Gorno-Tempini, M. L., Rosen, H. J., Miller, B. L., & Seeley, W. W. (2017). Network degeneration and dysfunction in presymptomatic C9ORF72 expansion carriers. *NeuroImage: Clinical*, *14*, 286–297. https://doi.org/10.1016/j.nicl.2016.12.006

Lehmann, M., Rohrer, J. D., Clarkson, M. J., & Ridgway, G. R. (2010). *Reduced Cortical Thickness in the Posterior Cingulate Gyrus is Characteristic of Both Typical and Atypical Alzheimer ' s Disease*. *20*, 587–598. https://doi.org/10.3233/JAD-2010-1401

Lv, H., Wang, Z., Tong, E., Williams, L. M., Zaharchuk, G., Zeineh, M., Goldstein-Piekarski, A. N., Ball, T. M., Liao, C., & Wintermark, M. (2018). Resting-state functional MRI: Everything that nonexperts have always wanted to know. In *American Journal of Neuroradiology* (Vol. 39, Issue 8, pp. 1390–1399). American Society of Neuroradiology. https://doi.org/10.3174/ajnr.A5527

Mahoney, C. J., Beck, J., Rohrer, J. D., Lashley, T., Mok, K., Shakespeare, T., Yeatman, T., Warrington, E. K., Schott, J. M., Fox, N. C., Rossor, M. N., Hardy, J., Collinge, J., Revesz, T., Mead, S., & Warren, J. D. (2012). Frontotemporal dementia with the C9ORF72

hexanucleotide repeat expansion: Clinical, neuroanatomical and neuropathological features. *Brain*, *135*(3), 736–750. https://doi.org/10.1093/brain/awr361

Mahoney, C. J., Malone, I. B., Ridgway, G. R., Buckley, A. H., Downey, L. E., Golden, H. L., Ryan, N. S., Ourselin, S., Schott, J. M., Rossor, M. N., Fox, N. C., & Warren, J. D. (2013). White matter tract signatures of the progressive aphasias. *Neurobiology of Aging*, *34*(6), 1687–1699. https://doi.org/10.1016/j.neurobiolaging.2012.12.002

Mahoney, C. J., Ridgway, G. R., Malone, I. B., Downey, L. E., Beck, J., Kinnunen, K. M., Schmitz, N., Golden, H. L., Rohrer, J. D., Schott, J. M., Rossor, M. N., Ourselin, S., Mead, S., Fox, N. C., & Warren, J. D. (2014). Profiles of white matter tract pathology in frontotemporal dementia. *Human Brain Mapping*, *35*(8), 4163–4179. https://doi.org/10.1002/hbm.22468

Mahoney, C. J., Simpson, I. J. A., Nicholas, J. M., Fletcher, P. D., Downey, L. E., Golden, H. L., Clark, C. N., Schmitz, N., Rohrer, J. D., Schott, J. M., Zhang, H., Ourselin, S., Warren, J. D., & Fox, N. C. (2015). Longitudinal diffusion tensor imaging in rontotemporal dementia. *Annals of Neurology*, *77*(1), 33–46. https://doi.org/10.1002/ana.24296

Mansoor, Y., Jastrzab, L., Dutt, S., Miller, B. L., Seeley, W. W., & Kramer, J. H. (2015). Memory Profiles in Pathology or Biomarker Confirmed Alzheimer Disease and Frontotemporal Dementia. *Alzheimer Disease and Associated Disorders*, *29*(2), 135–140. https://doi.org/10.1097/WAD.0000000000000062

McCarthy, J., Collins, D. L., & Ducharme, S. (2018). Morphometric MRI as a diagnostic biomarker of frontotemporal dementia: A systematic review to determine clinical applicability. *NeuroImage: Clinical*, *20*, 685–696. https://doi.org/10.1016/J.NICL.2018.08.028

McInnes, M. D. F., Moher, D., Thombs, B. D., McGrath, T. A., Bossuyt, P. M., Clifford, T., Cohen, J. F., Deeks, J. J., Gatsonis, C., Hooft, L., Hunt, H. A., Hyde, C. J., Korevaar, D. A., Leeflang, M. M. G., Macaskill, P., Reitsma, J. B., Rodin, R., Rutjes, A. W. S., Salameh, J.-P., … Willis, B. H. (2018). Preferred Reporting Items for a Systematic Review and Meta-analysis of Diagnostic Test Accuracy Studies. *JAMA*, *319*(4), 388–396. https://doi.org/10.1001/jama.2017.19163

McMillan, Corey T., Avants, B. B., Cook, P., Ungar, L., Trojanowski, J. Q., & Grossman, M. (2014). The power of neuroimaging biomarkers for screening frontotemporal dementia. *Human Brain Mapping*, *35*(9), 4827–4840. https://doi.org/10.1002/hbm.22515

McMillan, Cory T., Brun, C., Siddiqui, S., Churgin, M., Libon, D., Yushkevich, P., Zhang, H., Boller, A., Gee, J., & Grossman, M. (2012). White matter imaging contributes to the multimodal diagnosis of frontotemporal lobar degeneration. *Neurology*, *78*(22), 1761–1768. https://doi.org/10.1212/WNL.0b013e31825830bd

Meeter, L. H., Dopper, E. G., Jiskoot, L. C., Sanchez-Valle, R., Graff, C., Benussi, L., Ghidoni, R., Pijnenburg, Y. A., Borroni, B., Galimberti, D., Laforce, R. J., Masellis, M., Vandenberghe, R., Ber, I. Le, Otto, M., van Minkelen, R., Papma, J. M., Rombouts, S. A., Balasa, M., … van Swieten, J. C. (2016). Neurofilament light chain: a biomarker for genetic frontotemporal dementia. *Annals of Clinical and Translational Neurology*, *3*(8), 623–636. https://doi.org/10.1002/acn3.325

Meeter, L. H., Kaat, L. D., Rohrer, J. D., & van Swieten, J. C. (2017). Imaging and fluid biomarkers in frontotemporal dementia. *Nature Reviews Neurology*, *13*(7), 406–419. https://doi.org/10.1038/nrneurol.2017.75

Mesulam, M., Wieneke, C., Rogalski, E., Cobia, D., Thompson, C., & Weintraub, S. (2009). Quantitative Template for Subtyping Primary Progressive Aphasia. *Archives of …*, *66*(12), 1545–1551. https://doi.org/10.1001/archneurol.2009.288

Meyer, S., Mueller, K., Stuke, K., Bisenius, S., Diehl-Schmid, J., Jessen, F., Kassubek, J., Kornhuber, J., Ludolph, A. C., Prudlo, J., Schneider, A., Schuemberg, K., Yakushev, I., Otto, M., & Schroeter, M. L. (2017). Predicting behavioral variant frontotemporal dementia with pattern classification in multi-center structural MRI data. *NeuroImage: Clinical*, *14*, 656–662. https://doi.org/10.1016/j.nicl.2017.02.001

Moher, D., Liberati, A., Tetzlaff, J., Altman, D. G., & The PRISMA Group. (2009). Preferred Reporting Items for Systematic Reviews and Meta-Analyses: The PRISMA Statement. *PLoS Medicine*, *6*(7), e1000097. https://doi.org/10.1371/journal.pmed.1000097

Möller, C., Hafkemeijer, A., Pijnenburg, Y. A. L., Rombouts, S. A. R. B., Van Der Grond, J., Dopper, E., Van Swieten, J., Versteeg, A., Pouwels, P. J. W., Barkhof, F., Scheltens, P., Vrenken, H., & Van Der Flier, W. M. (2015). Joint assessment of white matter integrity, cortical and subcortical atrophy to distinguish AD from behavioral variant FTD: A two-center study. *NeuroImage: Clinical*, *9*, 418–429. https://doi.org/10.1016/j.nicl.2015.08.022

Möller, C., Pijnenburg, Y. A. L., van der Flier, W. M., Versteeg, A., Tijms, B., de Munck, J. C., Hafkemeijer, A., Rombouts, S. A. R. B., van der Grond, J., van Swieten, J., Dopper, E., Scheltens, P., Barkhof, F., Vrenken, H., & Wink, A. M. (2016). Alzheimer Disease and Behavioral Variant Frontotemporal Dementia: Automatic Classification Based on Cortical Atrophy for Single-Subject Diagnosis. *Radiology*, *279*(3), 838–848. https://doi.org/10.1148/radiol.2015150220

Moore, K. M., Nicholas, J., Grossman, M., McMillan, C. T., Irwin, D. J., Massimo, L., Van Deerlin, V. M., Warren, J. D., Fox, N. C., Rossor, M. N., Mead, S., Bocchetta, M., Boeve, B. F., Knopman, D. S., Graff-Radford, N. R., Forsberg, L. K., Rademakers, R., Wszolek, Z. K., van Swieten, J. C., … Geschwind, D. (2020). Age at symptom onset and death and disease duration in genetic frontotemporal dementia: an international retrospective cohort study. *The Lancet Neurology*, *19*, 145–156. https://doi.org/10.1016/S1474-4422(19)30394-1

Muñoz-Ruiz, M. Á., Hartikainen, P., Koikkalainen, J., Wolz, R., Julkunen, V., Niskanen, E., Herukka, S. K., Kivipelto, M., Vanninen, R., Rueckert, D., Liu, Y., Lötjönen, J., & Soininen, H. (2012). Structural MRI in Frontotemporal Dementia: Comparisons between Hippocampal Volumetry, Tensor-Based Morphometry and Voxel-Based Morphometry. *PLoS ONE*, *7*(12). https://doi.org/10.1371/journal.pone.0052531

Mutsaerts, H. J. M. M., Mirza, S. S., Petr, J., Thomas, D. L., Cash, D. M., Bocchetta, M., De Vita, E., Metcalfe, A. W. S., Shirzadi, Z., Robertson, A. D., Tartaglia, M. C., Mitchell, S. B., Black, S. E., Freedman, M., Tang-Wai, D., Keren, R., Rogaeva, E., Van Swieten, J., Laforce, R., … Warren, J. D. (2019). Cerebral perfusion changes in presymptomatic genetic frontotemporal dementia: A GENFI study. *Brain*, *142*(4), 1108–1120. https://doi.org/10.1093/brain/awz039

Nichols, E., Szoeke, C. E. I., Vollset, S. E., Abbasi, N., Abd-Allah, F., Abdela, J., Aichour, M. T. E., Akinyemi, R. O., Alahdab, F., Asgedom, S. W., Awasthi, A., Barker-Collo, S. L., Baune, B. T., Béjot, Y., Belachew, A. B., Bennett, D. A., Biadgo, B., Bijani, A., Bin Sayeed, M. S., … Murray, C. J. L. (2019). Global, regional, and national burden of Alzheimer's disease and other dementias, 1990–2016: a systematic analysis for the Global Burden of Disease Study 2016. *The Lancet Neurology*, *18*(1), 88–106. https://doi.org/10.1016/S1474-4422(18)30403-4

Olm, C. A., McMillan, C. T., Irwin, D. J., Van Deerlin, V. M., Cook, P. A., Gee, J. C., & Grossman, M. (2018). Longitudinal structural gray matter and white matter MRI changes in presymptomatic progranulin mutation carriers. *NeuroImage: Clinical*, *19*, 497–506. https://doi.org/10.1016/j.nicl.2018.05.017

Olney, N. T., Ong, E., Goh, S. Y. M., Bajorek, L., Dever, R., Staffaroni, A. M., Cobigo, Y., Bock, M., Chiang, K., Ljubenkov, P., Kornak, J., Heuer, H. W., Wang, P., Rascovsky, K., Wolf, A., Appleby, B., Bove, J., Bordelon, Y., Brannelly, P., … Rosen, H. J. (2020). Clinical and volumetric changes with increasing functional impairment in familial frontotemporal lobar degeneration. *Alzheimer's and Dementia*, *16*(1), 49–59. https://doi.org/10.1016/j.jalz.2019.08.196

Onyike, C. U., & Diehl-Schmid, J. (2013). The epidemiology of frontotemporal dementia. *International Review of Psychiatry*, *25*(2), 130–137. https://doi.org/10.3109/09540261.2013.776523

Oxtoby, N. P., & Alexander, D. C. (2017). Imaging plus X: Multimodal models of neurodegenerative disease. In *Current Opinion in Neurology* (Vol. 30, Issue 4, pp. 371–379). Wolters Kluwer Health. https://doi.org/10.1097/WCO.0000000000000460

Oxtoby, N. P., Garbarino, S., Firth, N. C., Warren, J. D., Schott, J. M., & Alexander, D. C. (2017). Data-driven sequence of changes to anatomical brain connectivity in sporadic Alzheimer's disease. *Frontiers in Neurology*, *8*(NOV), 580. https://doi.org/10.3389/fneur.2017.00580

Oxtoby, N. P., Young, A. L., Cash, D. M., Benzinger, T. L. S., Fagan, A. M., Morris, J. C., Bateman, R. J., Fox, N. C., Schott, J. M., & Alexander, D. C. (2018). Data-driven models of dominantly-inherited Alzheimer's disease progression. *Brain*, *141*(5), 1529–1544.

https://doi.org/10.1093/brain/awy050

Pan, P. L., Song, W., Yang, J., Huang, R., Chen, K., Gong, Q. Y., Zhong, J. Z., Shi, H. C., Shang, H. F., & Departments. (2012). Gray Matter Atrophy in Behavioral Variant Frontotemporal Dementia: A Meta-Analysis of Voxel-Based Morphometry Studies. *Dementia and Geriatric Cognitive Disorders*, *33*, 141–148. https://doi.org/10.1159/000 338176

Pankov, A., Binney, R. J., Staffaroni, A. M., Kornak, J., Attygalle, S., Schuff, N., Weiner, M. W., Kramer, J. H., Dickerson, B. C., Miller, B. L., & Rosen, H. J. (2016). Data-driven regions of interest for longitudinal change in frontotemporal lobar degeneration. *NeuroImage: Clinical*, *12*, 332–340. https://doi.org/10.1016/J.NICL.2015.08.002

Panman, J. L., Jiskoot, L. C., Bouts, M. J. R. J., Meeter, L. H. H., van der Ende, E. L., Poos, J. M., Feis, R. A., Kievit, A. J. A., van Minkelen, R., Dopper, E. G. P., Rombouts, S. A. R. B., van Swieten, J. C., & Papma, J. M. (2019). Gray and white matter changes in presymptomatic genetic frontotemporal dementia: a longitudinal MRI study. *Neurobiology of Aging*, *76*, 115–124. https://doi.org/10.1016/j.neurobiolaging.2018.12.017

Panman, J. L., Venkatraghavan, V., Van Der Ende, E. L., Steketee, R. M. E., Jiskoot, L. C., Poos, J. M., Dopper, E. G. P., Meeter, L. H. H., Donker Kaat, L., Rombouts, S. A. R. B., Vernooij, M. W., Kievit, A. J. A., Premi, E., Cosseddu, M., Bonomi, E., Olives, J., Rohrer, J. D., Sánchez-Valle, R., Borroni, B., … Klein, S. (2021). Modelling the cascade of biomarker changes in GRN -related frontotemporal dementia. *Journal of Neurology, Neurosurgery and Psychiatry*, *92*(5), 494–501. https://doi.org/10.1136/jnnp-2020-323541

Papma, J. M., Jiskoot, L. C., Panman, J. L., Dopper, E. G., Den Heijer, T., Donker Kaat, L., Pijnenburg, Y. A. L., Meeter, L. H., Van Minkelen, R., Rombouts, S. A. R. B., & Van

Swieten, J. C. (2017). Cognition and gray and white matter characteristics of presymptomatic C9orf72 repeat expansion. *Neurology*, *89*(12), 1256–1264. https://doi.org/10.1212/WNL.0000000000004393

Pasquini, L., Nana, A. L., Toller, G., Brown, J. A., Deng, J., Staffaroni, A., Kim, E.-J., Hwang, J.-H. L., Li, L., Park, Y., Gaus, S. E., Allen, I., Sturm, V. E., Spina, S., Grinberg, L. T., Rankin, K. P., Kramer, J. H., Rosen, H. J., Miller, B. L., & Seeley, W. W. (2020). Salience Network Atrophy Links Neuron Type-Specific Pathobiology to Loss of Empathy in Frontotemporal Dementia. *Cerebral Cortex*, *June*, 5387–5399. https://doi.org/10.1093/cercor/bhaa119

Pievani, M., Paternicò, D., Benussi, L., Binetti, G., Orlandini, A., Cobelli, M., Magnaldi, S., Ghidoni, R., & Frisoni, G. B. (2014). Pattern of structural and functional brain abnormalities in asymptomatic granulin mutation carriers. *Alzheimer's and Dementia*, *10*(5), S354-S363.e1. https://doi.org/10.1016/j.jalz.2013.09.009

Popuri, K., Beg, M. F., Lee, H., Balachandar, R., Wang, L., Sossi, V., Jacova, C., Baker, M., Shahinfard, E., Rademakers, R., Mackenzie, I. R. A., & Hsiung, G. Y. R. (2021). FDG-PET in presymptomatic C9orf72 mutation carriers. *NeuroImage: Clinical*, *31*. https://doi.org/10.1016/j.nicl.2021.102687

Premi, E., Cauda, F., Costa, T., Diano, M., Gazzina, S., Gualeni, V., Alberici, A., Archetti, S., Magoni, M., Gasparotti, R., Padovani, A., & Borroni, B. (2016). Looking for Neuroimaging Markers in Frontotemporal Lobar Degeneration Clinical Trials: A Multi-Voxel Pattern Analysis Study in Granulin Disease. *Journal of Alzheimer's Disease*, *51*(1), 249–262. https://doi.org/10.3233/JAD-150340

Premi, E., Cauda, F., Gasparotti, R., Diano, M., Archetti, S., Padovani, A., & Borroni, B. (2014).

Multimodal fMRI resting-state functional connectivity in Granulin mutations: The case of fronto-parietal dementia. *PLoS ONE*, *9*(9), e106500. https://doi.org/10.1371/journal.pone.0106500

Prince, M., Bryce, R., Albanese, E., Wimo, A., Ribeiro, W., & Ferri, C. P. (2013). *The global prevalence of dementia: A systematic review and metaanalysis; The global prevalence of dementia: A systematic review and metaanalysis*. https://doi.org/10.1016/j.jalz.2012.11.007

Raamana, P. R., Rosen, H., Miller, B., Weiner, M. W., Wang, L., & Beg, M. F. (2014). Three-class differential diagnosis among Alzheimer disease, frontotemporal dementia, and controls. *Frontiers in Neurology*, *5 MAY*(May), 1–15. https://doi.org/10.3389/fneur.2014.00071

Rademakers, R., Neumann, M., & Mackenzie, I. R. (2012). Advances in understanding the molecular basis of frontotemporal dementia. *Nature Reviews Neurology*, *8*, 423–434. https://doi.org/10.1038/nrneurol.2012.117

Raj, A., Kuceyeski, A., & Weiner, M. (2012). A Network Diffusion Model of Disease Progression in Dementia. *Neuron*, *73*(6), 1204–1215. https://doi.org/10.1016/j.neuron.2011.12.040

Ranasinghe, K. G., Rankin, K. P., Pressman, P. S., Perry, D. C., Lobach, I. V., Seeley, W. W., Coppola, G., Karydas, A. M., Grinberg, L. T., Shany-Ur, T., Lee, S. E., Rabinovici, G. D., Rosen, H. J., Gorno-Tempini, M. L., Boxer, A. L., Miller, Z. A., Chiong, W., DeMay, M., Kramer, J. H., … Miller, B. L. (2016). Distinct subtypes of behavioral variant frontotemporal dementia based on patterns of network degeneration. *JAMA Neurology*, *73*(9), 1078–1088. https://doi.org/10.1001/jamaneurol.2016.2016

Rascovsky, K., Hodges, J. R., Knopman, D., Mendez, M. F., Kramer, J. H., Neuhaus, J., Van Swieten, J. C., Seelaar, H., Dopper, E. G. P., Onyike, C. U., Hillis, A. E., Josephs, K. A.,

Boeve, B. F., Kertesz, A., Seeley, W. W., Rankin, K. P., Johnson, J. K., Gorno-Tempini, M. L., Rosen, H., … Miller, B. L. (2011). Sensitivity of revised diagnostic criteria for the behavioural variant of frontotemporal dementia. *Brain*, *134*, 2456–2477. https://doi.org/10.1093/brain/awr179

Rathore, S., Habes, M., Iftikhar, M. A., Shacklett, A., & Davatzikos, C. (2017). A review on neuroimaging-based classification studies and associated feature extraction methods for Alzheimer's disease and its prodromal stages. *NeuroImage*, *155*(March), 530–548. https://doi.org/10.1016/j.neuroimage.2017.03.057

Rogalski, E., Cobia, D., Martersteck, A., Rademaker, A., Wieneke, C., Weintraub, S., & Mesulam, M. M. (2014). Asymmetry of cortical decline in subtypes of primary progressive aphasia. *Neurology*, *83*(13), 1184–1191. https://doi.org/10.1212/WNL.0000000000000824

Rohrer, J. D., Nicholas, J. M., Cash, D. M., van Swieten, J., Dopper, E., Jiskoot, L., van Minkelen, R., Rombouts, S. A., Cardoso, M. J., Clegg, S., Espak, M., Mead, S., Thomas, D. L., De Vita, E., Masellis, M., Black, S. E., Freedman, M., Keren, R., MacIntosh, B. J., … Rossor, M. N. (2015). Presymptomatic cognitive and neuroanatomical changes in genetic frontotemporal dementia in the Genetic Frontotemporal dementia Initiative (GENFI) study: a cross-sectional analysis. *The Lancet Neurology*, *14*, 253–262. https://doi.org/10.1016/S1474-4422(14)70324-2

Rohrer, J. D., Ridgway, G. R., Modat, M., Ourselin, S., Mead, S., Fox, N. C., Rossor, M. N., & Warren, J. D. (2010). Distinct profiles of brain atrophy in frontotemporal lobar degeneration caused by progranulin and tau mutations. *NeuroImage*, *53*(3), 1070–1076. https://doi.org/10.1016/j.neuroimage.2009.12.088

Rohrer, J. D., Woollacott, I. O. C., Dick, K. M., Brotherhood, E., Gordon, E., Fellows, A., Toombs, J., Druyeh, R., Cardoso, M. J., Ourselin, S., Nicholas, J. M., Norgren, N., Mead, S., Andreasson, U., Blennow, K., Schott, J. M., Fox, N. C., Warren, J. D., & Zetterberg, H. (2016). Serum neurofilament light chain protein is a measure of disease intensity in frontotemporal dementia. *Neurology*, *87*(13), 1329–1336. https://doi.org/10.1212/WNL.0000000000003154

Rojas, J. C., Wang, P., Staffaroni, A. M., Heller, C., Cobigo, Y., Wolf, A., Goh, S. Y. M., Ljubenkov, P. A., Heuer, H. W., Fong, J. C., Taylor, J. B., Veras, E., Song, L., Jeromin, A., Hanlon, D., Yu, L., Khinikar, A., Sivasankaran, R., Kieloch, A., … Boxer, A. L. (2021). Plasma Neurofilament Light for Prediction of Disease Progression in Familial Frontotemporal Lobar Degeneration. *Neurology*, *96*(18), e2296–e2312. https://doi.org/10.1212/WNL.0000000000011848

Rosen, H. J., Boeve, B. F., & Boxer, A. L. (2020). Tracking disease progression in familial and sporadic frontotemporal lobar degeneration: Recent findings from ARTFL and LEFFTDS. In *Alzheimer's and Dementia* (Vol. 16, Issue 1, pp. 71–78). John Wiley and Sons Inc. https://doi.org/10.1002/alz.12004

Rytty, R., Nikkinen, J., Paavola, L., Abou Elseoud, A., Moilanen, V., Visuri, A., Tervonen, O., Renton, A. E., Traynor, B. J., Kiviniemi, V., & Remes, A. M. (2013). GroupICA dual regression analysis of resting state networks in a behavioral variant of frontotemporal dementia. *Frontiers in Human Neuroscience*, *7*(AUG). https://doi.org/10.3389/fnhum.2013.00461

Salloway, S., Sperling, R., Fox, N. C., Blennow, K., Klunk, W., Raskind, M., Sabbagh, M., Honig,

L. S., Porsteinsson, A. P., Ferris, S., Reichert, M., Ketter, N., Nejadnik, B., Guenzler, V., Miloslavsky, M., Wang, D., Lu, Y., Lull, J., Tudor, I. C., … Brashear, H. R. (2014). Two Phase 3 Trials of Bapineuzumab in Mild-to-Moderate Alzheimer's Disease. *New England Journal of Medicine*, *370*(4), 322–333. https://doi.org/10.1056/nejmoa1304839

Santillo, A. F., Nilsson, C., & Englund, E. (2013). von Economo neurones are selectively targeted in frontotemporal dementia. *Neuropathology and Applied Neurobiology*, *39*(5), 572–579. https://doi.org/10.1111/nan.12021

Santillo, Alexander F., & Englund, E. (2014). Greater loss of von Economo neurons than loss of layer II and III neurons in behavioral variant frontotemporal dementia. *American Journal of Neurodegenerative Diseases*, *3*(2), 64–71. /pmc/articles/PMC4162587/?report=abstract

Schroeter, M. L., Laird, A. R., Chwiesko, C., Deuschl, C., Schneider, E., Bzdok, D., Eickhoff, S. B., & Neumann, J. (2014). Conceptualizing neuropsychiatric diseases with multimodal data-driven meta-analyses - The case of behavioral variant frontotemporal dementia. *Cortex*, *57*, 22–37. https://doi.org/10.1016/j.cortex.2014.02.022

Schwindt, G. C., Graham, N. L., Rochon, E., Tang-Wai, D. F., Lobaugh, N. J., Chow, T. W., & Black, S. E. (2013). Whole-brain white matter disruption in semantic and nonfluent variants of primary progressive aphasia. *Human Brain Mapping*, *34*(4), 973–984. https://doi.org/10.1002/hbm.21484

Seeley, W. W., Carlin, D. A., Allman, J. M., Macedo, M. N., Bush, C., Miller, B. L., & DeArmond, S. J. (2006). Early frontotemporal dementia targets neurons unique to apes and humans. *Annals of Neurology*, *60*(6), 660–667. https://doi.org/10.1002/ana.21055

Seeley, W. W., Crawford, R. K., Zhou, J., Miller, B. L., & Greicius, M. D. (2009).

Neurodegenerative Diseases Target Large-Scale Human Brain Networks. *Neuron*, *62*, 42–52. https://doi.org/10.1016/j.neuron.2009.03.024

Sha, S. J., Takada, L. T., Rankin, K. P., Yokoyama, J. S., Rutherford, N. J., Fong, J. C., Khan, B., Karydas, A., Baker, M. C., De Jesus-Hernandez, M., Pribadi, M., Coppola, G., Geschwind, D. H., Rademakers, R., Lee, S. E., Seeley, W., Miller, B. L., & Boxer, A. L. (2012). Frontotemporal dementia due To C9ORF72 mutations clinical and imaging features. *Neurology*, *79*(10), 1002–1011. https://doi.org/10.1212/WNL.0b013e318268452e

Smith, R. E., Tournier, J. D., Calamante, F., & Connelly, A. (2012). Anatomically-constrained tractography: Improved diffusion MRI streamlines tractography through effective use of anatomical information. *NeuroImage*, *62*(3), 1924–1938. https://doi.org/10.1016/j.neuroimage.2012.06.005

Smith, R. E., Tournier, J. D., Calamante, F., & Connelly, A. (2015). SIFT2: Enabling dense quantitative assessment of brain white matter connectivity using streamlines tractography. *NeuroImage*, *119*, 338–351. https://doi.org/10.1016/j.neuroimage.2015.06.092

Soares, J. M., Marques, P., Alves, V., & Sousa, N. (2013). A hitchhiker's guide to diffusion tensor imaging. *Frontiers in Neuroscience*, *7*(7 MAR). https://doi.org/10.3389/fnins.2013.00031

Song, H. L., Shim, S., Kim, D. H., Won, S. H., Joo, S., Kim, S., Jeon, N. L., & Yoon, S. Y. (2014). β-Amyloid is transmitted via neuronal connections along axonal membranes. *Annals of Neurology*, *75*(1), 88–97. https://doi.org/10.1002/ana.24029

Staffaroni, A. M., Bajorek, L., Casaletto, K. B., Cobigo, Y., Goh, S. Y. M., Wolf, A., Heuer, H. W., Elahi, F. M., Ljubenkov, P. A., Dever, R., Kornak, J., Appleby, B., Bove, J., Bordelon, Y., Brannelly, P., Brushaber, D., Caso, C., Coppola, G., Dheel, C., … Rosen, H. J. (2020).

Assessment of executive function declines in presymptomatic and mildly symptomatic familial frontotemporal dementia: NIH-EXAMINER as a potential clinical trial endpoint. *Alzheimer's and Dementia*, *16*(1), 11–21. https://doi.org/10.1016/j.jalz.2019.01.012

Staffaroni, A. M., Cobigo, Y., Goh, S. Y. M., Kornak, J., Bajorek, L., Chiang, K., Appleby, B., Bove, J., Bordelon, Y., Brannelly, P., Brushaber, D., Caso, C., Coppola, G., Dever, R., Dheel, C., Dickerson, B. C., Dickinson, S., Dominguez, S., Domoto-Reilly, K., … Rosen, H. J. (2020). Individualized atrophy scores predict dementia onset in familial frontotemporal lobar degeneration. *Alzheimer's and Dementia*, *16*(1), 37–48. https://doi.org/10.1016/j.jalz.2019.04.007

Tahmasian, M., Shao, J., Meng, C., Grimmer, T., Diehl-Schmid, J., Yousefi, B. H., Forster, S., Riedl, V., Drzezga, A., & Sorg, C. (2016). Based on the Network Degeneration Hypothesis: Separating Individual Patients with Different Neurodegenerative Syndromes in a Preliminary Hybrid PET/MR Study. *Journal of Nuclear Medicine*, *57*(3), 410–415. https://doi.org/10.2967/jnumed.115.165464

Tong, T., Ledig, C., Guerrero, R., Schuh, A., Koikkalainen, J., Tolonen, A., Rhodius, H., Barkhof, F., Tijms, B., Lemstra, A. W., Soininen, H., Remes, A. M., Waldemar, G., Hasselbalch, S., Mecocci, P., Baroni, M., Lötjönen, J., Flier, W. van der, & Rueckert, D. (2017). Five-class differential diagnostics of neurodegenerative diseases using random undersampling boosting. *NeuroImage: Clinical*, *15*(March), 613–624. https://doi.org/10.1016/j.nicl.2017.06.012

Tournier, J. D., Calamante, F., & Connelly, A. (2007). Robust determination of the fibre orientation distribution in diffusion MRI: Non-negativity constrained super-resolved spherical deconvolution. *NeuroImage*, *35*(4), 1459–1472.

https://doi.org/10.1016/j.neuroimage.2007.02.016

Tournier, J. D., Smith, R., Raffelt, D., Tabbara, R., Dhollander, T., Pietsch, M., Christiaens, D., Jeurissen, B., Yeh, C. H., & Connelly, A. (2019). MRtrix3: A fast, flexible and open software framework for medical image processing and visualisation. *NeuroImage*, *202*, 116137. https://doi.org/10.1016/j.neuroimage.2019.116137

Tsai, R. M., & Boxer, A. L. (2016). Therapy and clinical trials in frontotemporal dementia: past, present, and future. *Journal of Neurochemistry*, *138*(Suppl. 1), 211–221. https://doi.org/10.1111/jnc.13640

Tu, S., Leyton, C. E., Hodges, J. R., Piguet, O., & Hornberger, M. (2015). Divergent longitudinal propagation of white matter degradation in logopenic and semantic variants of primary progressive aphasia. *Journal of Alzheimer's Disease*, *49*(3), 853–861. https://doi.org/10.3233/JAD-150626

van der Ende, E. L., Meeter, L. H., Poos, J. M., Panman, J. L., Jiskoot, L. C., Dopper, E. G. P., Papma, J. M., de Jong, F. J., Verberk, I. M. W., Teunissen, C., Rizopoulos, D., Heller, C., Convery, R. S., Moore, K. M., Bocchetta, M., Neason, M., Cash, D. M., Borroni, B., Galimberti, D., … van Swieten, J. C. (2019). Serum neurofilament light chain in genetic frontotemporal dementia: a longitudinal, multicentre cohort study. *The Lancet Neurology*, *18*, 1103–1111. https://doi.org/10.1016/S1474-4422(19)30354-0

Vemuri, P., Simon, G., Kantarci, K., Whitwell, J. L., Senjem, M. L., Przybelski, S. A., Gunter, J. L., Josephs, K. A., Knopman, D. S., Boeve, B. F., Ferman, T. J., Dickson, D. W., Parisi, J. E., Petersen, R. C., & Jack, C. R. (2011). Antemortem differential diagnosis of dementia pathology using structural MRI: Differential-STAND. *NeuroImage*, *55*(2), 522–531.

https://doi.org/10.1016/j.neuroimage.2010.12.073

Venkatraghavan, V., Bron, E. E., Niessen, W. J., & Klein, S. (2019). Disease progression timeline estimation for Alzheimer's disease using discriminative event based modeling. *NeuroImage*, *186*, 518–532. https://doi.org/10.1016/j.neuroimage.2018.11.024

Vijverberg, E. G. B., Schouws, S., Meesters, P. D., Verwijk, E., Comijs, H., Koene, T., Schreuder, C., Beekman, A., Scheltens, P., Stek, M., Pijnenburg, Y., & Dols, A. (2017). Cognitive deficits in patients with neuropsychiatric symptoms: A comparative study between behavioral variant frontotemporal dementia and primary psychiatric disorders. *Journal of Clinical Psychiatry*, *78*(8), e940–e946. https://doi.org/10.4088/JCP.16m11019

Vijverberg, E. G. B., Wattjes, M. P., Dols, A., Krudop, W. A., Möller, C., Peters, A., Kerssens, C. J., Gossink, F., Prins, N. D., Stek, M. L., Scheltens, P., Van Berckel, B. N. M., Barkhof, F., & Pijnenburg, Y. A. L. (2016). Diagnostic Accuracy of MRI and Additional [18F]FDG-PET for Behavioral Variant Frontotemporal Dementia in Patients with Late Onset Behavioral Changes. *Journal of Alzheimer's Disease*, *53*(4), 1287–1297. https://doi.org/10.3233/JAD-160285

Wang, J., Redmond, S. J., Bertoux, M., Hodges, J. R., & Hornberger, M. (2016). A comparison of magnetic resonance imaging and neuropsychological examination in the diagnostic distinction of Alzheimer's disease and behavioral variant frontotemporal dementia. *Frontiers in Aging Neuroscience*, *8*(JUN), 1–10. https://doi.org/10.3389/fnagi.2016.00119

Whiting, P. F., Rutjes, A. W. S., Westwood, M. E., Mallett, S., Deeks, J. J., Reitsma, J. B., Leeflang, M. M. G., Sterne, J. A. C., & Bossuyt, P. M. M. (2011). QUADAS-2: A Revised Tool for the Quality Assessment of Diagnostic Accuracy Studies. *Annals of Internal*

Medicine, *155*(8), 529–536. https://doi.org/10.7326/0003-4819-155-8-201110180-00009

Whitwell, J. L., Avula, R., Senjem, M. L., Kantarci, K., Weigand, S. D., Samikoglu, A., Edmonson, H. A., Vemuri, P., Knopman, D. S., Boeve, B. F., Petersen, R. C., Josephs, K. A., & Jack, C. R. (2010). Gray and white matter water diffusion in the syndromic variants of frontotemporal dementia. *Neurology*, *74*(16), 1279–1287. https://doi.org/10.1212/WNL.0b013e3181d9edde

Whitwell, J. L., Boeve, B. F., Weigand, S. D., Senjem, M. L., Gunter, J. L., Baker, M. C., DeJesus-Hernandez, M., Knopman, D. S., Wszolek, Z. K., Petersen, R. C., Rademakers, R., Jack, C. R., & Josephs, K. A. (2015). Brain atrophy over time in genetic and sporadic frontotemporal dementia: A study of 198 serial magnetic resonance images. *European Journal of Neurology*, *22*(5), 745–752. https://doi.org/10.1111/ene.12675

Whitwell, J. L., Jack, C. R., Przybelski, S. A., Parisi, J. E., Senjem, M. L., Boeve, B. F., Knopman, D. S., Petersen, R. C., Dickson, D. W., & Josephs, K. A. (2011). Temporoparietal atrophy: A marker of AD pathology independent of clinical diagnosis. *Neurobiology of Aging*, *32*(9), 1531–1541. https://doi.org/10.1016/j.neurobiolaging.2009.10.012

Whitwell, J. L., Josephs, K. A., Avula, R., Tosakulwong, N., Weigand, S. D., Senjem, M. L., Vemuri, P., Jones, D. T., Gunter, J. L., Baker, M., Wszolek, Z. K., Knopman, D. S., Rademakers, R., Petersen, R. C., Boeve, B. F., & Jack, C. R. (2011). Altered functional connectivity in asymptomatic MAPT subjects A comparison to bvFTD. *Neurology*, *77*(9), 866–874. https://doi.org/10.1212/WNL.0b013e31822c61f2

Whitwell, J. L., Przybelski, S. A., Weigand, S. D., Ivnik, R. J., Vemuri, P., Gunter, J. L., Senjem, M. L., Shiung, M. M., Boeve, B. F., Knopman, D. S., Parisi, J. E., Dickson, D. W., Petersen,

R. C., Jack, C. R., & Josephs, K. A. (2009). Distinct anatomical subtypes of the behavioural variant of frontotemporal dementia: A cluster analysis study. *Brain*, *132*(11), 2932–2946. https://doi.org/10.1093/brain/awp232

Whitwell, J. L., Weigand, S. D., Boeve, B. F., Senjem, M. L., Gunter, J. L., DeJesus-Hernandez, M., Rutherford, N. J., Baker, M., Knopman, D. S., Wszolek, Z. K., Parisi, J. E., Dickson, D. W., Petersen, R. C., Rademakers, R., Jack, C. R., & Josephs, K. A. (2012). Neuroimaging signatures of frontotemporal dementia genetics: C9ORF72, tau, progranulin and sporadics. *Brain : A Journal of Neurology*, *135*(3), 794–806. https://doi.org/10.1093/brain/aws001

Wilson, S. M., Ogar, J. M., Laluz, V., Growdon, M., Jang, J., Glenn, S., Miller, B. L., Weiner, M. W., & Gorno-tempini, M. L. (2009). Automated MRI-based classification of primary progressive aphasia variants. *NeuroImage*, *47*(4), 1558–1567. https://doi.org/10.1016/j.neuroimage.2009.05.085.Automated

Woolley, J. D., Khan, B. K., Murthy, N. K., Miller, B. L., & Rankin, K. P. (2011). The diagnostic challenge of psychiatric symptoms in neurodegenerative disease: Rates of and risk factors for prior psychiatric diagnosis in patients with early neurodegenerative disease. *Journal of Clinical Psychiatry*, *72*(2), 126–133. https://doi.org/10.4088/JCP.10m06382oli

Young, A. L., Marinescu, R. V, Oxtoby, N. P., Bocchetta, M., Yong, K., Firth, N. C., Cash, D. M., Thomas, D. L., Dick, K. M., Cardoso, J., van Swieten, J., Borroni, B., Galimberti, D., Masellis, M., Tartaglia, M. C., Rowe, J. B., Graff, C., Tagliavini, F., Frisoni, G. B., … Furst, A. J. (2018). Uncovering the heterogeneity and temporal complexity of neurodegenerative diseases with Subtype and Stage Inference. *Nature Communications*, *9*, 4273. https://doi.org/10.1038/s41467-018-05892-0

Young, A. L., Oxtoby, N. P., Daga, P., Cash, D. M., Fox, N. C., Ourselin, S., Schott, J. M., & Alexander, D. C. (2014). A data-driven model of biomarker changes in sporadic Alzheimer's disease. *Brain*, *137*(9), 2564–2577. https://doi.org/10.1093/brain/awu176

Zhang, Y., Tartaglia, M. C., Schuff, N., Chiang, G. C., Ching, C., Rosen, H. J., Gorno-Tempini, M. L., Miller, B. L., & Weiner, M. W. (2013). MRI Signatures of Brain Macrostructural Atrophy and Microstructural Degradation in Frontotemporal Lobar Degeneration Subtypes NIH Public Access. *J Alzheimers Dis*, *33*(2), 431–444. https://doi.org/10.3233/JAD-2012-121156

Zhou, J., Gennatas, E. D. D., Kramer, J. H. H., Miller, B. L. L., & Seeley, W. W. W. (2012). Predicting Regional Neurodegeneration from the Healthy Brain Functional Connectome. *Neuron*, *73*(6), 1216–1227. https://doi.org/10.1016/J.NEURON.2012.03.004

Zhou, J., Greicius, M. D., Gennatas, E. D., Growdon, M. E., Jang, J. Y., Rabinovici, G. D., Kramer, J. H., Weiner, M., Miller, B. L., & Seeley, W. W. (2010). Divergent network connectivity changes in behavioural variant frontotemporal dementia and Alzheimer's disease. *Brain*, *133*(5), 1352–1367. https://doi.org/10.1093/brain/awq075

Zhu, N., Santos-Santos, M., Illán-Gala, I., Montal, V., Estellés, T., Barroeta, I., Altuna, M., Arranz, J., Muñoz, L., Belbin, O., Sala, I., Sánchez-Saudinós, M. B., Subirana, A., Videla, L., Pegueroles, J., Blesa, R., Clarimón, J., Carmona-Iragui, M., Fortea, J., … Alcolea, D. (2021). Plasma glial fibrillary acidic protein and neurofilament light chain for the diagnostic and prognostic evaluation of frontotemporal dementia. *Translational Neurodegeneration*, *10*(1), 50. https://doi.org/10.1186/S40035-021-00275-W

Zou, Q. H., Zhu, C. Z., Yang, Y., Zuo, X. N., Long, X. Y., Cao, Q. J., Wang, Y. F., & Zang, Y. F.

(2008). An improved approach to detection of amplitude of low-frequency fluctuation (ALFF) for resting-state fMRI: Fractional ALFF. *Journal of Neuroscience Methods*, *172*, 137–141. https://doi.org/10.1016/j.jneumeth.2008.04.012